UNCLASSIFIED

AD NUMBER

AD243387

NEW LIMITATION CHANGE

TO

Approved for public release, distribution unlimited

FROM

Distribution authorized to U.S. Gov't. agencies and their contractors; Administrative/Operational Use; Jun 1960. Other requests shall be referred to Wright Air Development Center, Materials Lab., Wright-Patterson AFB, OH 45433.

AUTHORITY

Aeronautical Systems Div. ltr dtd 9 Oct 1974

THIS PAGE IS UNCLASSIFIED

File Copy
WWRCNP

WADD TECHNICAL REPORT 60-283

AD0243387

OFFICIAL FILE COPY

D-29

EVALUATION OF EXPERIMENTAL POLYMERS

Charles D. Doyle

General Electric Company

JUNE 1960

This report is not to be announced or distributed automatically to foreign governments (AFR 205-43A, paragraph 6d).

WRIGHT AIR DEVELOPMENT DIVISION

20040218277

NOTICES

When Government drawings, specifications, or other data are used for any purpose other than in connection with a definitely related Government procurement operation, the United States Government thereby incurs no responsibility nor any obligation whatsoever; and the fact that the Government may have formulated, furnished, or in any way supplied the said drawings, specifications, or other data, is not to be regarded by implication or otherwise as in any manner licensing the holder or any other person or corporation, or conveying any rights or permission to manufacture, use, or sell any patented invention that may in any way be related thereto.

Qualified requesters may obtain copies of this report from the Armed Services Technical Information Agency, (ASTIA), Arlington Hall Station, Arlington 12, Virginia.

Copies of WADD Technical Reports and Technical Notes should not be returned to the Wright Air Development Division unless return is required by security considerations, contractual obligations, or notice on a specific document.

WADD TECHNICAL REPORT 60-283

EVALUATION OF EXPERIMENTAL POLYMERS

Charles D. Doyle

General Electric Company

JUNE 1950

Materials Central
Contract No. AF 33(616)-5576
Project No. 7340

WRIGHT AIR DEVELOPMENT DIVISION
AIR RESEARCH AND DEVELOPMENT COMMAND
UNITED STATES AIR FORCE
WRIGHT-PATTERSON AIR FORCE BASE, OHIO

300 – September 1960 – 1-45

BEST AVAILABLE COPY

FOREWORD

This report was prepared by the General Engineering Laboratory of the General Electric Company and submitted by the Chemical Materials Department of the General Electric Company under USAF Contract AF 33(616)-5576. This contract was initiated under Project No. 7340, "Non-Metallic and Composite Materials," Task No. 73407, "New Chemicals and Methods." The work was administered under the direction of the Materials Central, Directorate of Advanced Systems Technology, Wright Air Development Division, with Dr. G. F. L. Ehlers acting as project engineer.

This report covers work conducted from March 1959 to March 1960.

The writer is indebted to Mrs. W. G. Spodnewski, of the General Engineering Laboratory, who painstakingly conducted all the thermogravimetric analyses and tc Mssrs. J. A. Coffman and R. L. Thorkildsen, also of the General Engineering Laboratory, for frequent helpful discussions.

ABSTRACT

Thermogravimetric analysis (TGA) in dry N_2 is considered in detail as a method for comparing the intrinsic thermal stabilities of experimental polymers on both empirical and fundamental grounds. Two procedural decomposition temperatures are defined and discussed. One, the "differential procedural decomposition temperature" (dpdt), is based on the locations of recognizable curve features, while the second, the "integral procedural decomposition temperature" (ipdt), is based on areas under the curve. Kinetic analysis of volatilization data is discussed on the basis of both the Arrhenius rate equation and its integral. Two quasi-kinetic methods are discussed, one based on empirical time-temperature superposition; the other, on an empirical relationship between isothermal times and temperatures in TGA. Two corroborative test methods, differential thermal analysis and thermoparticulate analysis are discussed briefly.

This report has been reviewed and is approved.

FOR THE COMMANDER:

A. M. Lovelace
Chief, Polymer Branch
Nonmetallic Materials Laboratory
Materials Central

TABLE OF CONTENTS

LIST OF ILLUSTRATIONS

LIST OF TABLES

I. INTRODUCTION[1]

In the preceding summary technical report (1), methods were considered for assessing the intrinsic thermal stabilities of experimental polymers rapidly, reproducibly and significantly. One of these methods, thermogravimetric analysis in dry nitrogen, was regarded as an especially promising technique worthy of intensive development.

In the subsequent development of TGA, interest has been centered on three salient needs:

1. Methods for interpreting TGA curves on a consistent empirical basis in spite of the great variety of volatilization histories displayed by real materials.

2. Methods for interpreting TGA curves on the basis of fundamental principles.

3. Corroborative test methods to be applied in certain questionable cases, especially those wherein reaction without weight change may be suspected.

Progress along these lines is summarized in this report.

---

[1] Manuscript released by the author May 1960 for publication as a WADD Technical Report

II. EMPIRICAL INTERPRETATION OF TGA CURVES

A. Procedural Decomposition Temperatures

It has been noted previously that the measured values of empirically determined decomposition temperatures are powerfully influenced by procedural details and by the choice of experimentally convenient criteria of decomposition (1). As a precaution against citing such trivial data out of context with their necessary qualifications, it has been the custom in this investigation to refer to them as "procedural decomposition temperatures."

Two general types of procedural decomposition temperature have so far been defined for TGA in inert atmosphere. One of these, called the "differential procedural decomposition temperature" (dpdt), is determined on the basis of consistently recognizable features of the TGA curve. The other, called the "integral procedural decomposition temperature" (ipdt), is determined on the basis of areas under the curve.

In this report, all TGA-pdt's and all other TGA data refer to 200 mg pulverized samples heated in a 000 Cours porcelain crucible in a Chevenard thermobalance (1) to 900 C at 180 degrees centigrade per hour in an atmosphere of dry N_2 flowing at 314 ml per minute, unless otherwise specifically noted. All samples requiring pulverization were either end-milled or ground in a mortar under liquid N_2.

1. Differential Procedural Decomposition Temperatures. As an empirical index of intrinsic thermal stability, the dpdt was devised as a means of locating knees in normalized TGA records (of residual weight fraction vs temperature). In some instances, it also serves as a practical index of the onset of decomposition. Further, by its definition, it has potential significance in the kinetic sense. It is, however, frequently worthless as a pdt.

Since many materials decompose in steps, the dpdt is neither a unique empirical end point nor a consistently unambiguous practical index of incipient decomposition. In cases of gradual decomposition, it may be hopelessly imprecise or even completely unavailable. Further, as will next be shown, it is often impractical to attempt to realize its potential kinetic significance in rapid screening tests. This, in turn, limits the validity of the dpdt as a basis for the equitable comparison of diverse materials.

Ideally, the dpdt is defined as the temperature, in degrees C, at which the volatilization rate calculated on the initial

sample weight increases through a prescribed value so chosen that diverse materials are compared on the basis of a single specific decomposition rate constant.

In practice, however, this ideal definition cannot be applied. This is true because only an implied relationship exists between the rate of decomposition and the rate of volatilization in inert atmosphere. Further, the rate of volatilization depends in part in unspecified ways on the geometry and degree of subdivision of the sample. Thus at the outset, the best kinetic basis available from TGA for comparing materials is an empirical rate constant defined as the specific rate constant for volatilization under fixed procedural conditions. As such, it is not an authentic specific decomposition rate constant, nor is it necessarily even a constant; the geometry and degree of subdivision of a sample may change with temperature or extent of volatilization. These problems will be discussed again in Section IV of this report, but meanwhile, the value of the dpdt as a kinetic basis for comparing materials can be challenged on other grounds, as will next be shown.

The apparent volatilization rate, $\frac{dv}{dt}$, is found by multiplying the point-slope, $-\frac{dw}{dT}$, of the normalized TGA curve by the constant heating rate, B:

$$\frac{dv}{dt} = -B\frac{dw}{dT} \qquad (1)$$

where:

$$v = 1 - w \qquad (2)$$

and where w is the residual weight fraction on initial weight.

If the dpdt is to bear a clear relationship to the empirical rate constant, however, it must first be based on the true, rather than the apparent volatilization rate. The true volatilization rate for a particular decomposition step is calculated on the extent of volatilization during that step, as illustrated in idealized form in Figure 1. From Figure 1, a true residual weight fraction, h, and a true fraction volatilized, 1 - h, can be defined as:

$$h = \frac{w - G}{H} \qquad (3)$$

$$1 - h = \frac{v - L}{H} \qquad (4)$$

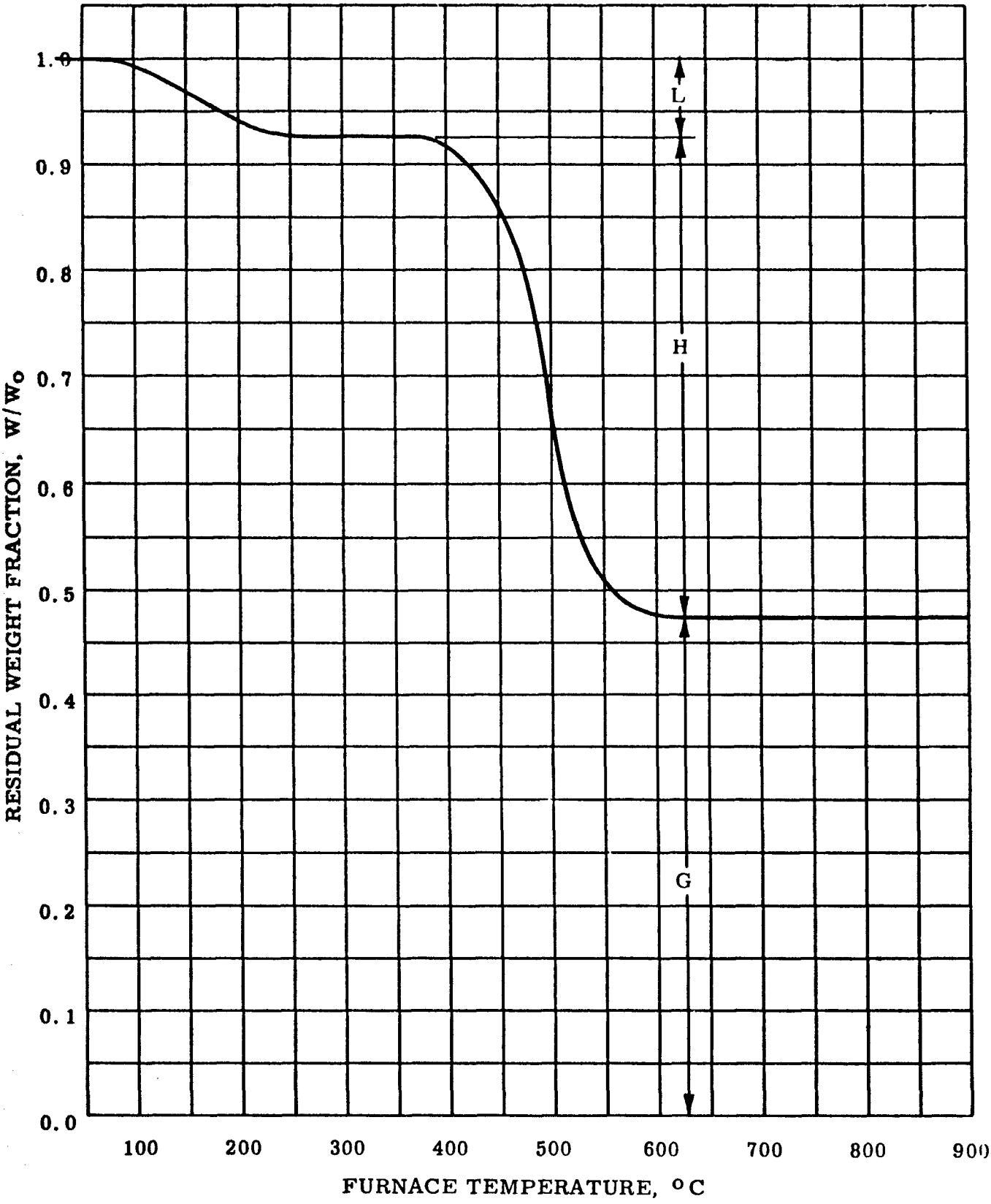

Figure 1 ILLUSTRATIVE TGA CURVE SHOWING THE QUANTITIES "G", "H" AND "L"

where L and H are the weight fractions volatilized prior to and during the decomposition of interest, and G is the weight fraction remaining after the decomposition has ceased. From Equation 4:

$$\frac{dv}{dt} = - H\frac{dh}{dt} \qquad (5)$$

Thus, the appropriate apparent rate of volatilization is equal to, or smaller than the prescribed true rate, depending on the value of H.

Next, the nature of the kinetic process must be taken into account. In general:

$$- \frac{dh}{dt} = \underline{k}f(h) \qquad (6)$$

where $\underline{k}$ is the empirical rate constant (whose constancy is dubious) and where the specific form of f(h) depends on the type of kinetic process.

Since the evaluation of f(h) from the TGA curve is formidably difficult in many cases, advantage is taken of the fact that when h is near unity, all forms of f(h) also approach unity, a condition which is satisfied when the prescribed true rate is chosen sufficiently small. In general, this requirement precludes the use of true rates which occur after the value of h has become less than about 0.95, as will be shown in Section IV of this report. Experience suggests that this, in turn, means that the end point true rate should not be chosen greater than about 50% per hour.

At the opposite extreme, the range of usable true rates is limited by the fact that the dpdt cannot be located with acceptance precision if the apparent rate of volatilization is chosen too small.

Further, as will be shown in Section IV of this report, the correlation between TGA temperatures and apparent volatilization rates smaller than about 8% per hour is confounded not only by imprecision but also by inherent inaccuracy. Thus, even if the maximum allowable apparent rate of 50H% per hour were prescribed, significant dpdt's could be cited only for materials whose H-values exceed 0.16. This would exclude many stable polymers from comparative rating.

Moreover, the evaluation of H often presents prohibitive difficulties insofar as rapid screening tests are concerned. In the data records for real materials, the values of L, H, and G are seldom as clearly defined as they are in the idealized curve of Figure 1. More commonly, consecutive decompositions

overlap and incomplete volatilizations have not entirely ceased when the analysis is ended at 900 C. Therefore, it has not been possible to devise a method for evaluating H without subjectivity.

Before the advent of a vastly superior empirical index of thermal stability in TGA in inert atmosphere, these frequently encountered difficulties of applying an equitable dpdt were circumvented by applying a single, convenient apparent rate (10% per hour) to all materials, regardless of their H-values and kinetic processes. Fortunately, it is now possible to abandon the use of this pseudo-kinetic dpdt for the unfair comparison of diverse materials on widely different empirical rate constants.

On the other hand, however, it is still expedient to retain the 10% per hour dpdt as a basis for comparing TGA in inert atmosphere with corroborative techniques whose data records can as yet be interpreted only in terms of the locations of curve features. For this purpose, 10% per hour dpdt's have been tabulated in Section III of this report for the 54 polymers so far examined. For the empirical comparison of the intrinsic thermal stabilities of diverse materials in TGA in inert atmosphere, however, the 10% per hour dpdt is now considered far less reliable than the ipdt, an index which takes into account the whole shape of the TGA curve.

2. Integral Procedural Decomposition Temperatures. The ipdt, being determined on the basis of areas under the curve, is always available from the normalized data record of TGA in inert atmosphere. Indeed, it is the consistent availability of the ipdt which so far sets TGA apart from all other rapid thermal stability methods as a uniquely versatile one. Further, although no ipdt having immediately apparent kinetic significance has yet been defined, at least one form having practical meaning can readily be determined from the data, as will next be shown.

In taking into account the whole shape of the TGA curve, the easiest way to sum up all of its dips and meanderings in a single number is to measure the area under the curve, as illustrated in Figure 2. In order to place all materials on an equal procedural footing, the curve is integrated on the basis of the total experimentally accessible temperature range from 25 to 900 C. The integration is accomplished quickly and easily by copying the curve and the outlines of the total plotting area on tracing paper, then cutting out and weighing the pieces on the analytical balance (preferably in a controlled humidity area). The weight of all of the crosshatched region in Figure 2 divided by the weight of the total rectangular plotting area is the total curve area, A*, normalized with respect to both residual weight and temperature.

A* is readily converted to a temperature, T_{A*}, by:

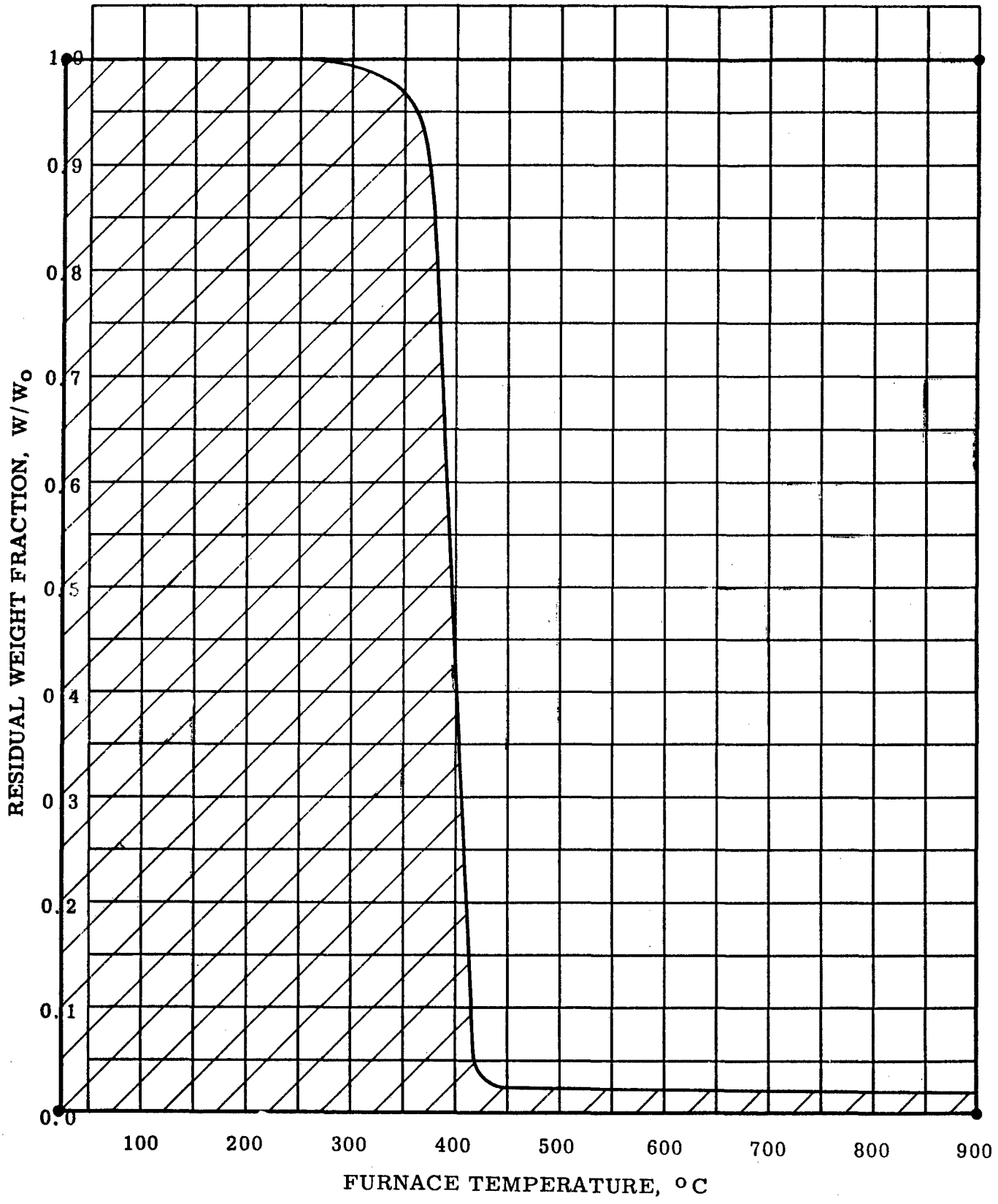

Figure 2 THE TGA CURVE AREA, A*

$$T_{A*} = 875A* + 25 \qquad (7)$$

In T_{A*}, it is pretended that all materials volatilize completely in TGA to 900 C and do so at a single temperature. Thus, T_{A*} represents a characteristic end-of-volatilization temperature, rather than an ipdt having practical significance. True, it does serve as a measure of refractoriness in TGA, but as such, it satisfies only one of two divergent points of view regarding thermal stability; many materials having high refractory weight fractions to 900 C begin to decompose at much lower temperatures. Further, high refractory fractions may be artificial, as in the case of a resin-glass laminate.

Thus, it is necessary to place materials on an equal footing not only with respect to the experimental temperature range, as in A*, but also with respect to their individual refractory contents in TGA. To this end, a second curve area, K*, was defined, as illustrated by the doubly crosshatched region in Figure 3. The ultimate boundaries of the lesser area, K*, are established by the characteristic end-of volatilization temperature, T_{A*}, and by the residual weight fraction at the fixed end-of-test temperature, 900 C.

The latter boundary is, of course, only one of several possible base lines for areas ending at T_{A*}. Others which have been considered include the lines at which the residual weight fraction has the values: zero, its value at T_{A*}, the value of A* (the integrated weight fraction) and the integrated weight fraction up to T_{A*}. The use of any of these base lines leads to an ipdt having practical meaning in some measure, but the most clearly significant ipdt is the one derived from the area shown in Figure 3. A further advantage of the final weight fraction line is that its value can be checked precisely in the analytical balance.

It is immediately apparent that the value of K* will approach unity in many cases of one-step, catastrophic volatilization. Thus, as an index of thermal stability, K* has little inherent significance; rather, it is a measure of a material's approach to the ideality pretended in T_{A*}, consistent with that material's refractory content at 900 C. For this reason, K* is applied as a coefficient of A*.

That the product A*K* represents a truly comprehensive index of intrinsic thermal stability is shown in Figure 4 for 54 polymers of widely different basic type. Here it is seen that the values of A*K* for real materials are not predominantly determined by the corresponding values of A*. Thus, materials which are highly refractory, but which begin to decompose at relatively low temperatures, have A*K* values which fall far short of their

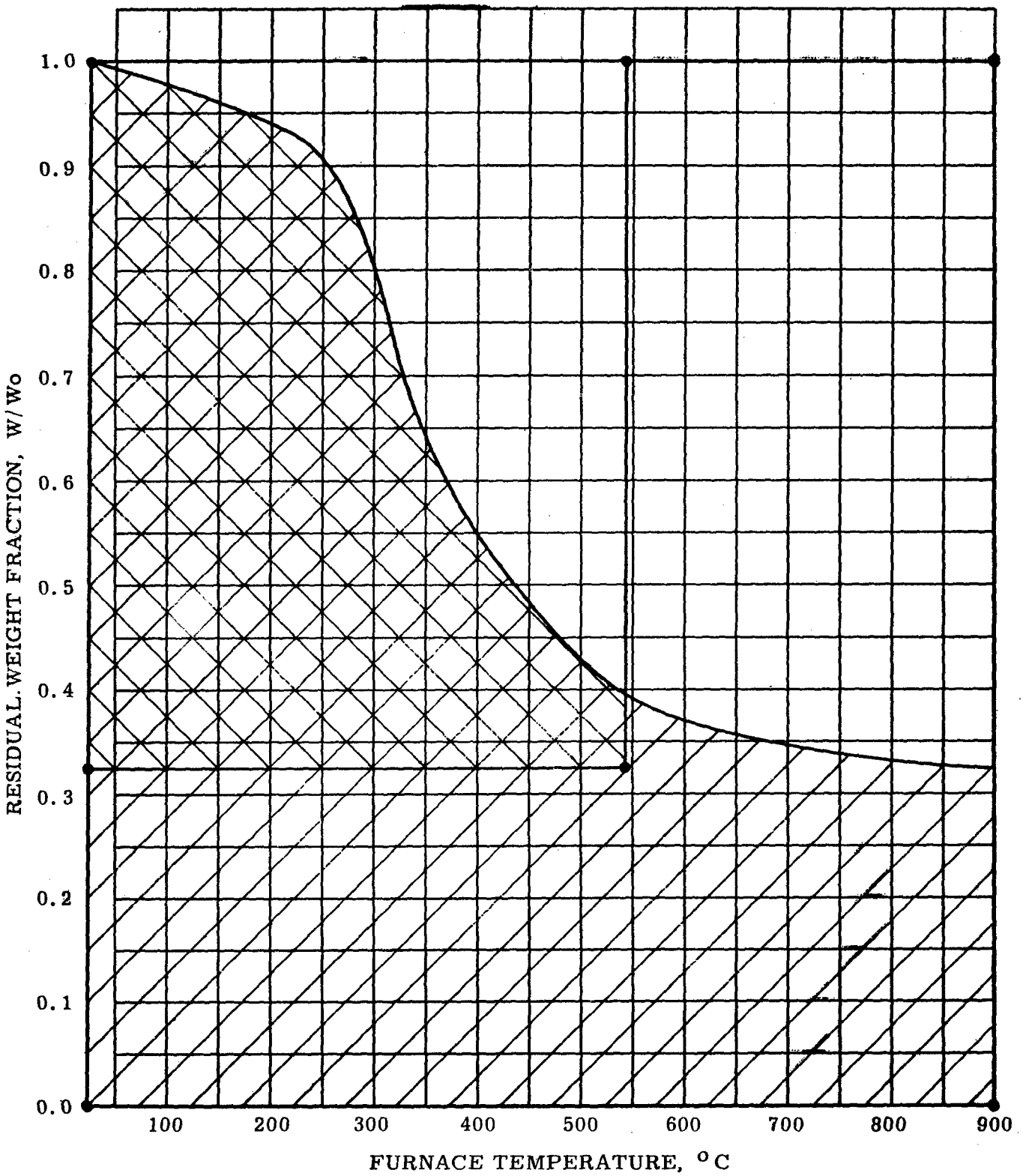

Figure 3 THE TGA CURVE AREAS, A* AND K*

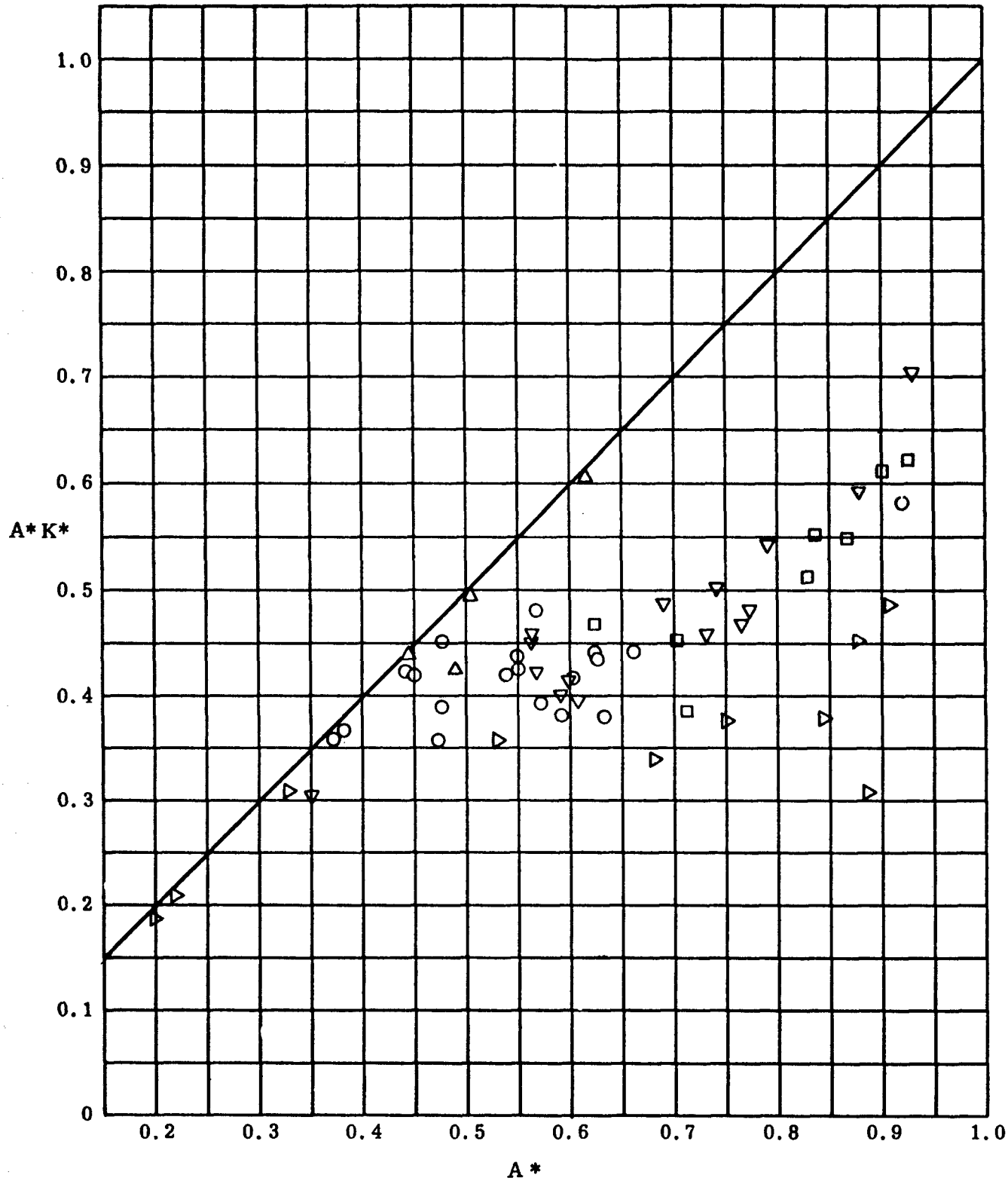

Figure 4 A*K* VS. A* FOR 54 POLYMERS CONTAINING:
⊙ C, H, N, O, △ F, □ Si, ▷ B, P, ▽ Cu, Zn, Be

potential levels, as shown by the partition line in Figure 4. Conversely, appropriately high A*K* values are found for some completely volatile materials which remain stable up to relatively high temperatures.

The ipdt determined by substituting A*K* for A* in Equation 7 has practical meaning as a remarkable type of half-volatilization temperature. Unlike the ordinary half-volatilization temperature, defined as the temperature at which half the ultimate volatilization has occurred, the ipdt based on the residual weight fraction at 900 C is appropriate whether decomposition occurs in a single step or in several consecutive steps. As shown in Figure 5, these two temperatures are closely related for many of the 54 polymers in Figure 4, but consideration of the individual cases shows that the exactness of the correlation decreases with increasing complexity of the TGA curve, or to put it the other way, with decreasing appropriateness of the ordinary half-volatilization temperature. The ipdt, on the other hand, having been determined on the basis of the whole shape of the TGA curve, is appropriate in all cases.

As a quantity derived from areas, the ipdt is also a highly reproducible datum whose value is only slightly affected by small vagaries or systematic errors in the TGA curve, especially as contrasted with indices derived on the basis of residual weight fraction end points alone. Happily, even small variations in heating rates in the neighborhood of 180 C degrees per hour produce little effect. Indeed, as shown in Figures 6 and 7, doubling the heating rate caused only a relatively small increase in curve area both in a case of complete and catastrophic volatilization and in one of gradual decomposition. The corresponding ipdt's were increased only from 555 to 575 C and from 355 to 370 C.

In summary, then, the ipdt based on the residual weight fraction in TGA to 900 C in inert atmosphere is a reproducible datum which can be determined in a consistent manner for diverse materials, and which represents both a truly comprehensive index of intrinsic thermal stability and a real temperature having practical significance.

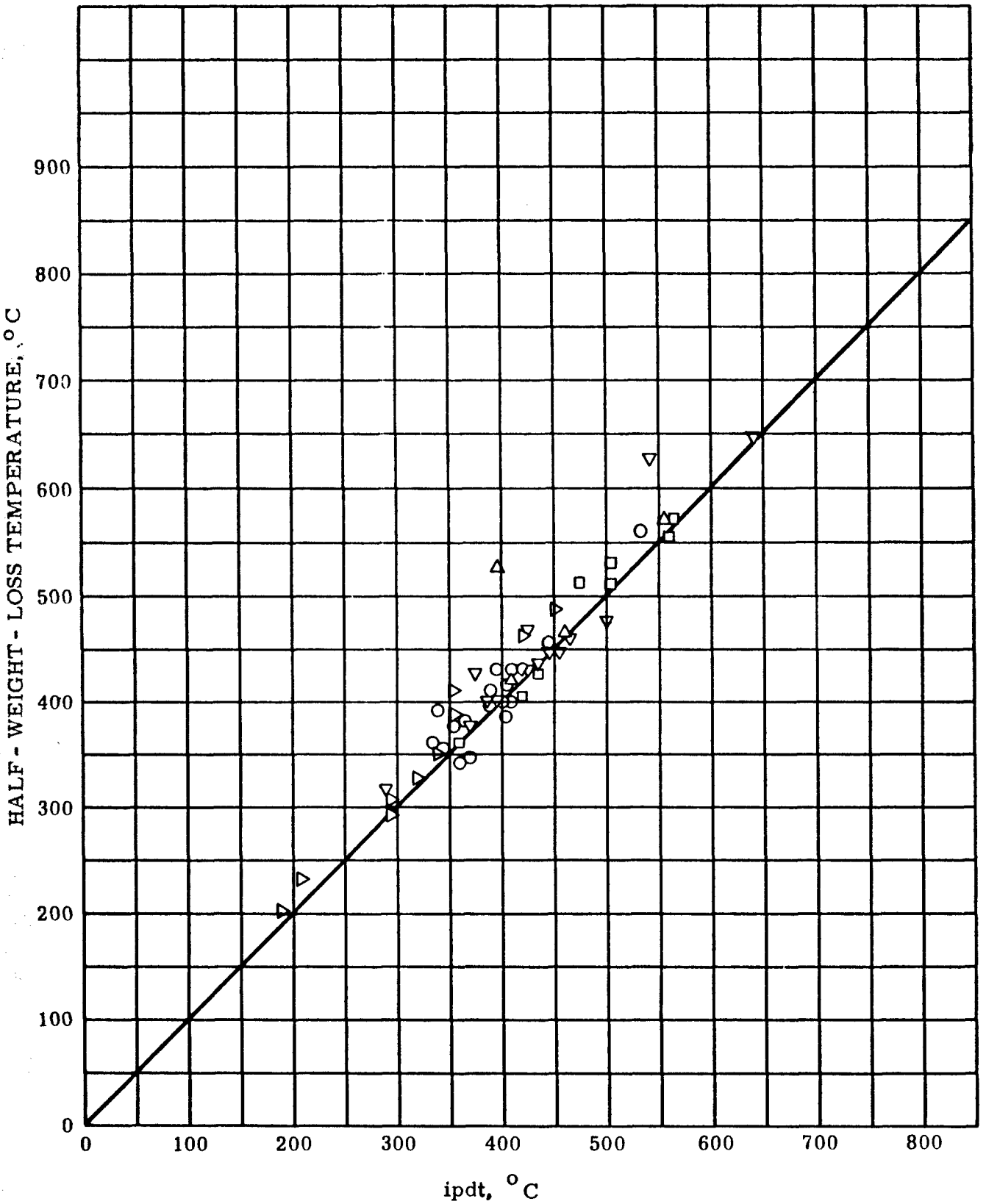

Figure 5 HALF - WEIGHT - LOSS TEMPERATURE VS. ipdt FOR 54 POLYMERS CONTAINING:
⊙ C, H, N, O △ F, □ Si, ▷ B, P ▽ Cu, Zn, Be

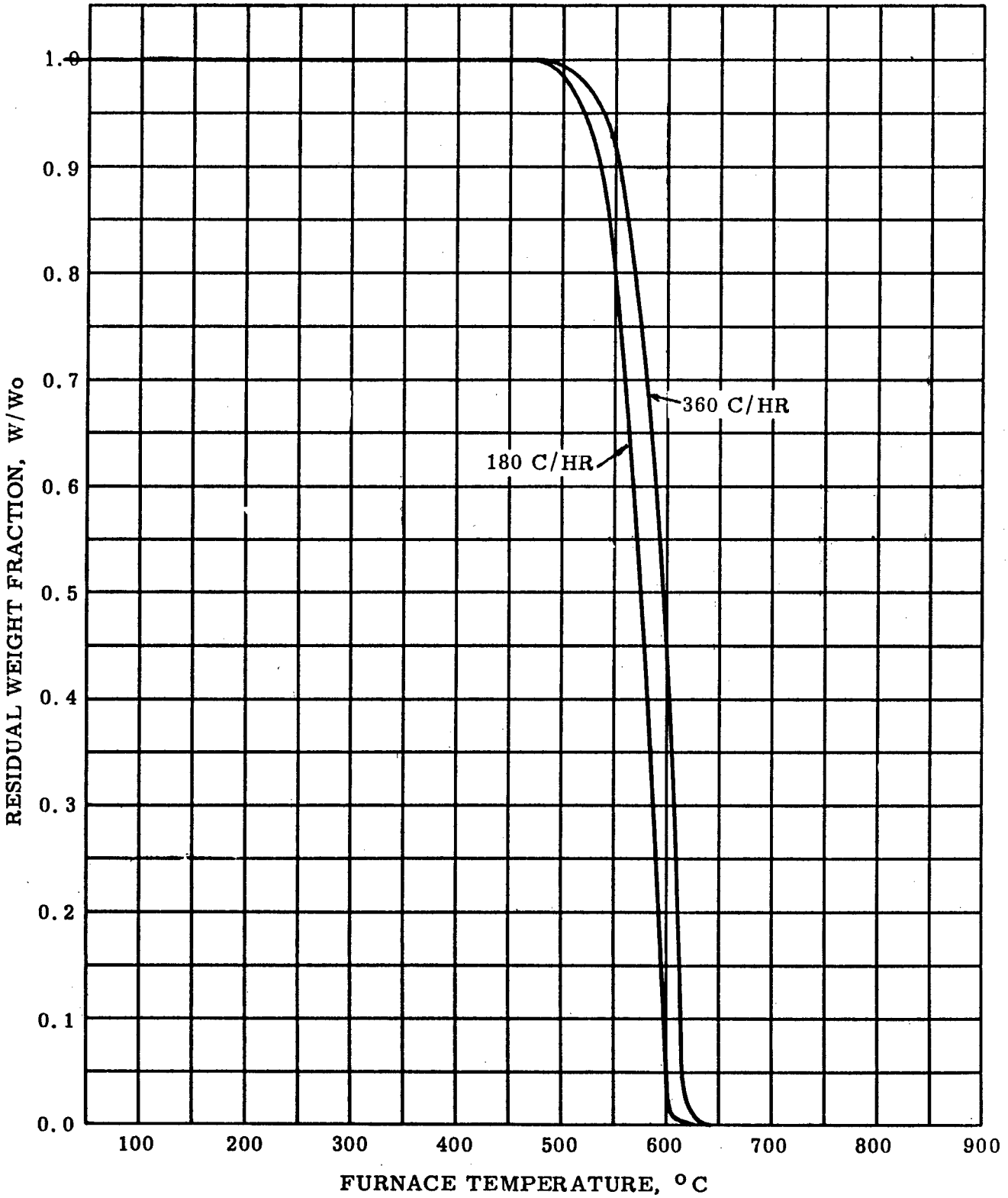

Figure 6 TGA IN DRY N_2 AT TWO DIFFERENT HEATING RATES, POLYTETRAFLUOROETHYLENE

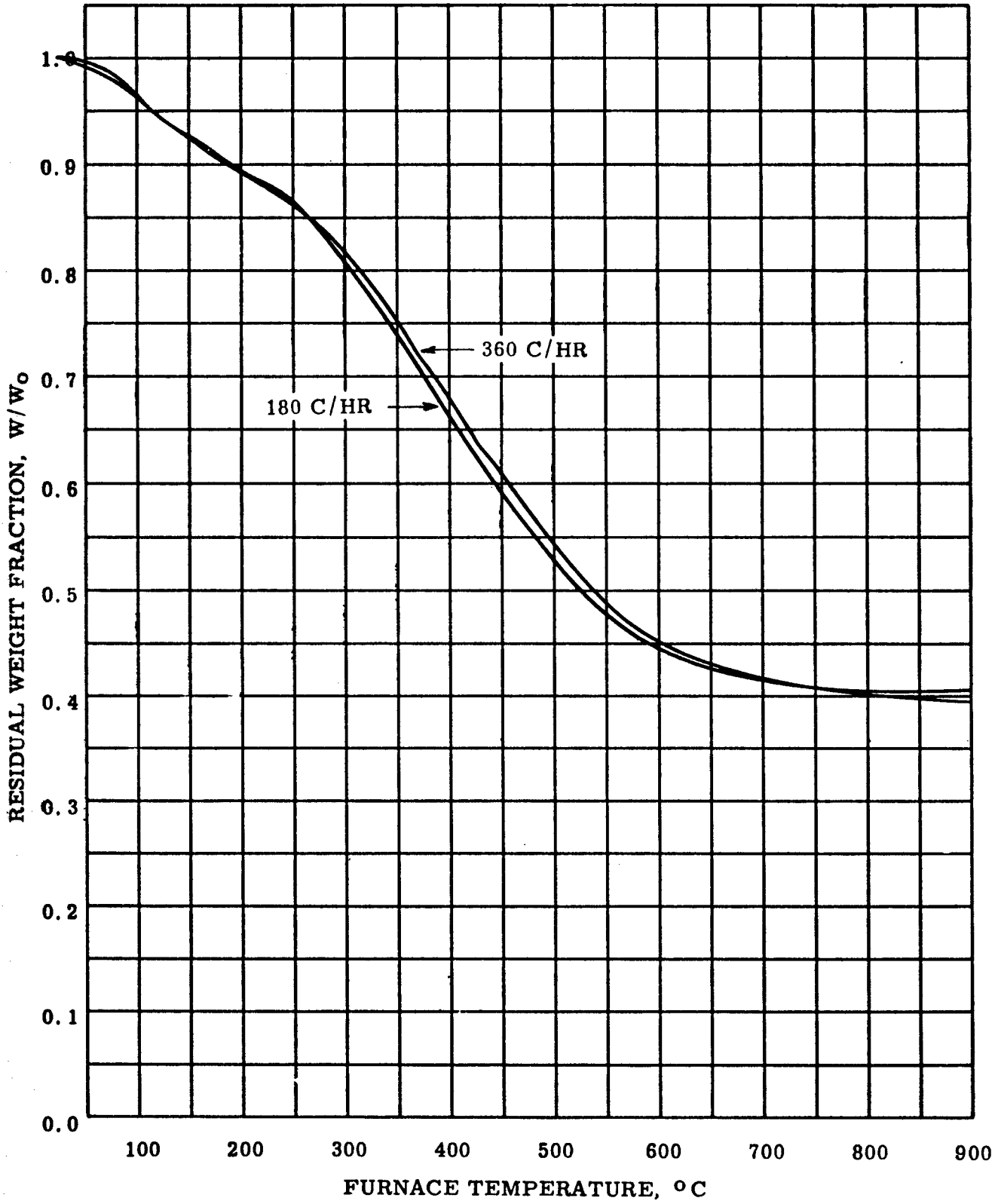

Figure 7 TGA IN DRY N_2 AT TWO DIFFERENT HEATING RATES, REACTION PRODUCT OF ACONITIC ACID AND ACETIC ANHYDRIDE, CODE 88, 8/58

III. TGA CURVES AND TABLES OF DATA FOR 54 POLYMERS

In the following Subsections IIIA through IIIK, TGA curves and pdt's (to the nearest 5°C) are given for the 54 polymers so far examined. For convenient comparison, related materials have been tabulated by groups and their TGA curves have been superposed. Since the descriptions of many of the polymers are rather involved, each has been assigned a sample number for convenient reference.

A. Cyclic Hydrocarbon Polymers

The data in Table 1 and Figure 8 for four cyclic hydrocarbon polymers, three of them open to vinyl depolymerization and the fourth cross-linked by strong ring-to-ring bonds, demonstrate the great importance of avoiding low-energy decomposition mechanisms in designing stable polymers. The stability of Material 25 approaches that of the ultimate benzenoid polymer, graphite, which suffers no weight-loss in TGA to 900 C in inert atmosphere.

Table 1

Cyclic Hydrocarbon Polymers

Sample	Polymer	Code	ipdt, °C	dpdt, °C
5CP	polystyrene	"Cadco"	395	330
16	anthracene-styrene copolymer	BDW-I-175	345	290
17	polyvinyl cyclohexane	AEG-82C	395	230
25	polyphenyl	PVB-L-7/25	535	510

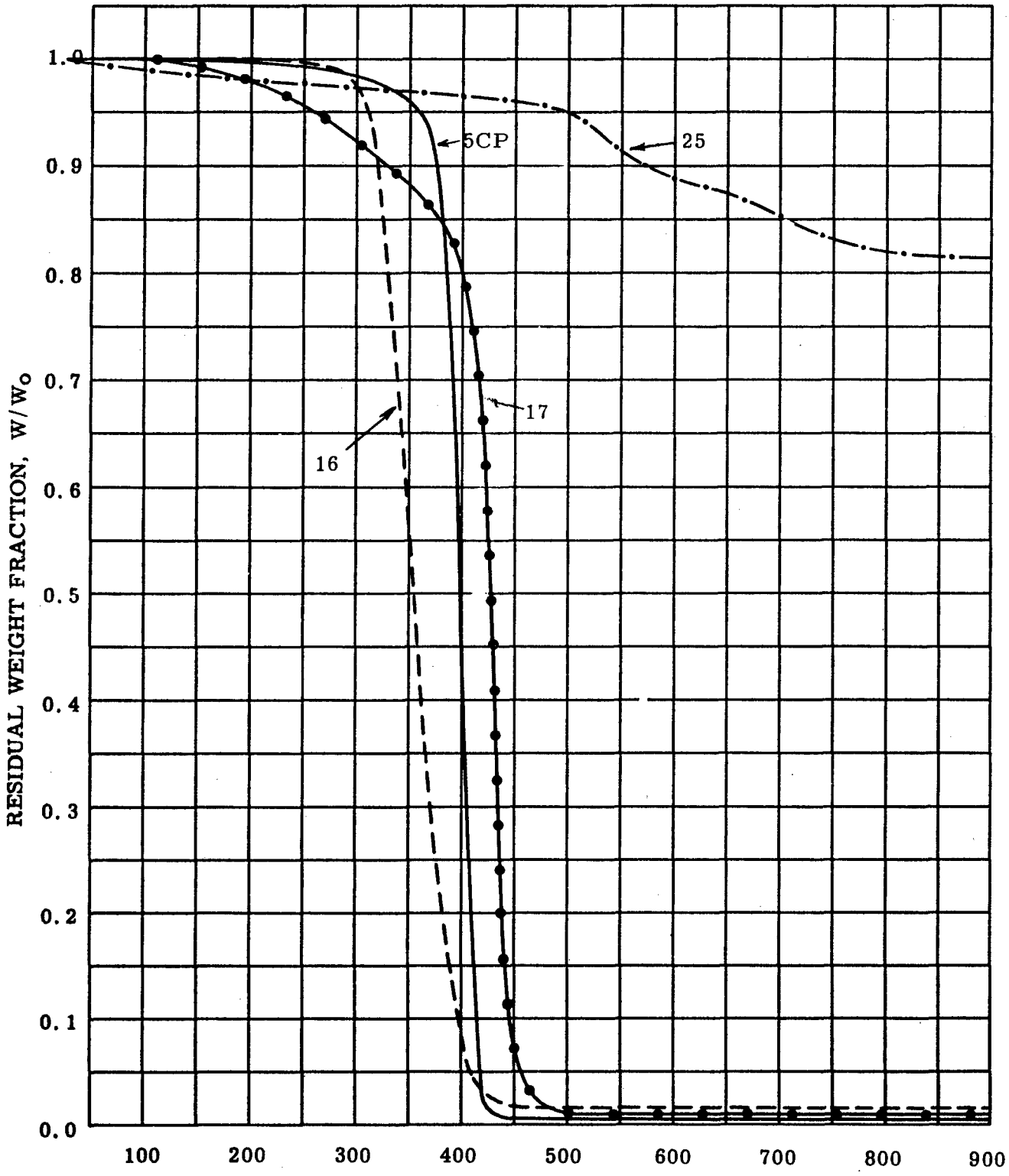

Figure 8 TGA IN DRY N_2 AT 180 C° PER HOUR
CYCLIC HYDROCARBON POLYMERS

B. Epoxy Resins

The data in Table 2 and Figure 9 for seven interesting epoxy resin-hardener variations illustrate the sensitivity of the ipdt to low-temperature vagaries in the TGA curve like those ascribable to excess hardener in the cases of Materials 40 and 43. In the rapid volatilization range, the TGA curves are remarkable alike, excepting the case of Material 42, whose hardener decomposes rapidly in the neighborhood of 300 C, yielding copious quantities of Cl_2. In those cases not complicated by excess hardener or by the release of Cl_2, however, it is seen again that increased initial cross-linking leads to increased final weight fractions and higher ipdt's.

Table 2

Epoxy Resins

Sample	Polymer	Code	ipdt, °C	dpdt, °C
39	E* + 1 mole maleic anhyd.	22/5	390	305
43	E* + 5 mole maleic anhyd.	22/17	340	110
45	E** + 1 mole maleic anhyd.	74/3	405	295
40	E* + 1 mole phthalic anhyd.	22/8	365	175, 295
41	E* + 0.5 mole pyromellitic dianhyd.	22/9	400	295
42	E* + 1 mole chlorendic anhyd.	22/10	370	270
44	E** + 1% BF_3-400	39/11	410	315

*bis-phenol A - epichlorohydrin resin, epoxy equivalent: 420
**Shell "Epon" 1031 resin, epoxy equivalent: 235

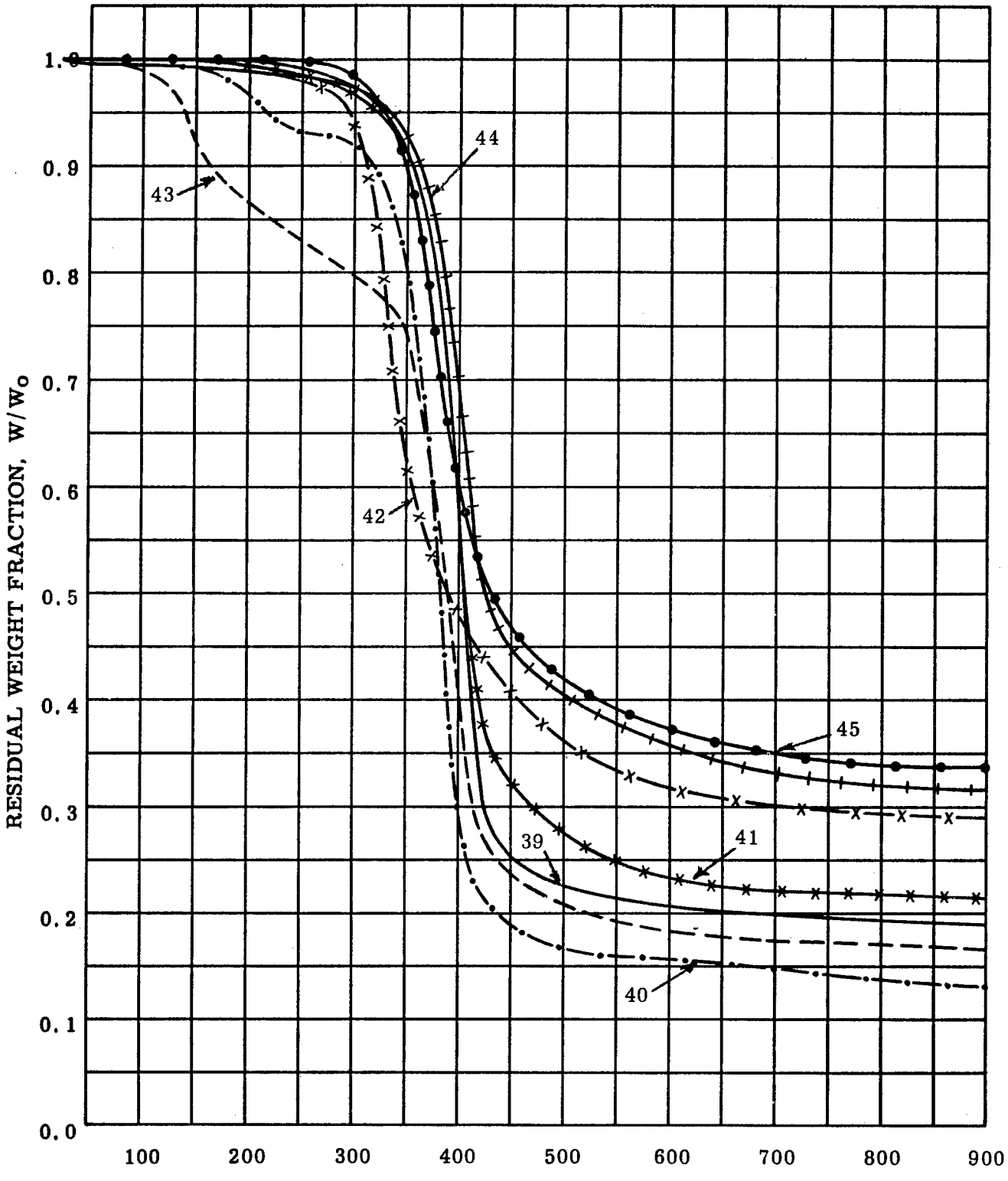

Figure 9 TGA IN DRY N_2 AT 180 C° PER HOUR

EPOXY RESINS

C. Miscellaneous Polymers

The data in Table 3 and Figure 10 for three conventional polymers and two experimental ones provide illustrations of the way in which the ipdt penalizes materials for decomposition at low temperatures while rewarding them for refractoriness. Also, the value found for Material 1CP probably represents a rock-bottom lower limit for the ipdt in studies of thermally stable polymers.

Table 3

Miscellaneous Polymers

Sample	Polymer	Code	ipdt, °C	dpdt, °C
1CP	(poly)methyl methacrylate	"Plexiglas"	345	280
4CP	6-6 nylon	"Zytel" 101	420	360
11CP	nylon-phenolic	("CTL-91-LD")	405	100, 340
35	aconitic acid + acetic anhyd.	88,8/58	355	70, 255
24	$[N = P(NCS)_2]_x^?$	(Audrieth)	390	140, 845

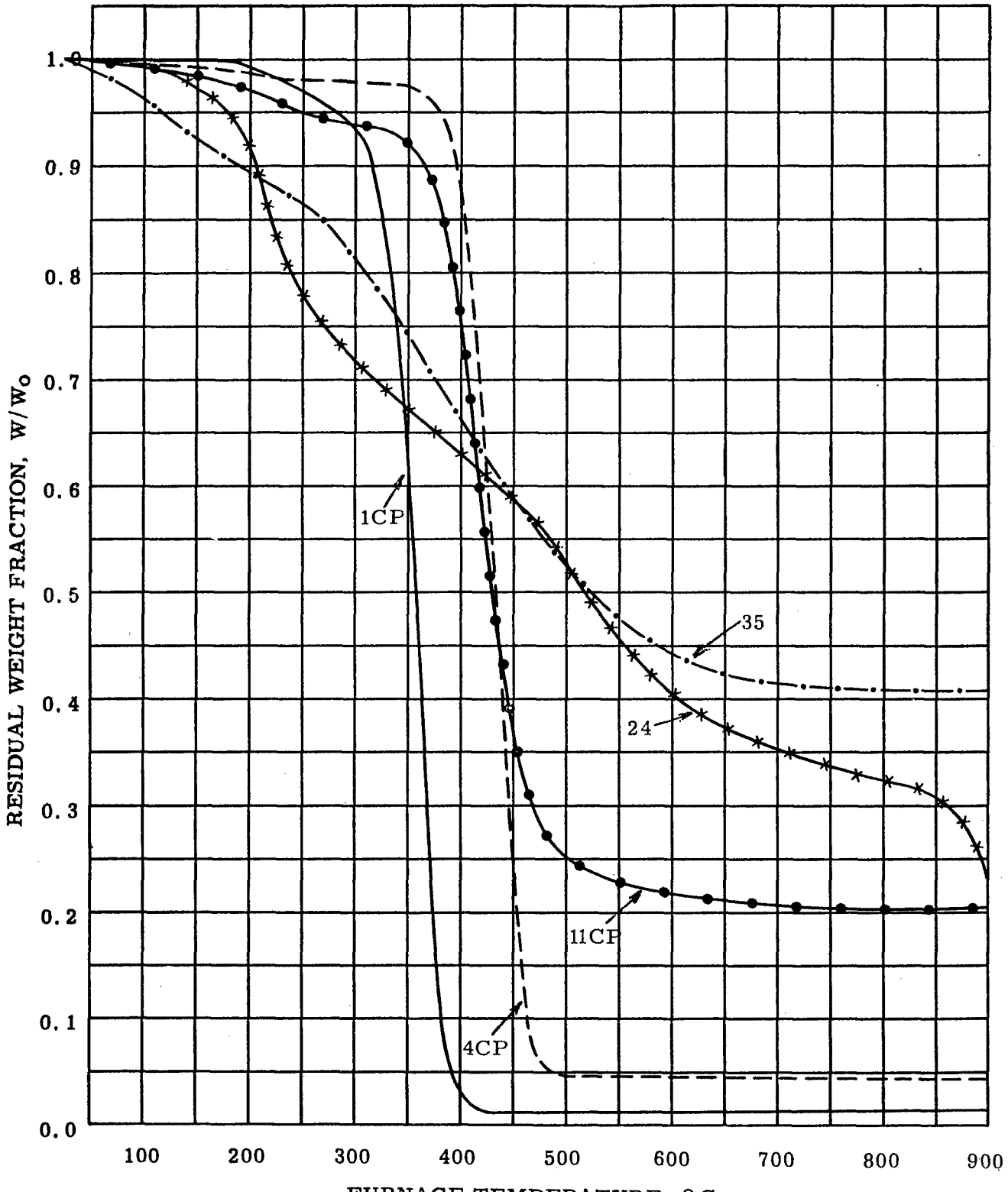

Figure 10 TGA IN DRY N_2 AT 180 C° PER HOUR

MISCELLANEOUS POLYMERS

D. Triazine Ring and Isocyanate Polymers

The data in Table 4 and Figure 11 again illustrate the stabilizing effect of cross-linking. It would appear also that the triazine ring structure and the benzenoid structure are about equally stable; as will be seen in the following Subsection IIIE, the residual stability of Material 10 at about 500 C is probably due to this polymer's fluorocarbon character, rather than to its triazine ring structure.

Table 4

Triazine Ring and Isocyanate Polymers

Sample	Polymers	Code	ipdt, °C	dpdt, °C
37	$(PhNCO)_3$	94/43 and 94/51, 10/58	335	285
38	toluene 2,4 diisocyanate polymer	94/25 and 94/32, 9/58	410	65,330
46	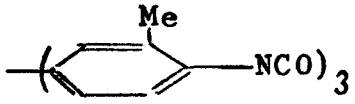	GE 150/50	360	225
47	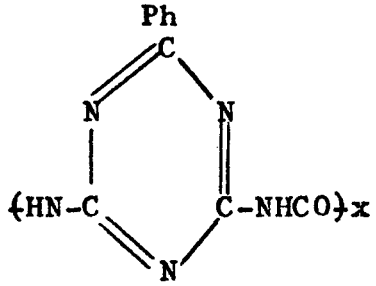	7HH30B	445	320
10	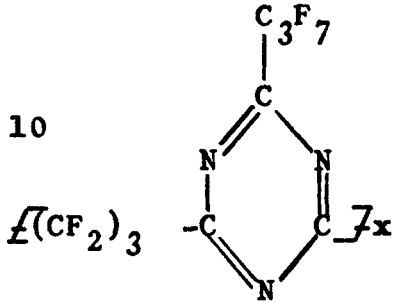	282	400	155

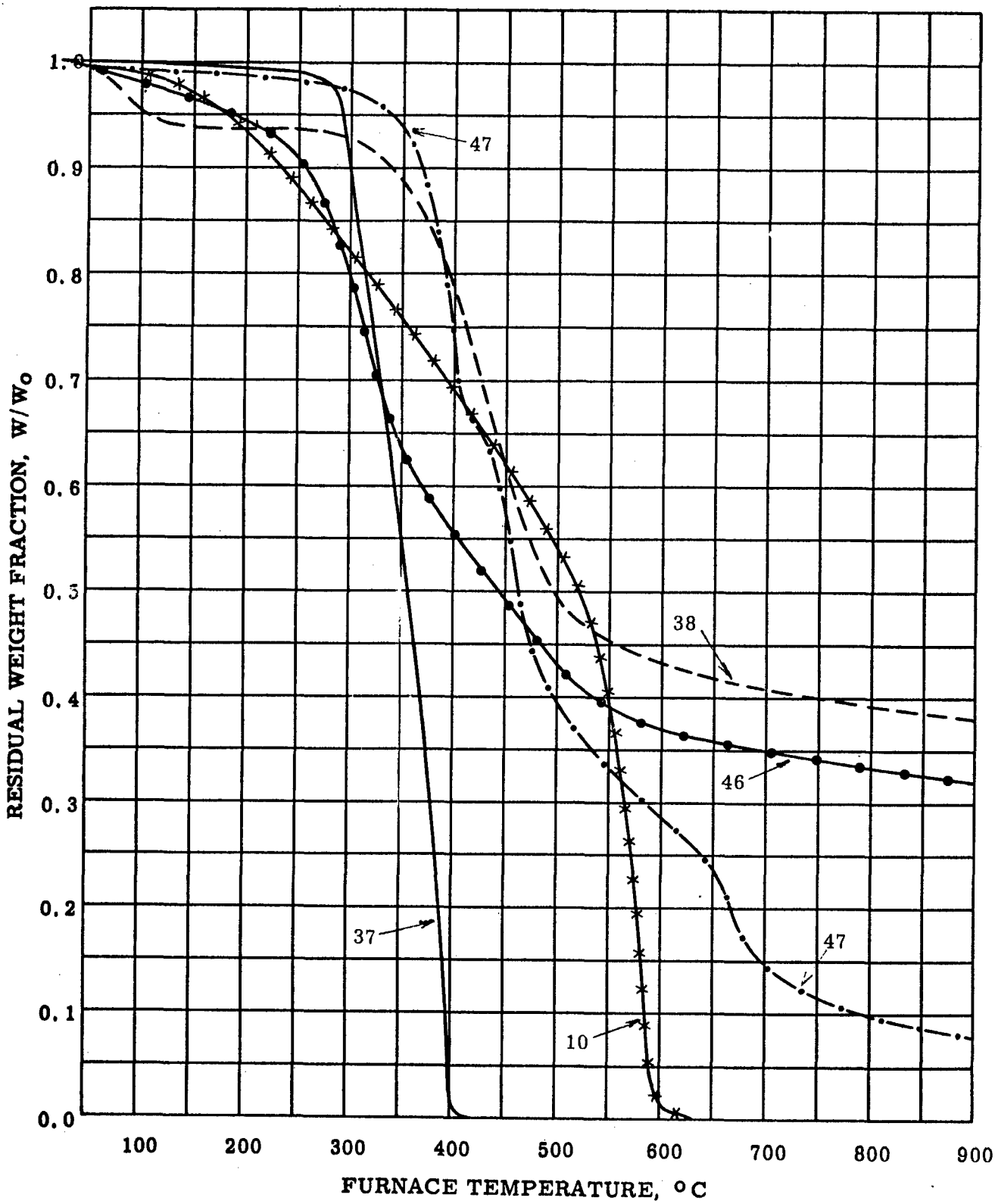

Figure 11 TGA IN DRY N_2 AT 180 C° PER HOUR

TRIAZINE RING AND ISOCYANATE POLYMERS

E. Polymers Containing Fluorine

The data in Table 5 and Figure 12 for three commercial fluorocarbon polymers and one experimental one illustrate the great sacrifice of intrinsic thermal stability resulting from the substitution of other atoms for some of the F-atoms on the carbon chain. Material 7CP, for example, is little better than some of the more stable hydrocarbons. Experimental difficulty was encountered in the TGA of Material 8CP, whose decomposition products extensively attacked the porcelain crucible normally used. The curve in Figure 12 represents an analysis conducted in a Pt crucible.

Table 5

Polymers Containing Fluorine

Sample	Polymer	Code	ipdt, °C	dpdt, °C
10	(cf Table 4)	282	400	155
6CP	polytetrafluoro-ethylene	"Teflon"	555	490
7CP	polychlorotrifluoro-ethylene	"Kel-f"	410	355
8CP	polyfluoropropylene-vinylidene fluoride copolymer	"Viton A"	450	405

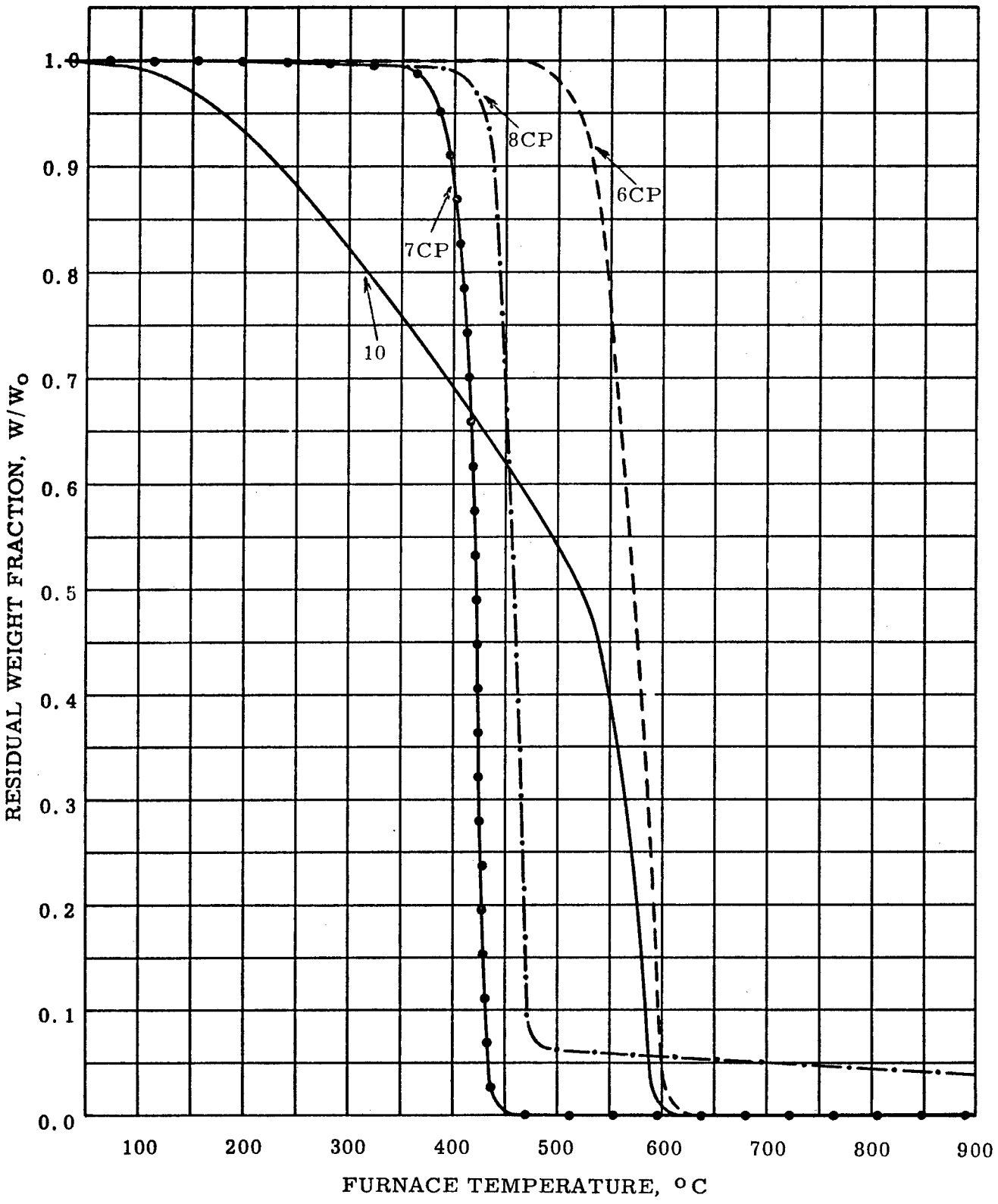

Figure 12 TGA IN DRY N_2 AT 180°C PER HOUR

POLYMERS CONTAINING FLUORINE

F. Polymers Containing Silicon

The data in Table 6 and Figure 13 for six silicon-containing polymers illustrate several interesting points. The beneficial effect of thorough curing is shown explicitly in the case of Material 2CP, and implicitly in those of Materials 20 and 21. The comparatively modest stability of Materials 18 and 19 can be attributed to the fact that these polymers are difunctional and remain so until degenerative cross-linking occurs. Clear evidence of degenerative cross-linking is given in the case of Material 18, whose curve displays a knee near 550 C in common with siloxanes of higher functionality.

Table 6

Polymers Containing Silicon

Sample	Polymer	Code	ipdt, °C	dpdt, °C
2CP	silicone resin	"SR 32"		
-1	uncured		475	465
-2	short cure		505	455
-3	long cure		505	450
20	precondensate of monomethylated $Cl_3SiC_6H_4SiPhCl_2$ with 80 mole% of $PhSiCl_3$			
	long cure	501-3-2	565	510
21	precondensate of 4,4'-bis-methyl-diethoxysilyl-diphenyl ether			
	long cure	B501-3-3	560	480
36	$\left[Si(-1,4-C_6H_4-)2-\right]x$?	113,10/58	360	160
18	$(Ph_2SiO)_{3.4}(Me_2SnO)_1$	62115A	420	275,560
19	$(Ph_2SiO)_{10}(Ph_2SnO)_1$	N68314B	435	315

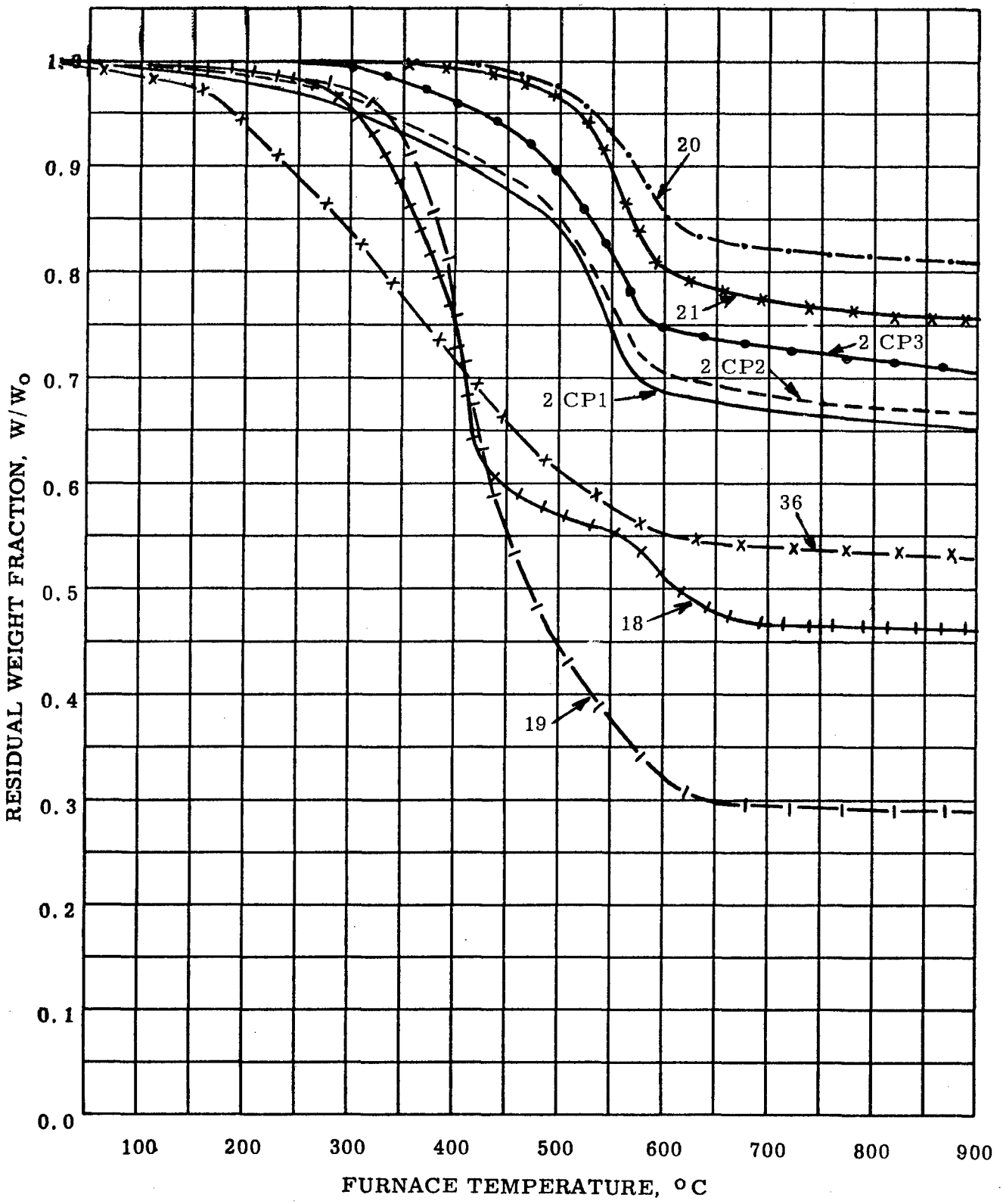

Figure 13 TGA IN DRY N_2 AT 180 C° PER HOUR
POLYMERS CONTAINING SILICON

G. Decaborane Adducts and Related Polymers

The data in Table 7 and Figure 14 for four decaborane adducts and one probable decaborane adduct provide excellent examples of the type of TGA curve which defied quantitative interpretation until the advent of the ipdt. Comparison of the curves for Materials 1, 3, and 4 shows how the ipdt succeeds in penalizing early volatilizers in proportion to their refractoriness in TGA. The true-rate dpdt, on the other hand, is unavailable, except in the case of Material 1, and the fixed-rate dpdt's given in Table 7 are both highly imprecise and highly inequitable as indices of thermal stability.

Table 7

Decaborane Adducts and Related Polymers

Sample	Polymer	Code	ipdt, °C	dpdt, °C
1	$\left[OCN(CH_2)_6NCO\right]B_{10}H_{14}$	L-197-40	355	50,280
3	$\left[H_2N(CH_2)_2NH\right]_2B_{10}H_{12}$	L-176-59	295	80
4	$\left[HN(CH_2)_2NHCH_2CH_2\right]_2B_{10}H_{14}$	L-176-63	355	80,510
9	Resin of $Me_2N + Me_2P + B + H$	(Burg)	450	485
33	$\left[(Me_2P)_4B_{10}H_9\right]x$	(Burg)	420	460

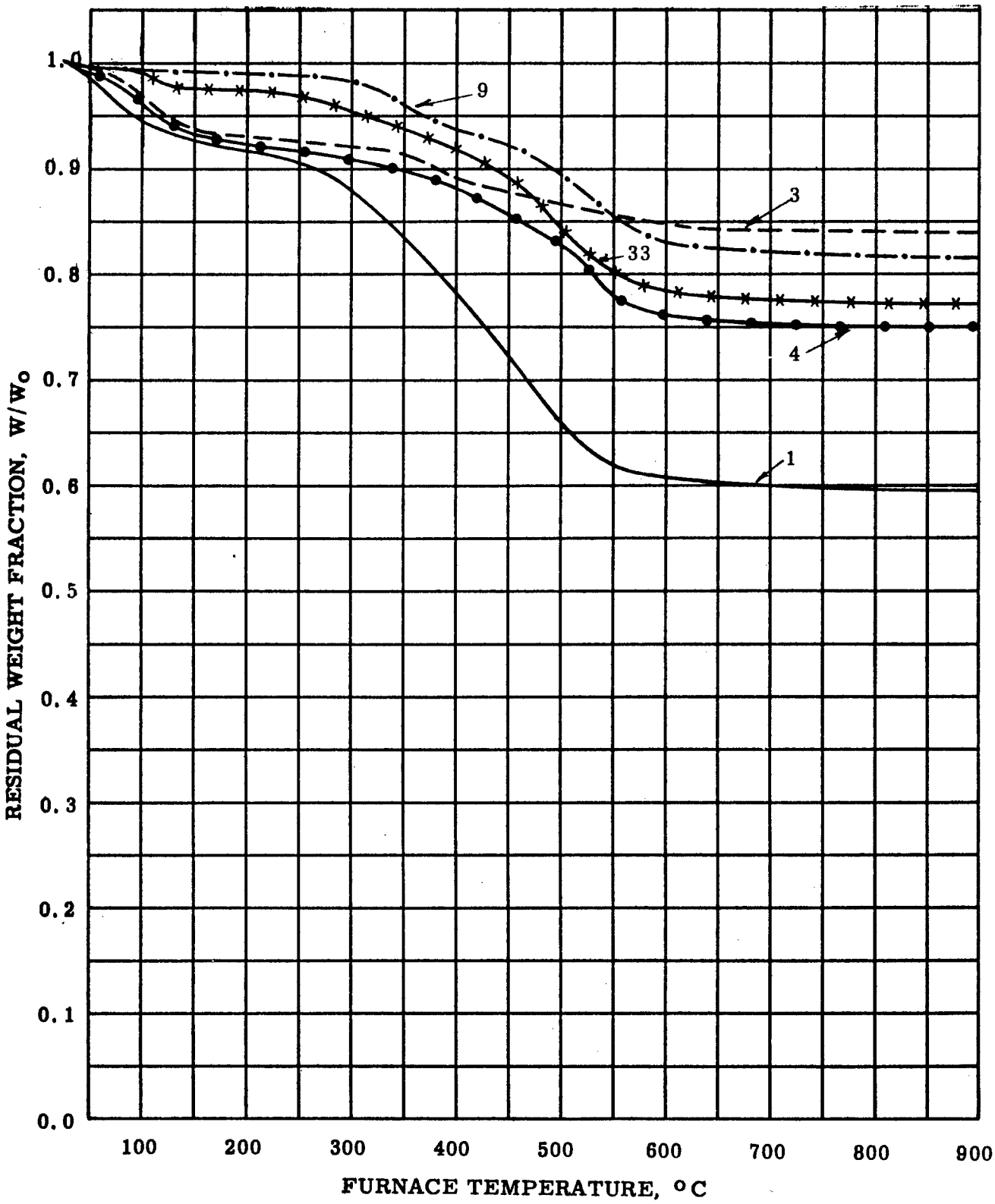

Figure 14 TGA IN DRY N_2 AT 180 C° PER HOUR

DECABORANE ADDUCTS AND RELATED POLYMERS

H. Phosphinoborine Polymers

The data in Table 8 and Figure 15 for five phosphinoborine polymers again illustrate the increased refractoriness resulting from increased cross-linking. The general tendency of these polymers to begin decomposing appreciably at moderate temperatures does not inspire confidence in them as promising high-temperature materials.

Table 8

Phosphinoborine Polymers

Sample	Polymer	Code	ipdt, °C	dpdt, °C
5	$(Me_2PBH_2)_3$	57W-177	190	80
6	$(MeEtPBH_2)_3$	57W-179*	210	130
7	$(Me_2PBH_2)x(MePBH)y$	57W-19	320	110
8	$(Me_2PBH_2)x$ $\left[(CH_2)_3(MePBH_2)_2\right]y$	58W-20	340	130,275
34	$(MeEtPBH_2)x$	(Amer. Pot. and Chem. Co.)	295	200

*Liquid at room temperature.

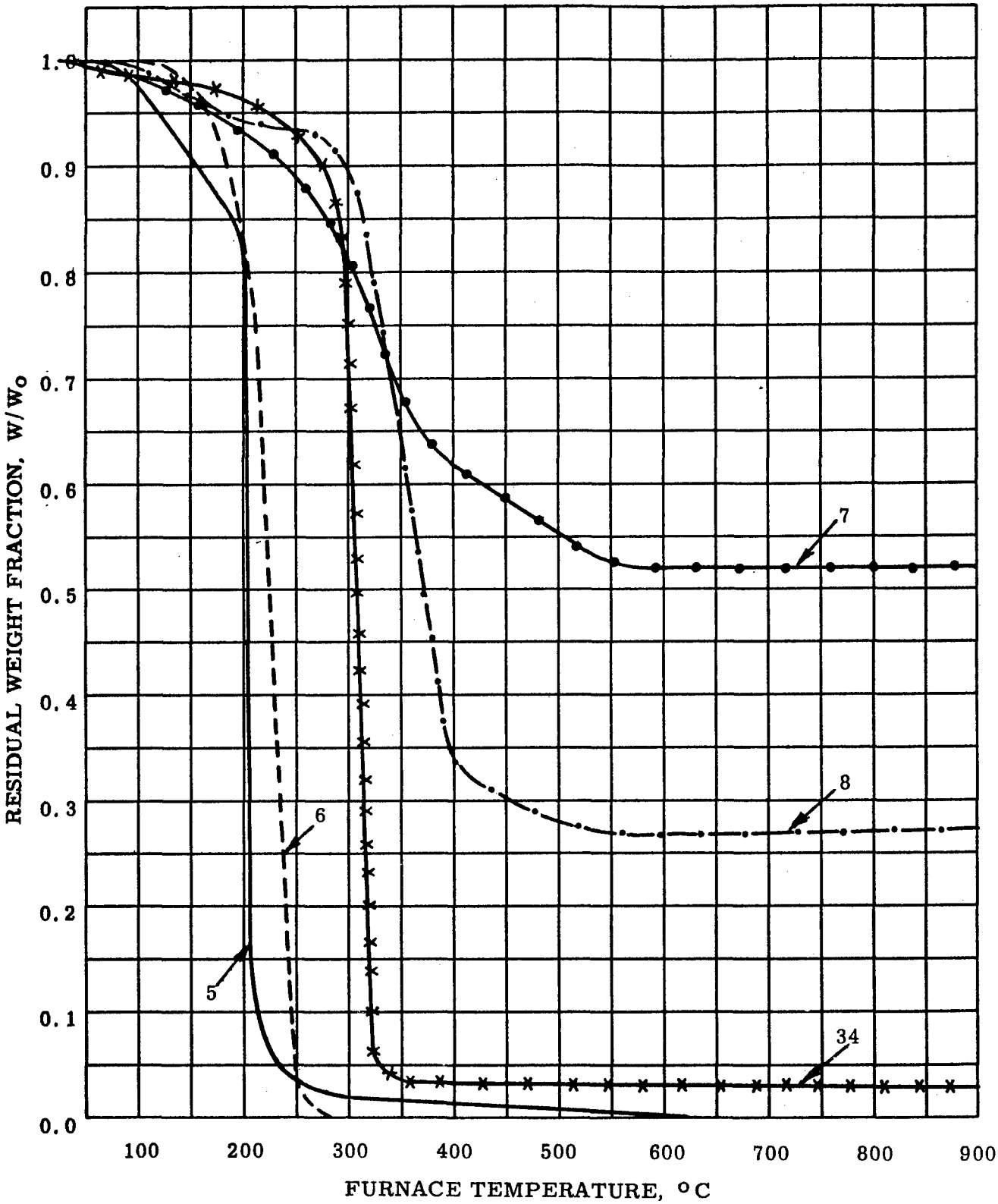

Figure 15 TGA IN DRY N_2 AT 180 C° PER HOUR

PHOSPHINOBORINE POLYMERS

I. Copper Phthalocyanine Polymers

The data in Table 9 and Figure 16 for three copper phthalocyanine polymers show that something was radically wrong with Material 15. Materials 22 and 23 display the order of thermal stability expected of copper phthalocyanine. During the TGA of Material 15, much busy brushing was necessitated by the condensation of copious quantities of fluffy, needle-like crystals of (probably) ortho-phthalic anhydride on moving parts of the balance.

Table 9

Copper Phthalocyanine Polymers

Sample	Polymer	Code	ipdt, °C	dpdt, °C
15	(polymer)	(Bailar)	425	285
22	(blue)	(Marshall)	640	585,715
23	(polymeric)	(Marvel)	540	590

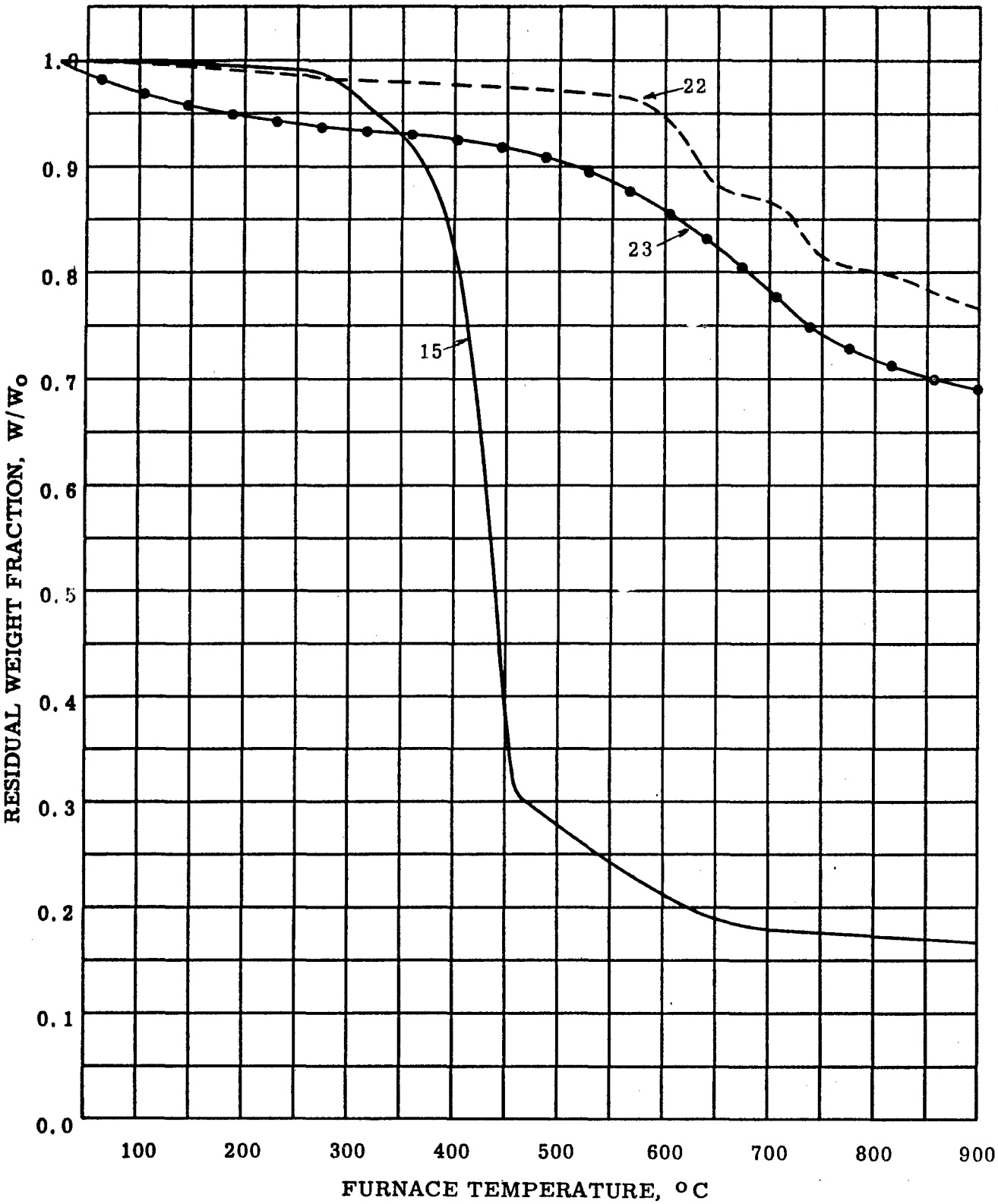

Figure 16 TGA IN DRY N_2 AT 180 C° PER HOUR
COPPER PHTHALOCYANINE POLYMERS

J. Zinc Chelate Polymers

The data in Table 10 and Figure 17 for four zinc chelate polymers clearly illustrate the difficulties and frustrations which attend attempts to compare the thermal stabilities of similar materials. In terms of major knee temperatures, for example, the material numbers can be ranked: 11>13>12>14. In terms of ultimate residual weight fractions, however, the order is: 14>11>12>13. In terms of the ipdt, which takes both of these oppositely directed indices of quality into account, the order is: 11>12>13>14. The ipdt also includes the effects of small dips in the TGA curve, like the one near 150 C in the pattern for Material 14. X-ray analysis has shown that this minor dip represents decomposition with the formation of cubic βZnS, a reaction not found in Material 11 in the same temperature range.

Table 10

Zinc Chelate Polymers*

Sample	Polymer	Code	ipdt, °C	dpdt, °C
11	R_2	(Bailar)	500	435
12	R_2O	(Bailar)	465	415
13	R_2SO_2	(Bailar)	455	425
14	R_2CO	(Bailar)	435	180,380

*Zinc 4,4'-bis-thiopicolinamido: -diphenyl,-diphenyl ether, -diphenyl sulfone and -dibenzophenone

"R" is:

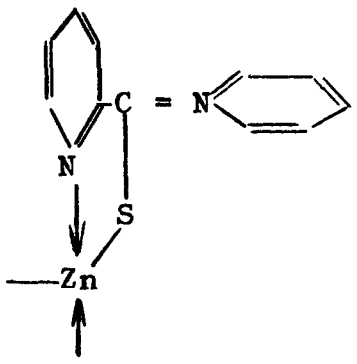

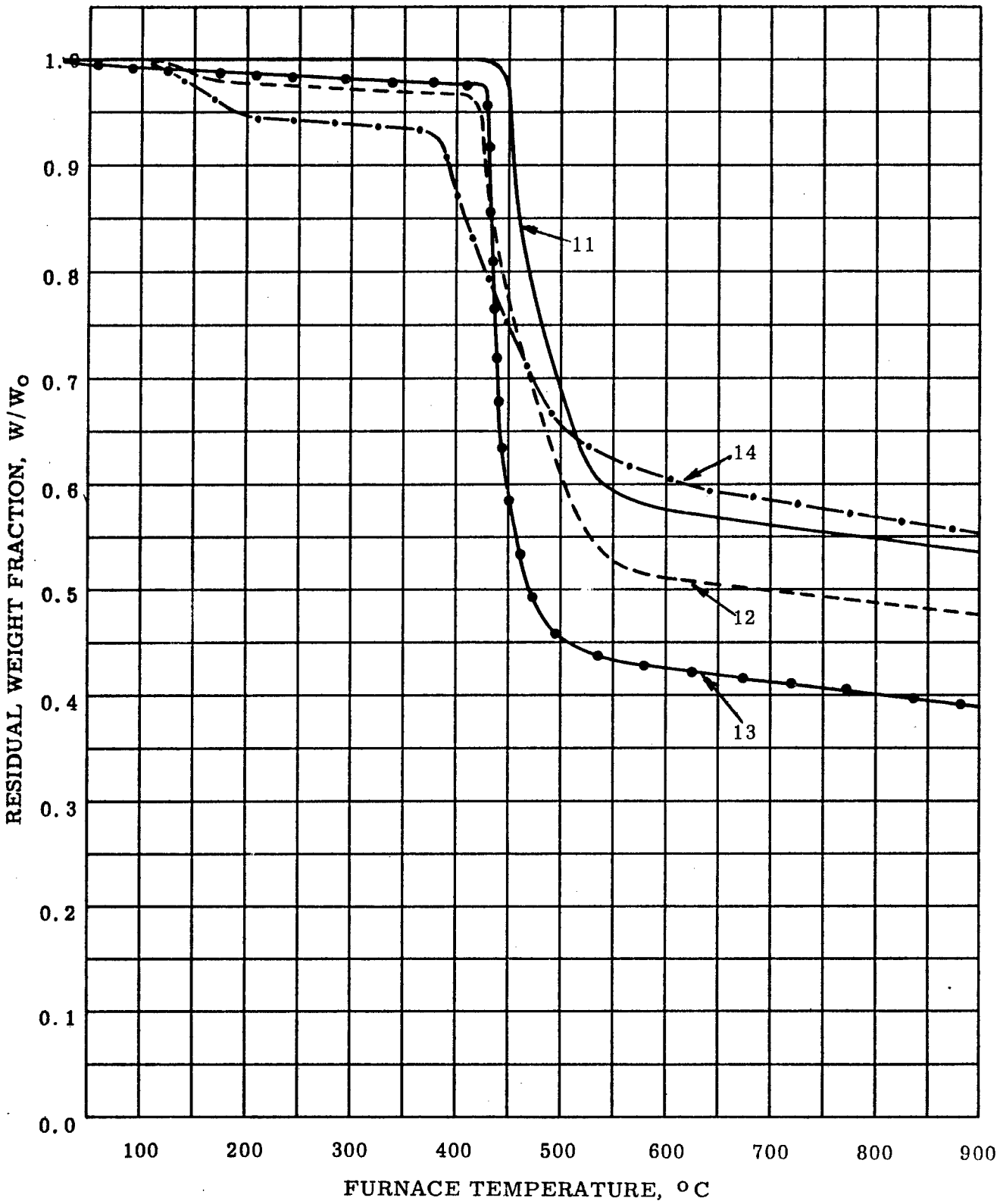

Figure 17 TGA IN DRY N_2 AT 180 C° PER HOUR
ZINC CHELATE POLYMERS

K. Beryllium Chelate Polymers

The data in Table 11 and Figure 18 for seven beryllium chelate polymers again attest to the difficulty of comparing without the help of the ipdt, similar materials whose differences in TGA take opposite directions.

Table 11

Beryllium Chelate Polymers

Sample	Polymer	Code	ipdt, °C	dpdt, °C
--	$Be(CHAc_2)_2$ with:	(Fernelius)		
31	$[(PhCO)_2\underline{CH}]_2$		290	25,80,230
26	$[(PhCO)_2\underline{CH}]_2CH_2$		420	255
28	$(Ac_2CH)_2CH_2$		370	215
27	$[(PhCO)Ac\underline{CH}]_2CHPh$		395	235
29	$1,4\text{-}C_6H_4(CH_2CHAc_2)_2$		385	215
	Be^{++} salt with:	(Fernelius)		
30	$(PhCOCH_2CO)_2$		375	65,170,420
32	$1,4\text{-}C_6H_4(MeCOCH_2CO)_2$		425	25,370

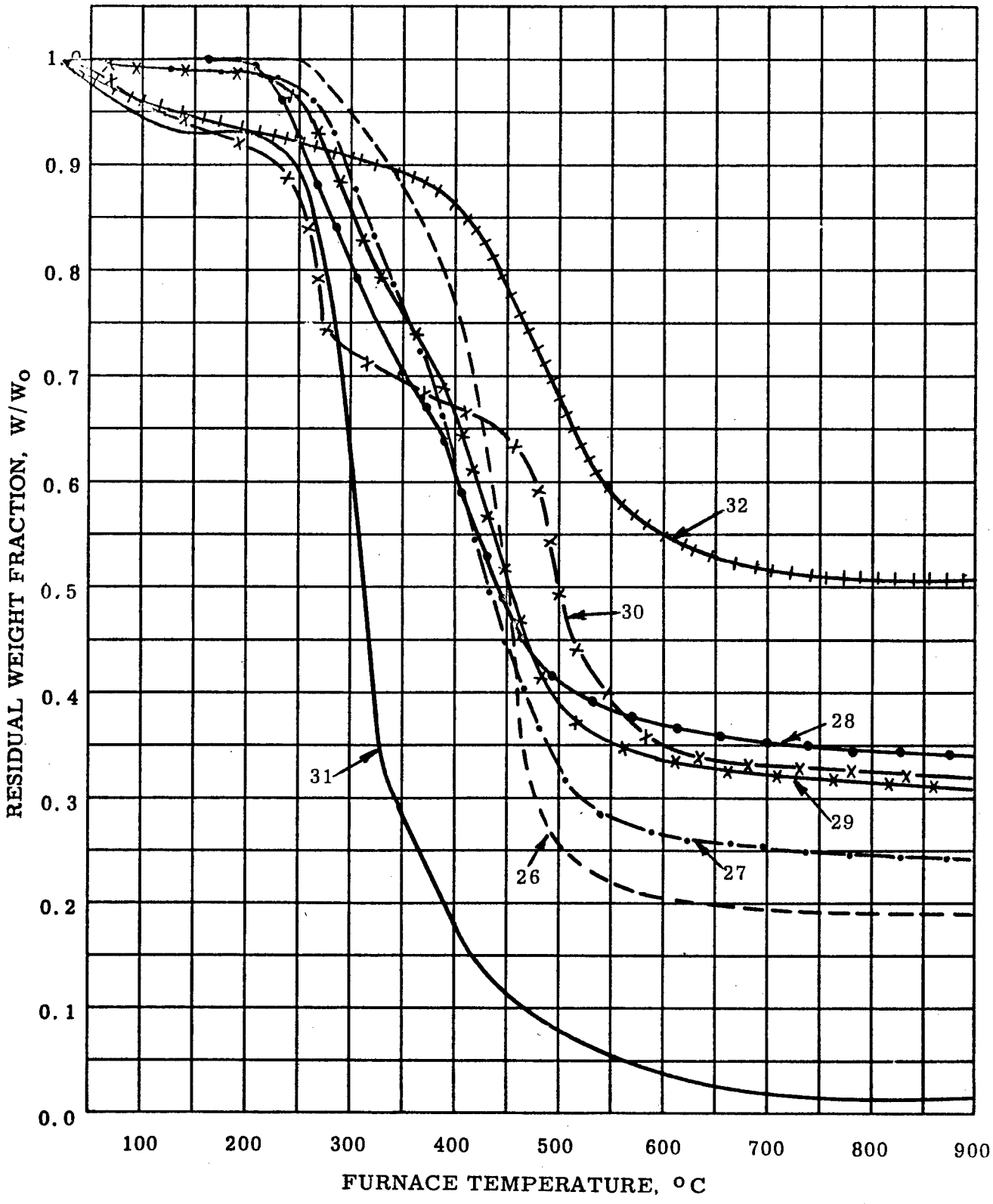

Figure 18 TGA IN DRY N_2 AT 180 C° PER HOUR
BERYLLIUM CHELATE POLYMERS

IV. KINETIC ANALYSIS OF TGA CURVES

It was noted in Section II of this report that only an empirical rate constant, $\underline{k}$, is available from the data record for TGA in inert atmosphere and that the constancy of $\underline{k}$ is dubious. Consequently, the authenticity and constancy of the primary kinetic constants derived from values of $\underline{k}$ are also questionable. Thus, the simplified Arrhenius relationship between $\underline{k}$ and the absolute temperature, T, must be expressed in this report as:

$$\underline{k} \cong \underline{A} e^{-\frac{E}{RT}} \qquad (8)$$

where $\underline{A}$ is the empirical frequency factor, expressed here in reciprocal hours, $\underline{E}$ is the empirical activation energy in calories and R is the molar gas constant, 1.987 calories per degree Kelvin per mole.

In general, the authenticity of $\underline{A}$ as the frequency factor for decomposition is only as good as that of $\underline{k}$ as the specific reaction rate constant, so that values of $\underline{A}$ are almost certain to be trivially dependent on procedural conditions. Values of $\underline{E}$, on the other hand, are not always trivial; if the temperature-dependence of the trivial $\underline{k}$ and the authentic specific decomposition rate constant are the same, $\underline{E}$ is the authentic activation energy for the decomposition reaction. Until proven otherwise by corroborative studies, however, $\underline{E}$ must be regarded as unauthentic.

In view of the inherent unauthenticity of $\underline{A}$ and $\underline{E}$, the value of subjecting TGA data records to kinetic analysis might well be questioned. The answer, of course, is that the findings provide starting points for more significant investigations. In the chemical sense, the authenticity of $\underline{E}$ and sometimes of $\underline{A}$ can subsequently be confirmed or disproved by studies of reaction products and their yields and by studies of the effects of varying the geometry and degree of subdivision of the sample. In the practical sense, only the latter study may be required, together with investigations conducted under expected environmental conditions.

Two methods will be given for determining $\underline{A}$ and $\underline{E}$ from the data record for TGA in inert atmosphere. In the first of these, the Arrhenius rate equation will be applied, and advantage will be taken of the fact that the findings can be directly compared with those from similar isothermal aging tests. In the second method, the Arrhenius integral will be applied as the equation of the TGA curve. Since the object here is merely to illustrate the analytical techniques, single data records will be used in all cases, it being taken as self evident that convincing

estimates of A and E are attainable only by appropriately intensive replication.

A. The Arrhenius Rate Equation

In Subsection II A1 of this report, it was noted that the empirical rate constant, k, can be found at a given temperature from the corresponding apparent volatilization rate, provided the true residual weight fraction, h, and the rate function appropriate to the kinetic process, f(h), are known. It was noted further that insofar as the comparison of materials is concerned, the need to evaluate the elusive f(h) can be circumvented by considering only those small rates which correspond to values of h near unity, in which case all forms of f(h) also approach unity.

This same simplification can sometimes be applied in the kinetic analysis of TGA data records and isothermal aging curves. As illustrated in Figure 19, aging curves of h vs time corresponding to the simpler rate processes do not differ greatly until the true residual weight fraction has decreased to about 0.95. This is less true of rate processes of transcendental order or of fractional order less than one, in which cases the linear range of h may be so short that the need to evaluate f(h) cannot be avoided. In many simpler cases, however, the quasi-linear range of h is sufficiently long to permit the direct use of initial true volatilization rates from isothermal aging and small true volatilization rates from the TGA curve as reasonably accurate estimates of the corresponding values of k.

Because this is true of the volatilization of polytetrafluoroethylene, this polymer was selected for preliminary study. Of additional interest is the fact that the work of other investigators suggests that over quite a broad temperature range, the temperature-dependence of the empirical rate constant for minute samples of polytetrafluoroethylene in vacuo is the same as that for the specific rate constant for decomposition of the polymer predominantly to monomer (2). From the ensuing comparison of small volatilization rates from TGA with initial rates from isothermal aging, however, it will be seen that the range of values of k having authentic temperature-dependence is quite limited in the case of the TGA of 200 mg samples of pulverized polytetrafluoroethylene in dry N_2.

1. Isothermal Aging Tests on Polytetrafluoroethylene. In theory, sample-to-sample error can be eliminated from isothermal aging data by subjecting a single sample to stepwise aging in the thermobalance, as shown in Figure 20. In practice, however, such tests usually run afoul of the limitations imposed by normal working hours. Further, fallacious initial volatilization rates arising from the loss of impurities may operate for considerable periods of time at the lower aging temperatures, so

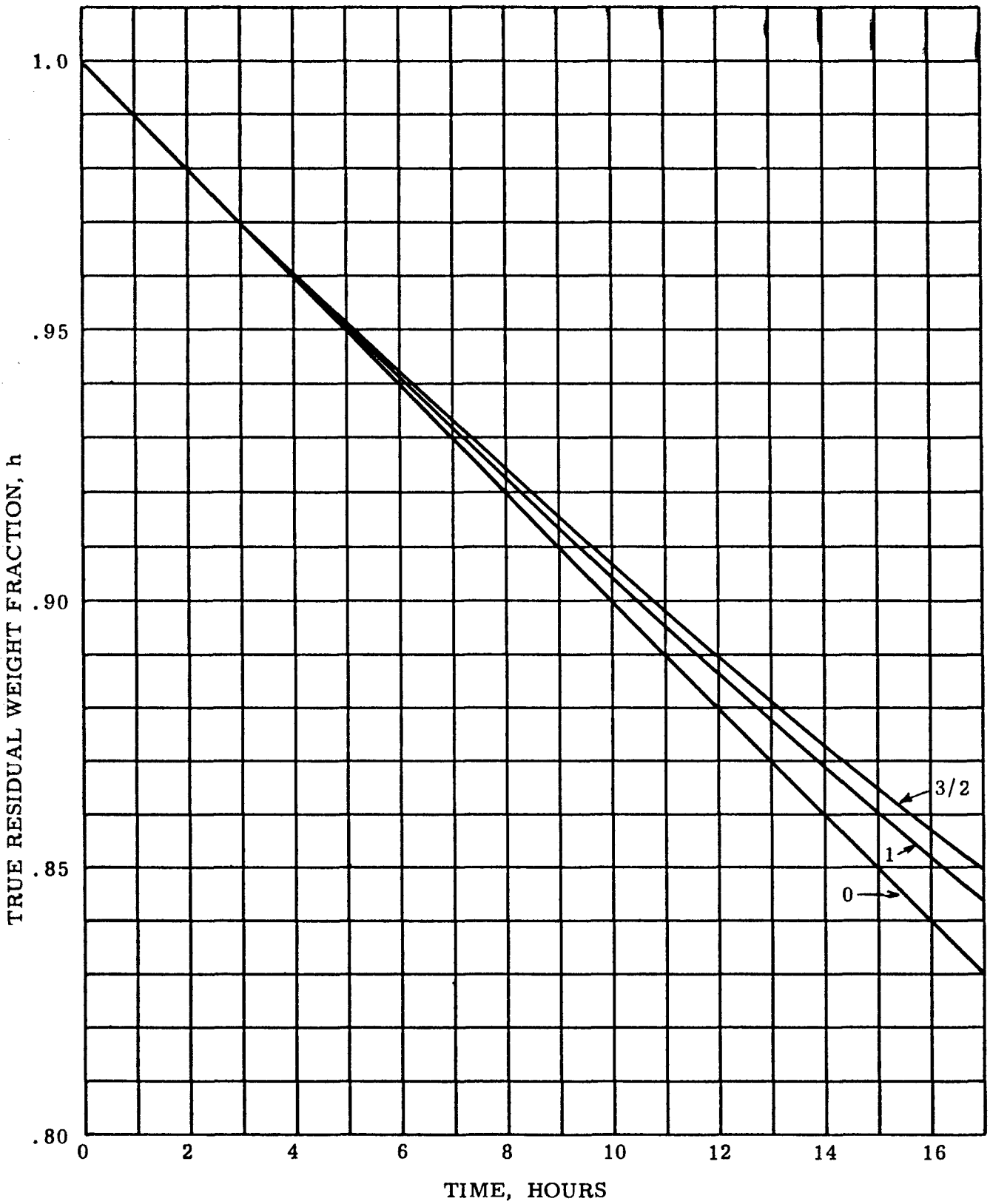

Figure 19 ARTIFICIAL WEIGHT LOSS CURVES FOR 0-, 1- AND 3/2-ORDER RATE PROCESSES HAVING THE SAME SPECIFIC RATE CONSTANT 0.01 PER HOUR

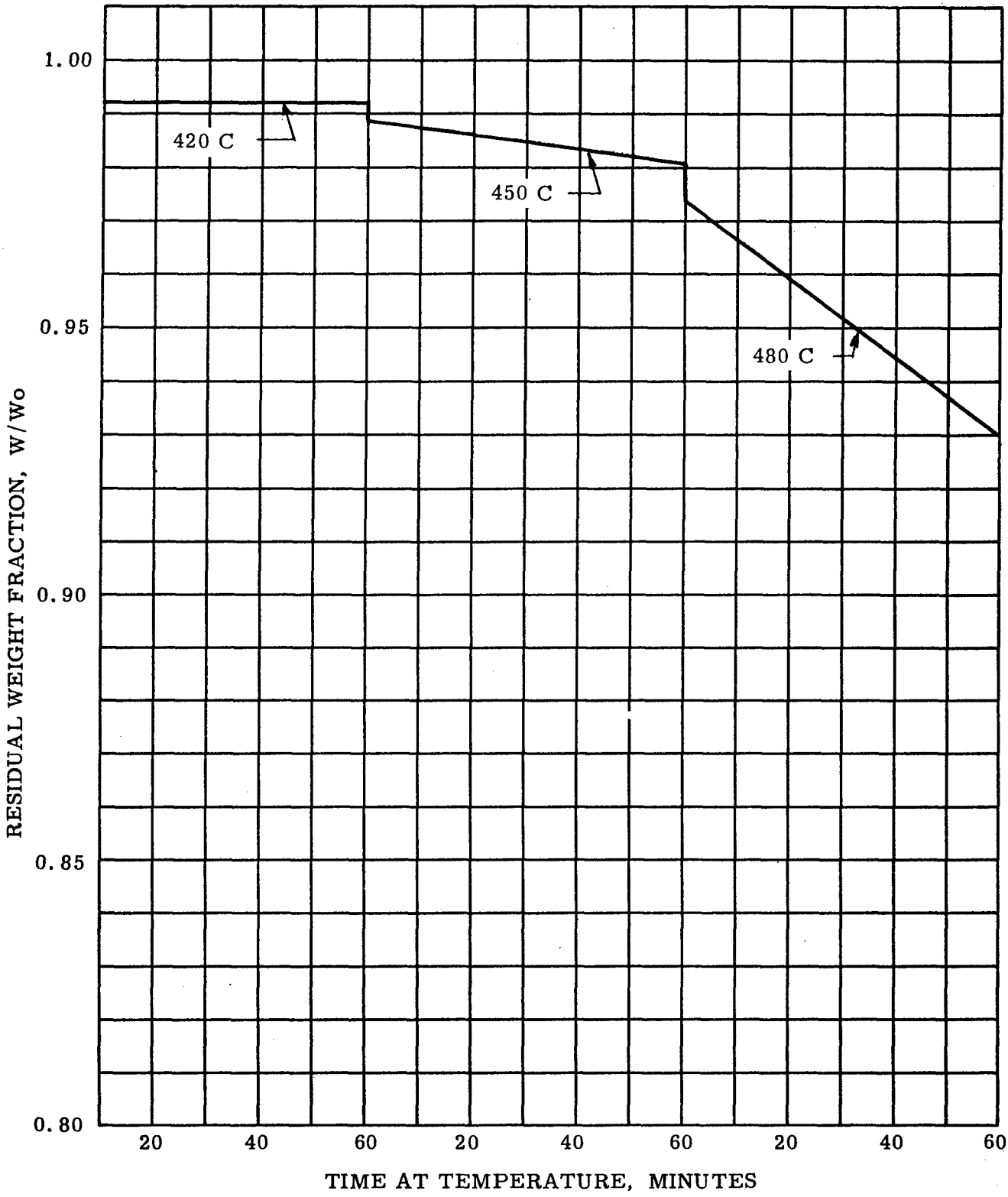

Figure 20 STEPWISE TGA IN DRY N_2, POLYTETRAFLUOROETHYLENE

that the experimenter cannot be sure when it is advisable to proceed to the next higher aging temperature. Most importantly, however, volatilization rates found at the higher temperature steps are progressively less amenable to treatment by the method of initial rates. Therefore, the isothermal aging tests were conducted by heating separate 200 mg samples at 180 C degrees per hour to each of the aging temperatures, which were then maintained within $\neq 0.5^{\circ}$ C for 24 hours or to complete volatilization.

The resulting plots of residual weight fraction vs time for a pulverized commercial "Teflon" gasketing material are shown in Figure 21. It should be noted that the curves in Figure 21 have been altered slightly for the sake of clarity. Otherwise, some of the curves would not have begun precisely at unit residual weight fraction, because the drift of the thermobalance varies from heat-up run to heat-up run and cannot be exactly compensated by reference to the average correction curve (1). This arbitrary concession to neatness has been made only in illustrative plots; in all other cases, actual values have been taken.

Since polytetrafluoroethylene volatilizes completely in TGA to about 610 C, the apparent volatilization rate is the true volatilization rate, so that the slopes of all aging curves in the range of residual weight fraction from 1.0 down to 0.95 can be taken as reasonable good estimates of the corresponding values of $\underline{k}$. It turns out, however, that the quasi-linear range is even more extensive than this in the present case, as shown by the rate plot in Figure 22.

There is room for controversy regarding the shapes of the rate curves in Figure 22. It must be admitted that the volatilization rates corresponding to the higher aging temperatures are so large that they cannot be read with good precision even with the help of a mirror and expanded plots of the steeper aging curves. The rate plot in Figure 22 does represent, however, a synthesis of smoothed rate plots prepared independently by two observers. Both found extensive ranges of zero-order volatilization at all aging temperatures, though studies conducted by other workers on minute samples of polytetrafluoroethylene volatilized in vacuo in the same temperature range led to first-order rate plots wherein the volatilization rate decreases linearly with residual weight fraction (2). In this connection, however, it is interesting to note that the 510 C data in Reference 2 can be represented quite faithfully by a curve like the corresponding one in Figure 22.

In any case, the apparently zero-order initial volatilization rates found in the present experiment lead to a linear Arrhenius plot at aging temperatures below 490 C, as shown in Figure 23. Further, the empirical activation energy, 80 K cal,

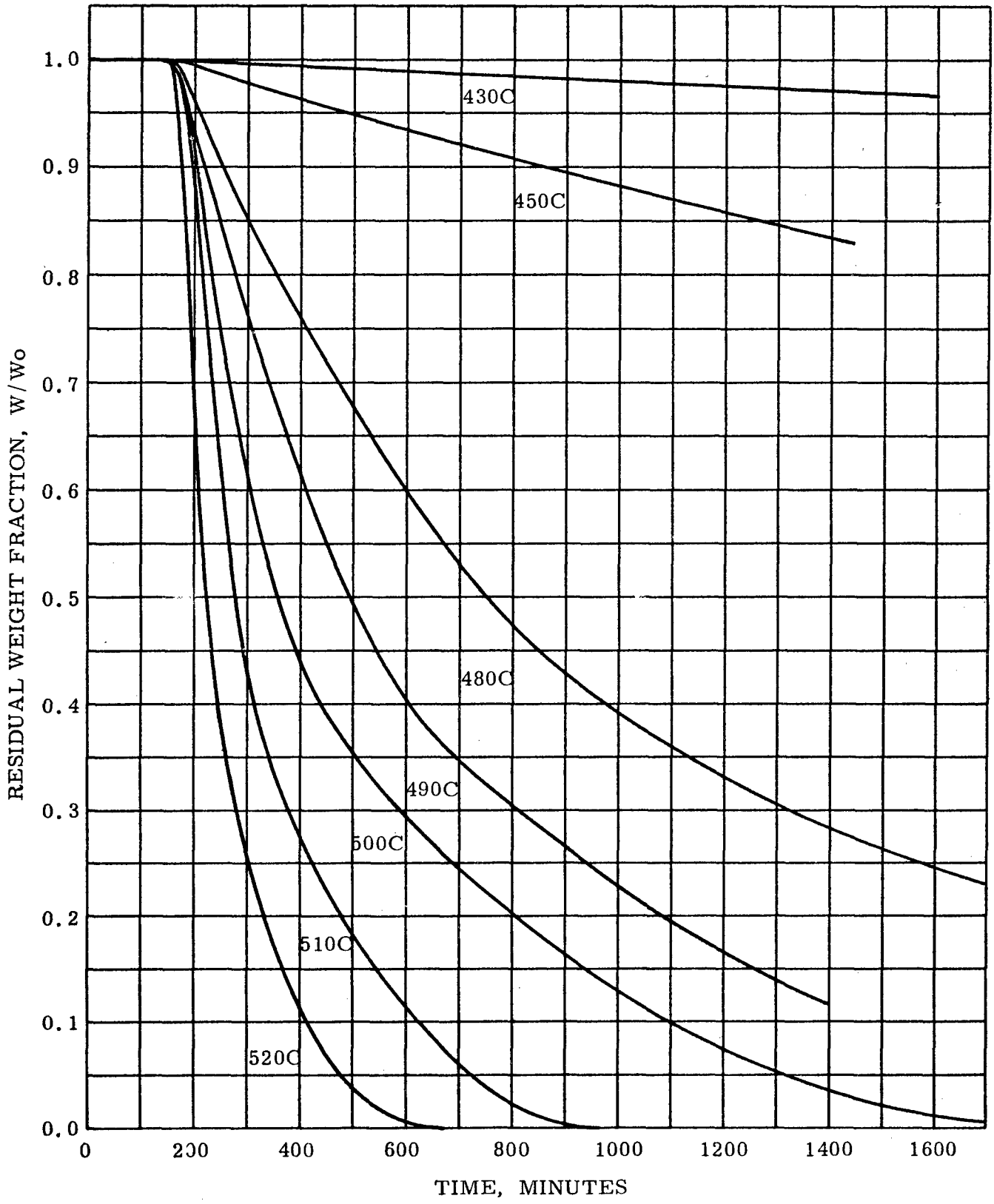

Figure 21 TGA IN DRY N_2 AT CONSTANT TEMPERATURE
POLYTETRAFLUOROETHYLENE

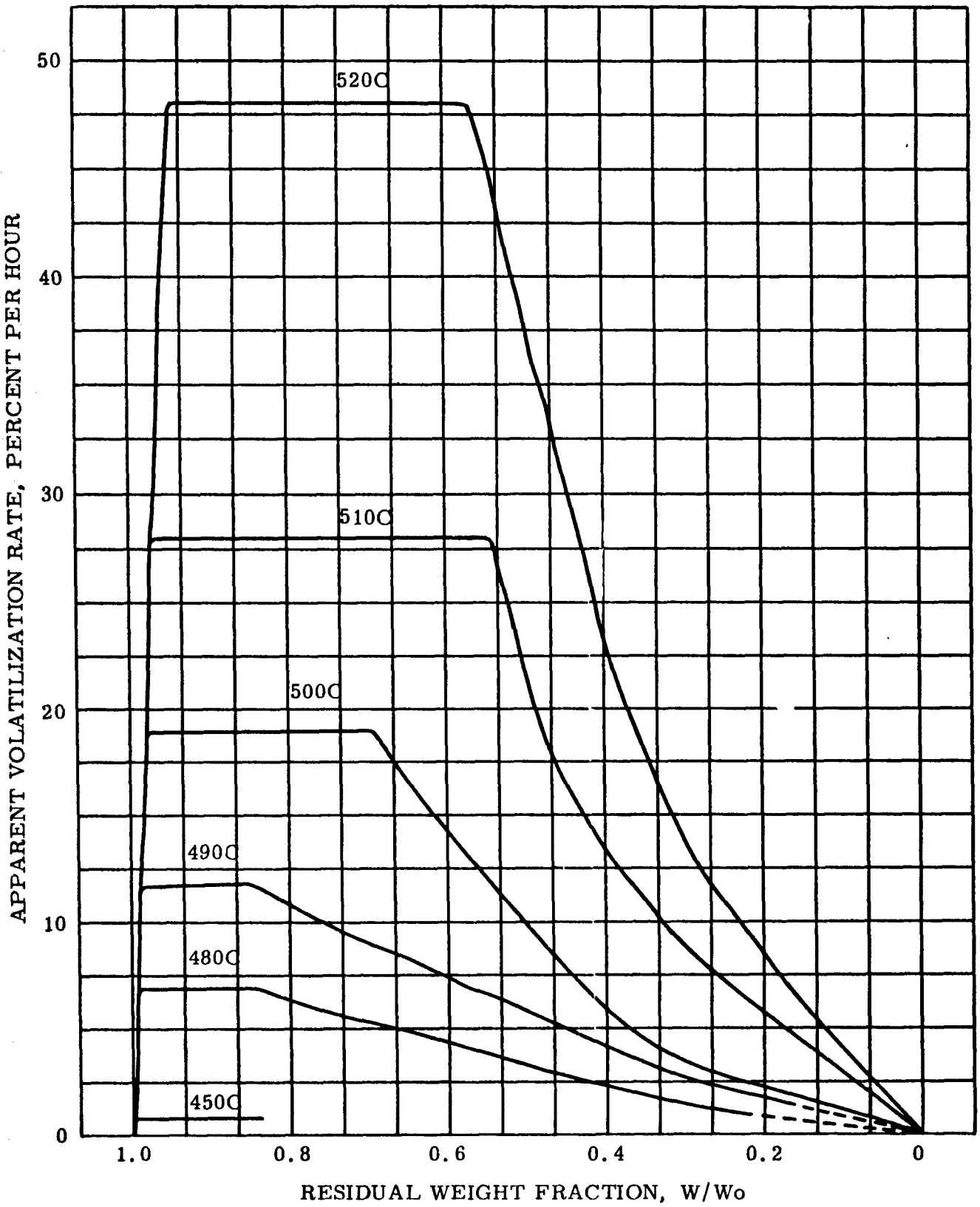

Figure 22 TGA IN DRY N_2 AT CONSTANT TEMPERATURE
APPARENT VOLATILIZATION RATES VS. RESIDUAL WEIGHT FRACTION,
POLYTETRAFLUOROETHYLENE

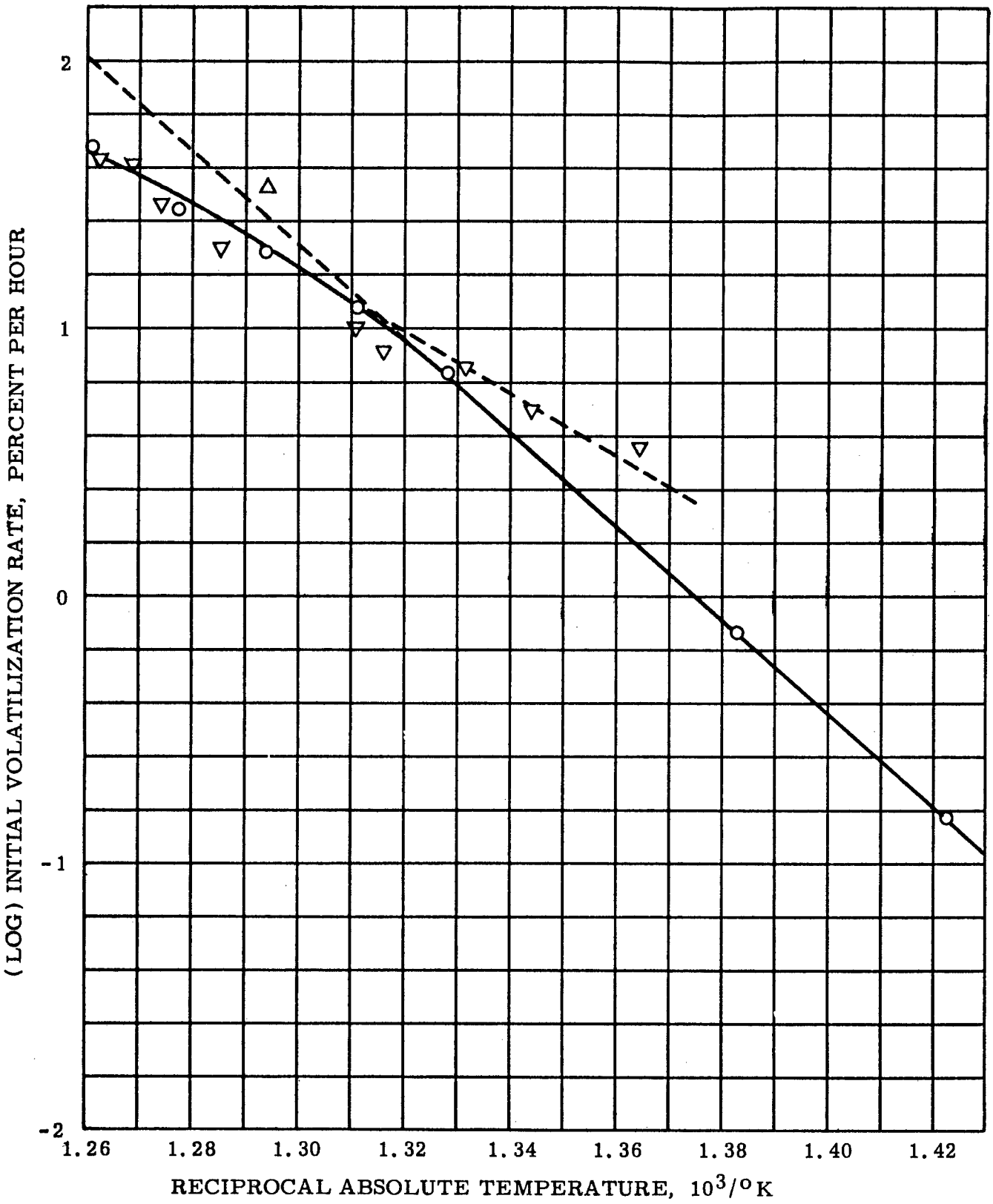

Figure 23 COMPARISON OF VOLATILIZATION RATES FROM THE MAGNIFIED THERMOGRAM "▽" WITH INITIAL VOLATILIZATION RATES FROM ISOTHERMAL AGING OF POLYTETRAFLUOROETHYLENE IN DRY N_2, "o" AND IN VACUO "△"

corresponding to the slope of the linear part of Figure 23 is in excellent agreement with published values for the decomposition of polytetrafluoroethylene to monomer. Surprisingly, even the values of k found at temperatures below 490 C lie only slightly below those found for minute samples volatilized in vacuo, as shown in Figure 23 by an extrapolation of the single rate datum given in Reference 2.

At temperatures above 490 C, however, the value of E found for polytetrafluoroethylene in the present experiment begins to diminish in marked disagreement with Reference 2, as would be expected from the disagreement between Figure 22 and its counterpart in Reference 2. Presumably, the curvature in Figure 23 does not reflect any change in the basic decomposition mechanism of the polymer at the higher aging temperatures since the yield of monomer remains large up to 510 C (2). Further, Figure 22 shows that initial volatilization rates measured at temperatures up to 520 C are reasonably accurate estimates of values of k. Apparently, then, the rate of escape of monomer after it has formed assumes increasing importance at aging temperatures above 490 C, so that initial volatilization rates no longer provide an uncomplicated measure of the corresponding decomposition rate constants under the procedural conditions of the present study. As will next be shown, this is also true of rates read from the TGA curve.

The isothermal volatilization rate data used in plotting Figure 23 are given for reference in Table 12.

Table 12

Initial Volatilization Rates for 200 mg Samples of Pulverized "Teflon" Aged in Dry N_2

Aging Temperature, °C	Initial Volatilization Rate, %/hr
400	(very small)
430	0.15
450	0.74
480	6.80
490	11.7
500	19.0
510	28.0
520	48.0

2. TGA of Polytetrafluoroethylene. In comparing the kinetics of static aging and TGA, the uncertainty of reading apparent volatilization rates from the TGA data record can be reduced considerably by using expanded plots of the knee region. Even so, imprecision remains a serious problem, as can be seen

from the data scatter in Figure 23. Also illustrated in Figure 23, though, is a far more serious limitation on the usefulness of TGA rate data, one which no amount of replication can remove since the problem is one of inherent inaccuracy rather than mere imprecision. Inherent inaccuracy is seen in Figure 23 in the range of volatilization rates smaller than about 8% per hour. Larger TGA rates lie near those found from isothermal aging because the same heating rate was employed in both cases and because this common heating rate was slow enough to maintain the sample near equilibrium during heat-up. Rates smaller than 8% per hour, on the other hand, tend toward a false limiting value.

This inherent inaccuracy of TGA at small rates of volatilization does not arise from such sources of imprecision as the volatilization of impurities or errors in computing thermobalance drift; it occurs because the total amount of volatilization arising from the infinite logarithmic range of small rates is eventually compressed into the width of the chart line in TGA. In isothermal tests, on the other hand, the sample can be held at low temperatures long enough for sensible volatilization to occur.

It is this unavoidable inaccuracy of TGA in the small rate range which, as was noted in Subsection II A1 of this report, imposes a lower limit on the prescription of end point rates for comparing materials. For the same reason, TGA is of no value in determining the long-time aging characteristics of materials.

Insofar as the kinetic analysis of TGA curves is concerned, the small-rate inaccuracy of TGA abbreviates the range of useful empirical rate constants, often with dismaying results: at best, it may be impossible to estimate an authentic value of $\underline{E}$; at worst, $\underline{E}$ may not be constant in the range of accurate empirical rate constants. From Figure 23, it is seen that both disasters have occurred in the present case wherein the range of inaccurate initial rates blends smoothly into the range of non-linear initial rates.

While the linear range of empirical rate constants could probably be extended by decreasing the initial weight of the sample, the resulting increase in the imprecision of TGA would be prohibitively large, especially for materials which volatilize only to a small extent. For this reason, means were sought for circumventing the need to deal with a broad range of volatilization rates. One way to do so is to integrate the Arrhenius rate equation, although the point in executing this maneuver might well be questioned on the grounds that the resulting relationship can be no more extrapolatable than the rate equation from which it was derived, nor can its empirical constants be any more authentic.

It might be argued that such skepticism is not entirely justifiable, since the Arrhenius integral is the general equation of the TGA curve. It turns out, though, that the form of the Arrhenius integral is such that an infinite number of combinations

of values of $\underline{A}$ and $\underline{E}$ fit the data curve well enough to require seeking the combination which affords the best fit. This approach, however, is thwarted by the concomitant need to take into account the effects of changing sample geometry and degree of subdivision, as well as the appropriate kinetic process for every part of the TGA curve, which information is unavailable from empirical rate constant data.

Thus, values of $\underline{E}$ can be estimated uniquely only from values of $\underline{A}$ which can be estimated uniquely. This, in turn, is possible only for the range of empirical rate constants which can be estimated with either sufficient accuracy or sufficient precision. In this sense then, the net result of integration is the substitution of a cumbersome equation for a simple one. All this will next be illustrated by deriving the Arrhenius integral and applying it to the TGA curve for polytetrafluoroethylene.

B. The Arrhenius Integral

From Equations 1 and 6 of Subsection II A1 of this report, Equation 8 can be written:

$$-\frac{dh}{dT} \cong \frac{\underline{A} f(h) e^{-\frac{\underline{E}}{RT}}}{B} \qquad (9)$$

The equation of the TGA curve is obtained by integrating Equation 9, treating $\underline{A}$ and $\underline{E}$ as constants:

$$-\int_{h_1}^{h} \frac{dh}{f(h)} = g(h) \cong \frac{\underline{A}}{B} \int_{T_o}^{T} e^{-\frac{\underline{E}}{RT}} dT \qquad (10)$$

where the specific form of g(h) depends on the nature of the kinetic process; all forms of g(h) approach zero as h approaches unity at T_o.

From Equation 9 and Equation 5 of Subsection II A1, $\frac{\underline{A}}{B}$, can be evaluated on the basis of a single apparent temperature-rate of volatilization, $\left(\frac{dv}{dT}\right)_a$, and the corresponding TGA temperature, T_a, where f(h) has the value, $f(h_a)$:

$$\frac{\underline{A}}{B} \cong \frac{e^{\frac{\underline{E}}{RT_a}}}{Hf(h_a)} \left(\frac{dv}{dT}\right)_a \qquad (11)$$

where the volatilization rate corresponding to $\left(\frac{dv}{dT}\right)_a$ must be an accurate measure of the empirical rate constant at T_a.

The integration of the right-hand member of Equation 10 is accomplished(3) by substituting u, having values, x, for $\frac{E}{RT}$:

$$\int_{T_o}^{T} e^{-\frac{E}{RT}} dT = \int_{T_o}^{T} e^{-u} dT \qquad (12)$$

Then, x_o being greater than x:

$$\int_{T_o}^{T} e^{-u} dT = -\frac{E}{R} \int_{x_o}^{x} \frac{e^{-u}}{u^2} du \qquad (13)$$

and:

$$-\frac{E}{R} \int_{x_o}^{x} \frac{e^{-u}}{u^2} du = \frac{E}{R} \frac{e^{-u}}{u} \Bigg|_{x_o}^{x} + \frac{E}{R} \int_{x_o}^{x} \frac{e^{-u}}{u} du \qquad (14)$$

From Equations 10 and 14, the equation of the TGA curve is:

$$g(h) \cong \frac{A}{B} \left(Te^{-x} - T_o e^{-x_o} + \frac{E}{R} \int_{x_o}^{\infty} \frac{e^{-u}}{u} du - \frac{E}{R} \int_{x}^{\infty} \frac{e^{-u}}{u} du\right) \qquad (15)$$

The exponential integrals in Equation 15 can be approximated in several ways*, but if the approximations are insufficiently exact, g(h), being determined from the sum of small differences between large quantities, will be greatly in error.

---

* One of these is especially interesting since it leads to a simple approximation of the equation of the TGA curve for values of x greater than about 15 (3). In this case, the exponential integral is taken as approximately equal to the sum of the first two terms of the asymptotic expansion, $e^{-x}\left(\frac{0!}{x} - \frac{1!}{x^2} + \frac{2!}{x^3} - \cdots\right)$. If terms having zero subscripts can be ignored, as is often the case, Equation 15 reduces to:

$$g(h) \cong \frac{ART^2}{BE} e^{-x}$$

Fortunately, however, the exponential integral is tabulated to enough significant figures in two references (4). Negative values are given under "Ei(-x)" for values of x up to 15 in one reference (5), in which case the required positive values are those of - Ei(-x). Positive values are given under "Ei*(x)" for values of x from 15 to 50 in the second reference (6). The value of g(h) can be found quite precisely if - Ei(-x) or Ei*(x) is taken to six significant figures. Interpolation between tabulated values is accomplished using:

$$\log S = \log S_1 + (\log S_2 - \log S_1)\left(\frac{x - x_1}{x_2 - x_1}\right) \qquad (16)$$

where S is - Ei(-x) or Ei*(x).

To find the value of $\underline{E}$ corresponding to a value of $\underline{A}$ found from Equation 11, Equations 11 and 15 are combined:**

$$g(h_a) \cong \frac{e^{x_a}}{Hf(h_a)}\left(\frac{dv}{dT}\right)_a \left[T_a e^{-x_a} - T_o e^{-x_o} + \frac{\underline{E}}{R}\ (S_o - S_a)\right] \qquad (17)$$

or:

$$\frac{\left(\frac{dv}{dT}\right)_a}{Hf(h_a)g(h_a)} \left[T_a - T_o e^{x_a - x_o} + \frac{\underline{E}e^{x_a}}{R}\ (S_o - S_a)\right] \cong 1 \qquad (18)$$

** If Equation 15a can be used, Equation 18 reduces to:

$$\underline{E} \cong \frac{RT_a^2}{Hf(h_a)g(h_a)} \left(\frac{dv}{dT}\right)_a \qquad (18a)$$

Next, Equations 11, 15, and 18 will be applied to the TGA data for polytetrafluoroethylene in order to illustrate the limited usefulness of the Arrhenius integral. This can be surmised from Equations 15 and 15a, but it is much more clearly recognizable in an actual example. Because they are more generally applicable, Equations 15 and 18 will be used even though the more convenient Equations 15a and 18a are valid for the case of polytetrafluoroethylene.

1. The TGA Curve for Polytetrafluoroethylene. In the case of polytetrafluoroethylene, the business of using Equation 18 is greatly simplified by virtue of the fact that $T_o(298K)$ is much lower than the temperature range of appreciable volatilization ($>770K$) from which T_a is chosen. Thus, even if $\underline{E}$ were as small as 20 K cal, all terms having zero subscripts could be neglected as being at least six orders of magnitude smaller than those having the subscript, "a".

Further simplification is inadvisable; as will presently be seen, appreciably inaccurate values of $\underline{E}$ are found from Equation 18 if $f(h_a)$ and $g(h_a)$ are not specifically evaluated, even when the calculation is limited to values of h_a greater than 0.95. In the present case, Figure 22 suggests zero-order initial volatilization, in which case $f(h_a)$ is unity and $g(h_a)$ is $1 - h_a$. Since the polymer volatilizes completely, H is unity and $1 - h_a$ is v, so that Equation 18 becomes:

$$N_a = \left[T_a - v_a\left(\frac{dT}{dv}\right)_a\right]R \cong \underline{E}S_a e^{x_a} \qquad (19)$$

where N_a is simply a number.

Equation 19 is more conveniently used in its logarithmic form:

$$\log N_a - \log \underline{E} - x_a \log e - \log S_a = \Delta \cong 0 \qquad (20)$$

where Δ is a difference which is positive for inappropriately small values of $\underline{E}$ and negative for those which are too large. If $f(h_a)$ and $g(h_a)$ have been correctly evaluated and if the three basic experimental quantities, $\left(\frac{dv}{dT}\right)_a$, T_a and h_a, have been determined precisely, Equation 20 is exactly true at T_a. Under these circumstances, the appropriate value of $\underline{E}$ for the value of $\underline{A}$ at T_a can be found by trial and error as the point where Δ passes through zero in a plot of Δ vs $\underline{E}$.

All this is difficult enough, but the use of the small difference equation is rendered even more difficult by its

extreme sensitivity to small errors. In the present case, for example, if log e is taken as 0.43429 instead of 0.434295, the resulting value of $\underline{E}$ is 2 K cal too high. Similarly, had first-order, rather than zero-order volatilization been assumed in deriving N_a, the value of $\underline{E}$ in the neighborhood of h = 0.95 would again have been about 2 K cal too high. The reason for this can be seen from the first-order expression for N_a:

$$N_a = \left[T_a + h_a\left(\frac{dT}{dv}\right)_a \ln 10 \log h_a\right]R \qquad (21)$$

where $h_a \ln 10 \log h_a$ is a negative number slightly smaller than v_a.

Still larger errors result from small errors in measuring the three basic experimental quantities. In the present case, if N_a is evaluated on the assumption of zero-order volatilization in the neighborhood of $h_a = .95$, an error of -.01 in h_a, or of -2^o in T_a, or of + 10% in $\left(\frac{dv}{dT}\right)_a$ can result in a -7 K cal error in $\underline{E}$. Such errors in measuring the experimental quantities are easily possible, so that $\underline{E}$ can be estimated precisely only by sufficient replication.

Even after this has been done, however, the result is valid only at T_a, unless $\underline{E}$ is a constant for the whole TGA curve. This, in turn, is possible only if volatilization rates are uniquely determined by temperature over the whole curve. In view of the dependence of volatilization rates partially on the nature of the apparent kinetic process, which may also change with temperature, such an ideal situation is highly unlikely.

That this is all too true even of the remarkably simple volatilization of polytetrafluoroethylene is readily shown by calculating $\frac{\underline{A}}{B}$ at several temperatures, using a constant value of $\underline{E}$ and observed values of h, $h_{obs.}$, in:

$$\frac{\underline{A}}{B} = \frac{g(h_{obs.})}{Te^{-x} - \frac{\underline{E}\,S}{R}} \qquad (22)$$

Using $\underline{E}$ = 68.2 K cal, found from Equations 19 and 20 evaluated at $h_a = .95$, $T_a = 794$ K and $\frac{dv}{dT}_a = \frac{1}{351}$, and solving for $\frac{\underline{A}}{B}$ at tabulated values of S in both the zero-order case (where $g(h_{obs.}) = v_{obs.}$) and the first-order case (where $g(h_{obs.}) = -\ln h_{obs.}$), Equation 22 yields the highly inconstant values of $\frac{\underline{A}}{B}$ given in Table 13.

Table 13

Values of A/B Found from Equation 22 for E = 68.2 K cal

x	Temp, °C	$h_{obs.}$	A/B per degree: Zero-order Case	A/B per degree: First Order Case
39	607.0	0.003	3.949×10^{15}	2.301×10^{16}
40	585.0	0.260	8.363×10^{15}	1.522×10^{16}
41	564.0	0.611	1.258×10^{16}	1.593×10^{16}
42	544.1	0.836	1.507×10^{16}	1.646×10^{16}
43	525.1	0.937	1.647×10^{16}	1.703×10^{16}
44	507.0	0.975	1.851×10^{16}	1.875×10^{16}
45	489.6	0.992	1.687×10^{16}	1.690×10^{16}

Clearly, the value of E found at 794 K (521 C) is invalid for most of the TGA curve for "Teflon," whether the volatilization is regarded as zero-order or first-order. Presumably though, the data curve can be roughly fitted using a single trivial value of E and an average value of $\frac{A}{B}$, especially in the first-order case wherein smaller discrepancies are found. This is not surprising since Figure 22 suggests first-order volatilization at the lower values of h, where the difference between zero-order and first-order aging curves becomes extremely large. In attempting to fit the data curve in the first-order case, values of h at various temperatures are calculated using:

$$\log h \cong -\left(\log e\left(\frac{A}{B}\right)_{ave}\right)\left(Te^{-x} - \frac{ES}{R}\right) \qquad (23)$$

As shown in Figure 24, Equation 23 fits most of the TGA curve for polytetrafluoroethylene within experimental error (h about $\pm$ 0.02) when E is taken as 68.2 K cal and $(A/B)_{ave.}$ is taken as 1.7615×10^{16} per degree. Figure 24 also shows, however, that had E been calculated as 61 K cal on, for example, a slightly different reading of $\frac{dv}{dT_a}$, an equally good fit could have been attained by taking $(A/B)_{ave.}$ as 1.8946×10^{14} per degree. These pairs of trivial values of E and $\frac{A}{B}$ are only two out of an infinite number of combinations which can be used in Equation 23 to reproduce the data curve within experimental error. From the form of Equation 23, it is seen that this would also be true even if E were a true constant for the whole TGA curve.

Of course, if g(h) could be evaluated appropriately over the whole curve, and if the dependence of volatilization rates

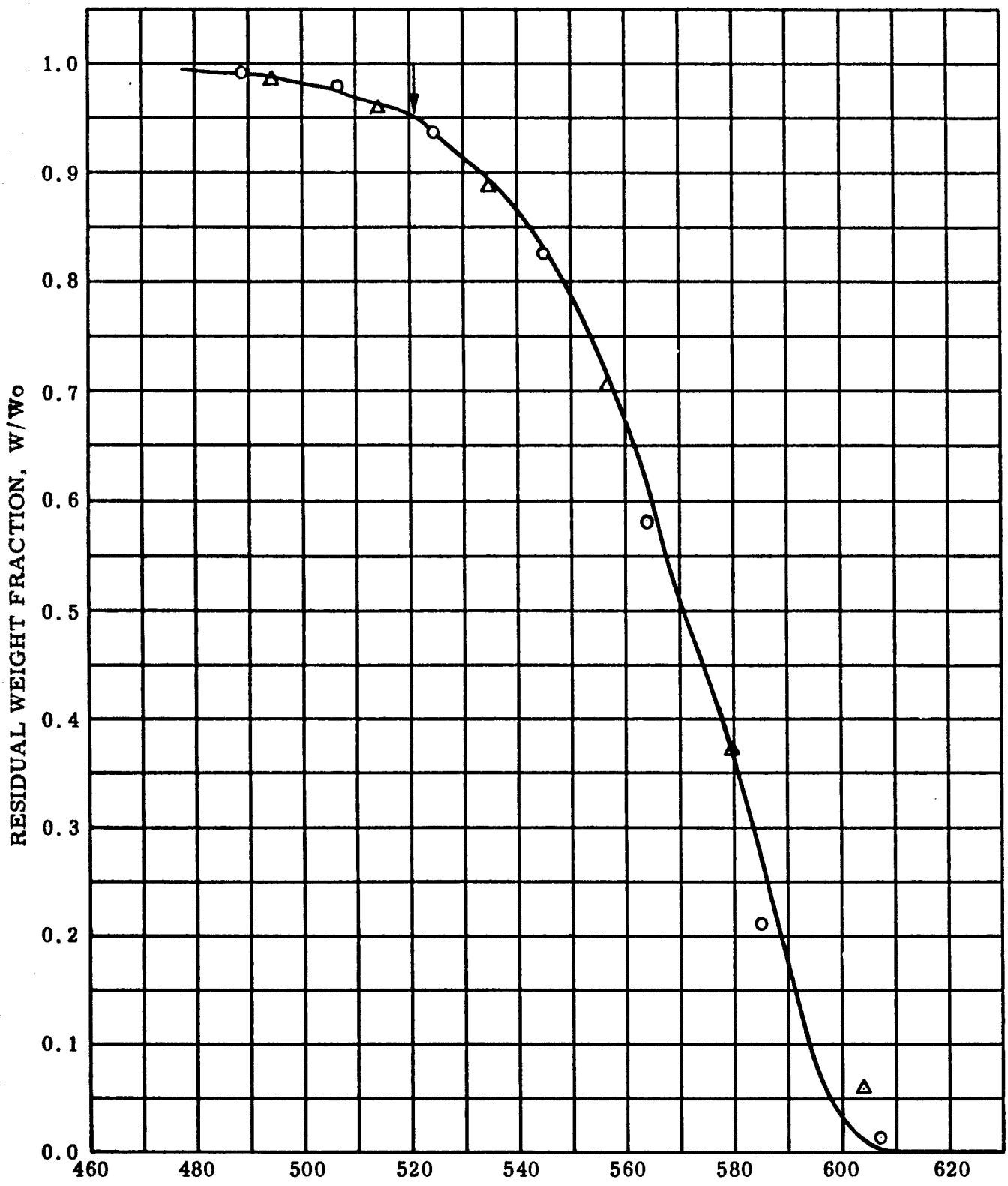

Figure 24 TGA IN DRY N_2 AT 180 C° PER HOUR, POLYTETRAFLUOROETHYLENE

——— EXPERIMENTAL DATA O, Δ CALCULATED POINTS

O : $\underline{E}$ = 68,200 CAL. Δ : $\underline{E}$ = 61,000 CAL.

on the changing geometry and degree of subdivision of the sample were quantitatively specifiable, it would be possible, given sufficient replication, to find a pair of values of $\underline{E}$ and $\underline{A}/B$ which affords a best fit to the curve. Given the same kind of corroborative information, however, these uniquely appropriate values of $\underline{E}$ and $\underline{A}$ could be found with far less computational effort from the least squares slope and intercept of the Arrhenius plot of the corresponding specific volatilization rate constants.

Since neither of these approaches can be applied in practice without the help of a great deal of corroborative information, the final result of kinetic analysis of weight-loss data alone is usually a set of trivial constants, valid only for a narrow temperature range as a rule, and unextrapolatable to other experimental conditions, at least on present knowledge. As such, the ultimate data represent little more than mere starting points for more significant studies, which can frequently be just as well begun on the basis of data found by simple quasi-kinetic methods. With this view in mind, two quasi-kinetic short-cuts will next be described and illustrated for four widely different polymers. The first technique to be described is one based on empirical time-temperature superposition; the second is based on an empirical relationship between time at constant temperature and temperature in TGA.

C. Two Quasi-kinetic Shortcuts

The great advantage of quasi-kinetic analysis of weight-loss data is simplicity, but it is simplicity gained at the cost of clear kinetic significance. For one thing, the techniques given in this subsection will involve only apparent weight fractions and volatilization rates, the relationship between the sometimes unspecifiable true volatilization rate and the actual decomposition rate usually being regarded as an experimentally inaccessible quantity. Further, the nature of the kinetic process will be ignored, except in explanatory passages and passing comments on interesting cases.

Surprisingly often, this cavalier approach to kinetic analysis leads to nearly linear relationships between rather extensive ranges of time and temperature under a given set of procedural conditions; only occasional cases require recourse to kinetic principles for the fulfillment of preliminary needs. This will be seen in the ensuing discussion of empirical time-temperature superposition and the subsequent discussion of an empirical relationship between aging times and TGA temperatures surmised from the similarity of the shapes of superposed aging curves and TGA curves. From the illustrative examples to be given, it will also be seen that an inherent advantage of the empirically superposed aging curve

over the analogous calculated TGA curve is greatly reduced ambiguity of practical meaning.

1. Empirical Time-temperature Superposition. In empirical time-temperature superposition, extensively valid relationships between time and temperature of aging are sought and proved by their usefulness as means of marshalling the data for several aging temperatures into a master curve at some single aging temperature, usually chosen from the middle of the experimental range (7). Such a master curve is constructed by measuring the aging times to various extents of volatilization at each of the aging temperatures, then multiplying each of these corresponding times, t_i, by an appropriate superposition factor, α_T, to find the corresponding time, t_{im}, at the master curve temperature:

$$\alpha_T t_i \cong t_{im} \qquad (24)$$

In rigorous kinetic analysis, Equation 24 would be exactly true; the value of α_T would be uniquely determined by the absolute temperature. By way of illustration, if it were possible to find from weight-loss data the true fraction remaining undecomposed, f, the general relationship between f and aging time could be written:

$$g(f) = kt \qquad (25)$$

where the specific form of g(f) depends on the nature of the kinetic process. At the same value of g(f):

$$kt_i = k_m t_{im} \qquad (26)$$

where k_m is the specific decomposition rate constant at the master aging temperature. In this sense, α_T represents the ratio of the specific decomposition rate constants:

$$\alpha_T = \frac{k}{k_m} \qquad (27)$$

Thus, by using the Arrhenius rate equation in Equation 27, α_T can be related to the absolute temperature of aging, T, and of the master curve, T_m, by:

$$\log \alpha_T = \frac{E}{R \ln 10}\left(\frac{1}{T_m} - \frac{1}{T}\right) \qquad (28)$$

Because Equations 25 through 28 are only partly true in quasi-kinetic analysis, Equation 28 is here rewritten as:

$$\log \alpha_T \cong b\left(\frac{1}{T_m} - \frac{1}{T}\right) \qquad (29)$$

where the empirical symbol, b, is used in order to emphasize the lack of clear kinetic significance in non-rigorous analysis. Defined as in Equation 29, α_T is expected to be only partially dependent on temperature. In some cases, it may be prohibitively non-linear, especially if the apparent kinetic process changes appreciably with extent of volatilization. Thus, in every instance, the linear range of α_T must be found by trial and error in quasi-kinetic analysis. This will next be done for four polymers having increasingly complex volatilization mechanisms, beginning with polytetrafluoroethylene.

a. Polytetrafluoroethylene.

In the absence of better information, values of b can be found from aging curves by patient trial and error, but in the case of polytetrafluoroethylene, superposition of the aging data is accomplished in straightforward fashion on the basis of the slopes of the Arrhenius plot in Figure 23. At temperatures below 487 C the slope is 17,483 ; above 487 C, an average slope of 13,330 was found. These values of b were used in Equation 29 to determine the values of log α_T given in Table 14, taking T_m as 760 K.

Table 14

Superposition Factors for 200 mg Samples of Pulverized "Teflon" Aged in Dry N_2

Aging Temperature, °C	log α_T
400	- 2.97675
430	- 1.86708
450	- 1.17845
480	- 0.21403
487	0
490	0.06892
500	0.29499
510	0.51520
520	0.72995

In constructing master curves, full representation of the data from all aging temperatures is conveniently attained by choosing equal residual weight fraction times which are about equally spaced on the logarithmic time-scale. In the case of the 24-hour tests of the present study, for example, the times chosen for multiplication by α_T were: 1/3, 1, 3-1/3, 10, and 20 hours. The corresponding values of W/W_o were then plotted

against the log of $t\alpha_T$, as shown for the case of polytetrafluoroethylene in Figure 25.

The superposition displayed in Figure 25 is remarkably precise, considering experimental error and the fact that only two values of b were used in constructing the curve. Further, because the complete curve could be found solely on the basis of initial rate data, it can be inferred that the only appreciable change in the value of b is the one which occurred near 487 C.

That such an inference can safely be drawn from Figure 25 illustrates an inherent advantage of the empirically superposed aging curve over the analogous calculated TGA curve; in pleasant contrast with the ambiguously paired constants of Equation 15 of Subsection IV B of this report, b can be determined uniquely for the procedural conditions employed. This, of course, is possible because the empirically superposed aging curve is found directly from observed values of w, thus obviating the need to guess about the relationship between g(h) and w. Thus, while the causes of a change in b cannot be surmised from weight-loss data alone, its single effect on the superposed curve can be determined unambiguously.

Since apparent volatilization rates can be determined from the TGA curve, the question might well be asked whether a few replicate TGA runs, assuming careful avoidance of the range of inherently inaccurate small rates, would not serve as well as several isothermal aging curves for the construction of an empirically superposed aging history. Reference to Figure 23 suggests that in the case of polytetrafluoroethylene, the question is largely one of relative costs. As will next be seen, this is true also of polystyrene. In the two subsequent cases, however, prohibitively brief ranges of directly usable TGA volatilization rates will be found, whereas the corresponding isothermal aging curves can be applied empirically in one way or another.

b. Polystyrene

Polystyrene is interesting not only as a widely studied polymer but also as a material whose aging curves in inert atmosphere lead to maximum-type rate curves, as shown in Figure 26. According to one view of vinyl depolymerization, the maximum true volatilization rate is related to the specific rate constant for depolymerization (2). Thus, examination of polystyrene affords an opportunity to determine the net activation energy of depolymerization from weight-loss data and, further, to compare empirical rate constants found from initial volatilization rates with those found from the theoretically significant maximum rates. The value of this study is limited, however, by the fact that the net activation energy for the depolymerization of polystyrene is subject to rather broad batch-to-batch variation, depending on residual catalyst content and other factors.

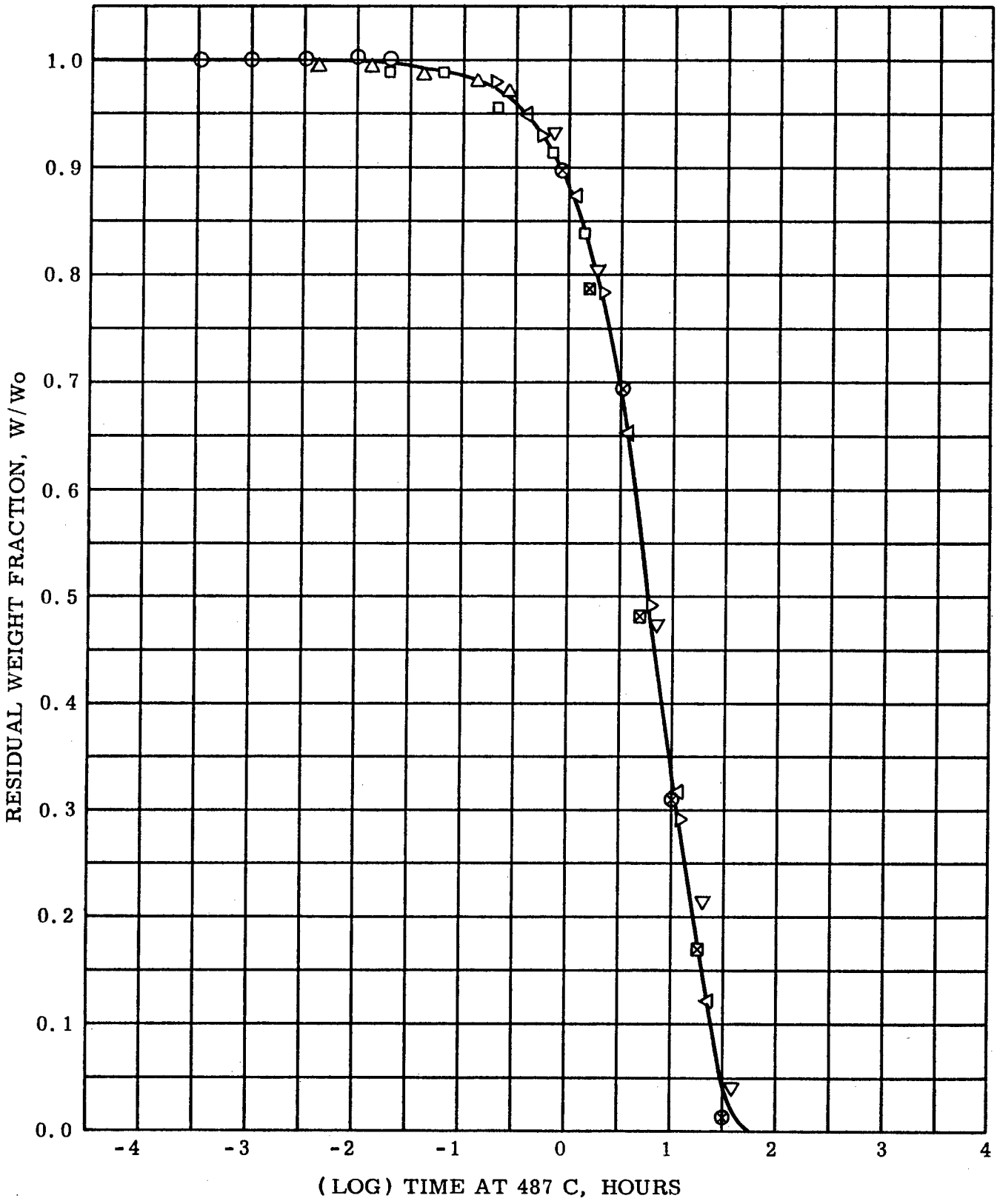

Figure 25 TIME-TEMPERATURE SUPERPOSITION OF AGING DATA FOR POLYTETRAFLUOROETHYLENE IN DRY N_2 AT: ○ 400 C, △ 430 C □ 450 C, ▷ 480 C, ◁ 490 C, ▽ 500 C, ⊗ 510 C, AND ⊠ 520 C

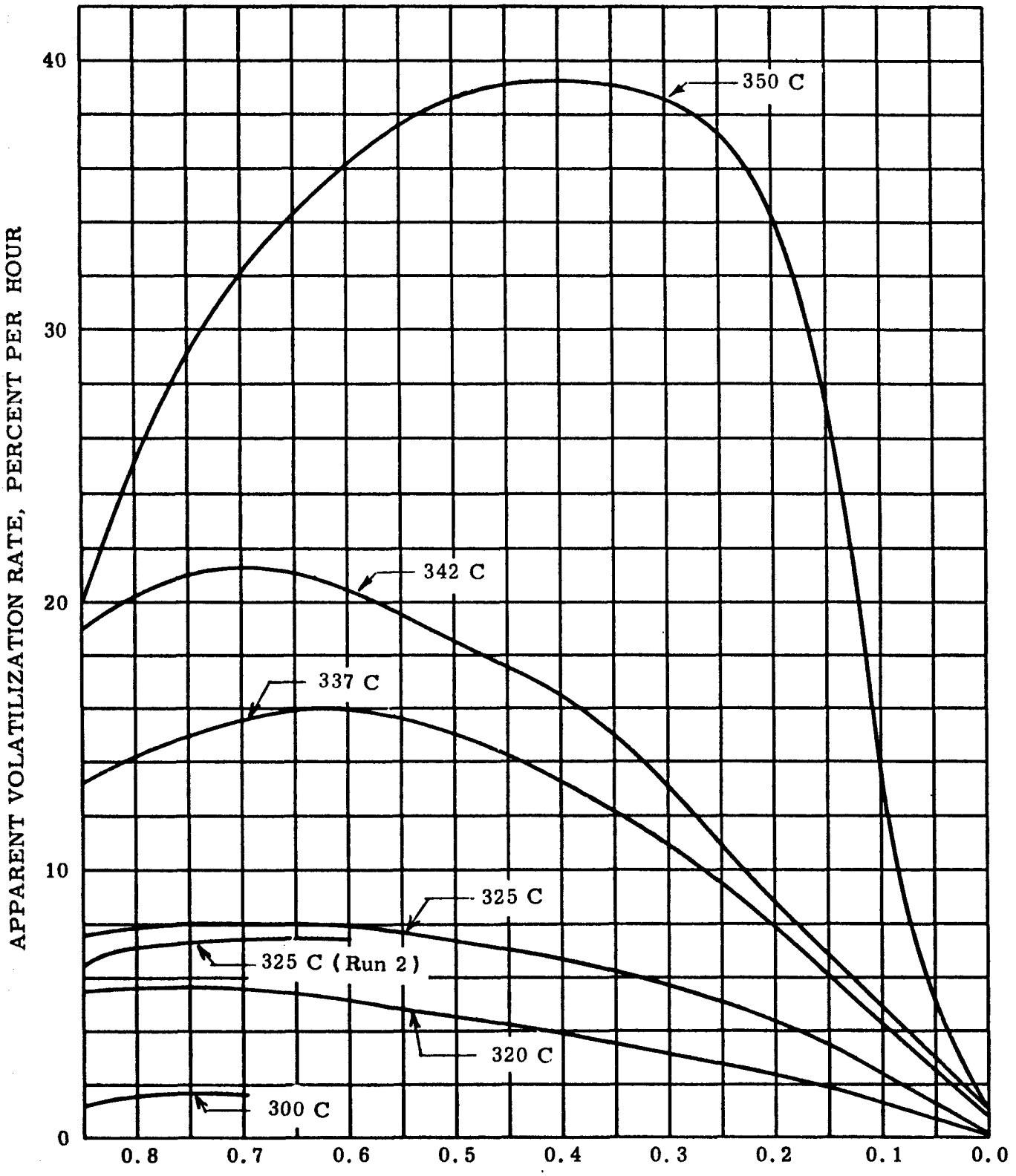

Figure 26 TGA IN DRY N_2 AT CONSTANT TEMPERATURE APPARENT VOLATILIZATION RATE VS. RESIDUAL WEIGHT FRACTION POLYSTYRENE

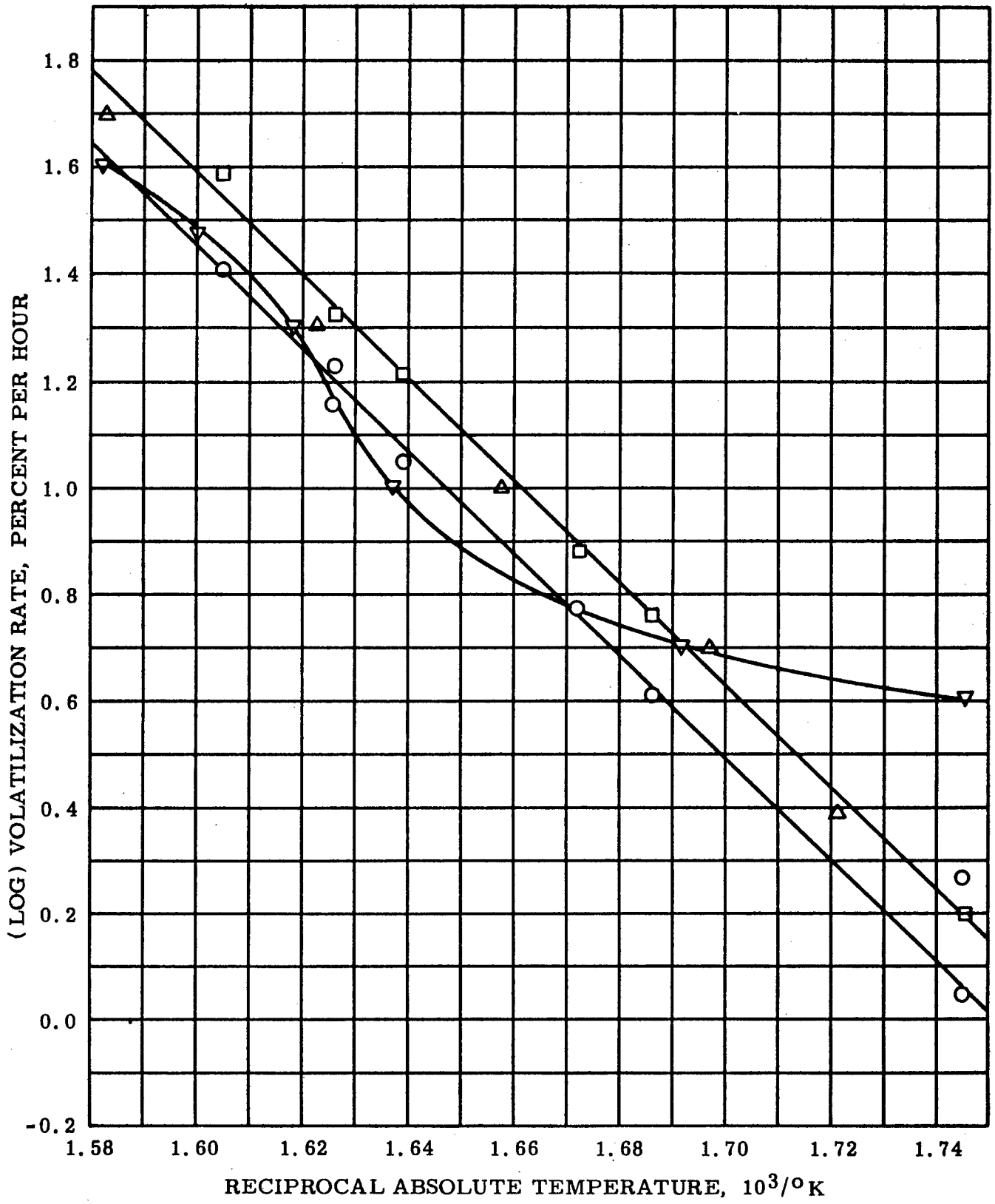

Figure 27 COMPARISON OF VOLATILIZATION RATES FROM THE UNMACNIFIED, "Δ" AND MAGNIFIED "∇" THERMOGRAMS, WITH INITIAL " O " AND MAXIMUM, "□" VOLATILIZATION RATES FROM ISOTHERMAL AGING OF POLYSTYRENE IN DRY N_2

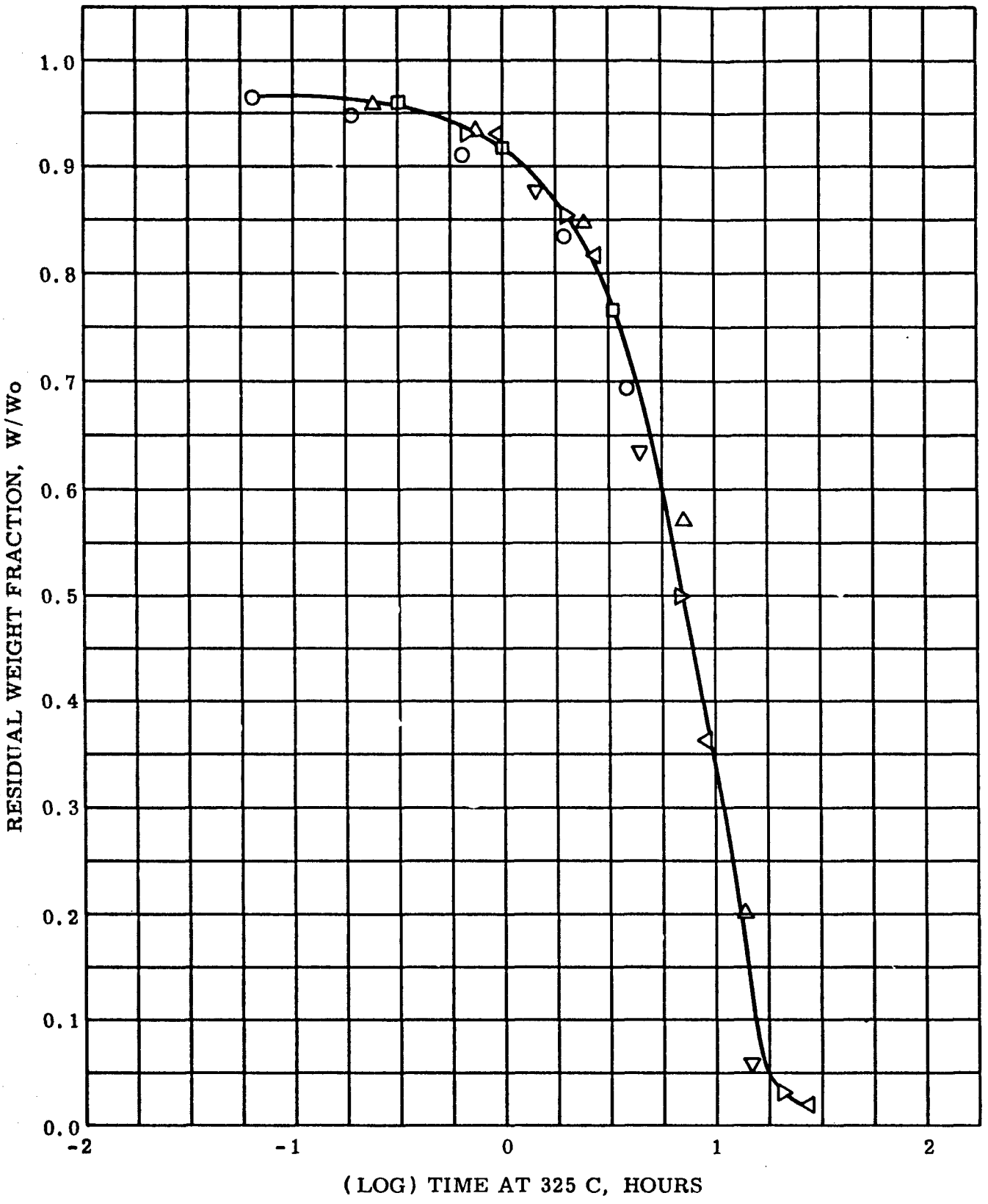

Figure 28 TIME-TEMPERATURE SUPERPOSITION OF AGING DATA FOR POLYSTYRENE IN DRY N_2 AT: ○ 300 C, △ 320 C, □ 325 C ▷ 337 C, ◁ 342 C AND ▽ 350 C

Initial and maximum volatilization rates found for a 200 mg sample of pulverized "Cadco" polystyrene are compared in Figure 27, where it is seen that the maximum rates are only slightly higher than the corresponding initial rates. Further, both have about the same temperature dependence, corresponding to a net activation energy of 44 K cal. Although further replication is clearly needed, the same is approximately true of TGA rates, except in the inherently inaccurate range.

Since the slopes in Figure 27 do not change, the polystyrene data were superposed on the basis of the single value of b = 9,615. The resulting values of log α_T with respect to 325 C are given along with the corresponding maximum and initial rate data in Table 15. Data for the experimentally incorrect Run 1 at 325 C are omitted.

Table 15

Rate and Superposition Data for 200 mg Samples of Pulverized Polystyrene Aged in Dry N_2

Aging Temperature, °C	Volatilization Rates, %/hr. Maximum	Initial	log α_T
300	1.58	1.12	- 0.70154
320	5.60	4.08	- 0.13558
325 (Run 2)	7.40	5.94	0
337	16.0	11.2	0.31635
342	21.3	16.8	0.44452
350	39.2	25.9	0.64529

As shown in Figure 28, the polystyrene data were superposed quite successfully on the basis of a single value of b, as expected from the constant value of the net activation energy found for the depolymerization. This, then, hardly represents a case of quasi-kinetic analysis. In the ensuing discussion of a chlorendic anhydride-hardened epoxy, however, kinetic principles will be largely ignored, except by way of explanation.

c. Chlorendic Anhydride-hardened Epoxy

The chlorendic anhydride-hardened epoxy, Code 22/10, hereinafter called simply "epoxy," does not volatilize completely in TGA. From curve number 42 in Figure 8, it is seen that the residue at 900 C is about 30%, so that the corresponding total fraction volatilized in the single weight-loss step is about 0.7. The use of apparent rather than true initial volatilization rates in such cases of incomplete volatilization leads to measurements of $\underline{K}Hf(h)$ rather than $\underline{K}f(h)$, as shown by Equations 5 and 6 in Subsection II A1 of this report. From the form of Equation 8, however, the value of $\underline{E}$ is unaffected by this so long as h is

near unity. The corresponding value of A, of course, will be too low, but this is of no importance in finding b. More troublesome is the fact that the accuracy of initial apparent rates as measures of kH depends on the magnitude of H, the range of w corresponding to $h > 0.95$ being limited to:

$$1 - L > w > 1 - L - .05H \qquad (30)$$

Thus, in the case of the epoxy, the range of directly usable apparent volatilization rates begins at w = 1 and ends at w = 0.965.

As can be seen from the aging curves in Figure 29, this limitation introduces the possibility of appreciable inaccuracy, especially at the higher aging temperatures. Further, multiple initial rates were encountered at all of the lower aging temperatures. To complicate matters still further, the aging curve at 240 C was confounded by some unknown experimental effect and could not, unfortunately, be redetermined because the sample supply had been exhausted.

In view of all these difficulties, all initial rates were included in a trial Arrhenius plot and only those which fell along a common line were retained, as shown in Figure 30. The slope of the line in Figure 30 corresponds to a value of b of 11,364, or an apparent activation energy of 52 K cal. Figure 30 also shows that the directly usable range of TGA rates is extremely limited, although matters can be improved by assuming first-order volatilization, as shown by the data points in parentheses.

The initial rate data and superposition factors with respect to 250 C are given for reference in Table 16.

Table 16

Rate and Superposition Data for 200 mg Samples of Pulverized Chlorendic Anhydride-hardened Epoxy Aged in Dry N_2

Aging Temperature, °C	Initial Volatilization Rate, %/hr.	log α_T
200	0.03	- 2.29682
240	0.33 ?	- 0.42352 ?
250	0.83	0
275	8.10	0.99125
300	70.0	1.89602

It is seen from the plot in Figure 31 that the epoxy data, excepting those from the dubious run at 240 C, were superposed with reasonably good success on initial apparent rates of limited

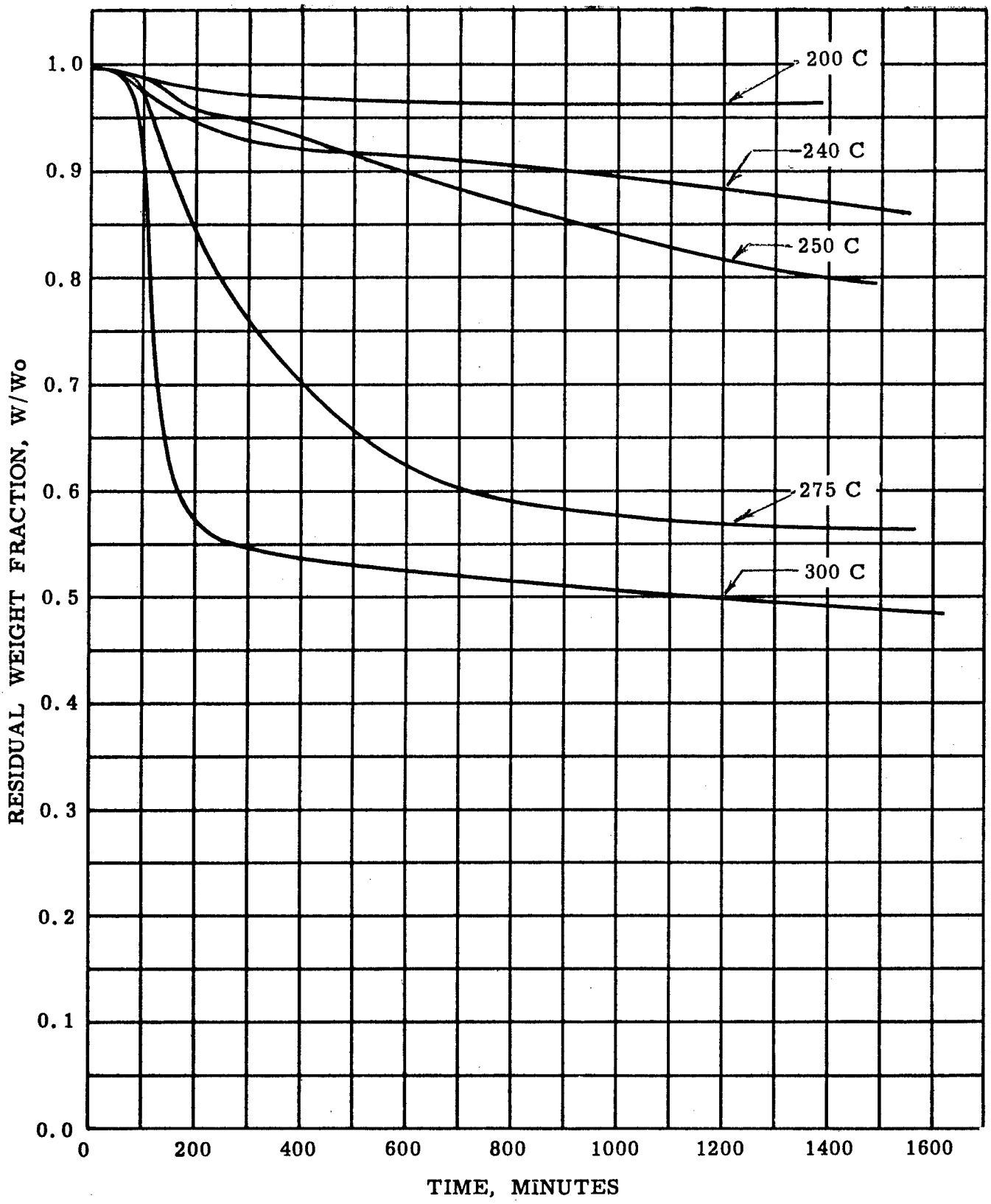

Figure 29 TGA IN DRY N_2 AT CONSTANT TEMPERATURE
CHLORENDIC ANHYDRIDE - HARDENED EPOXY, CODE 22/10

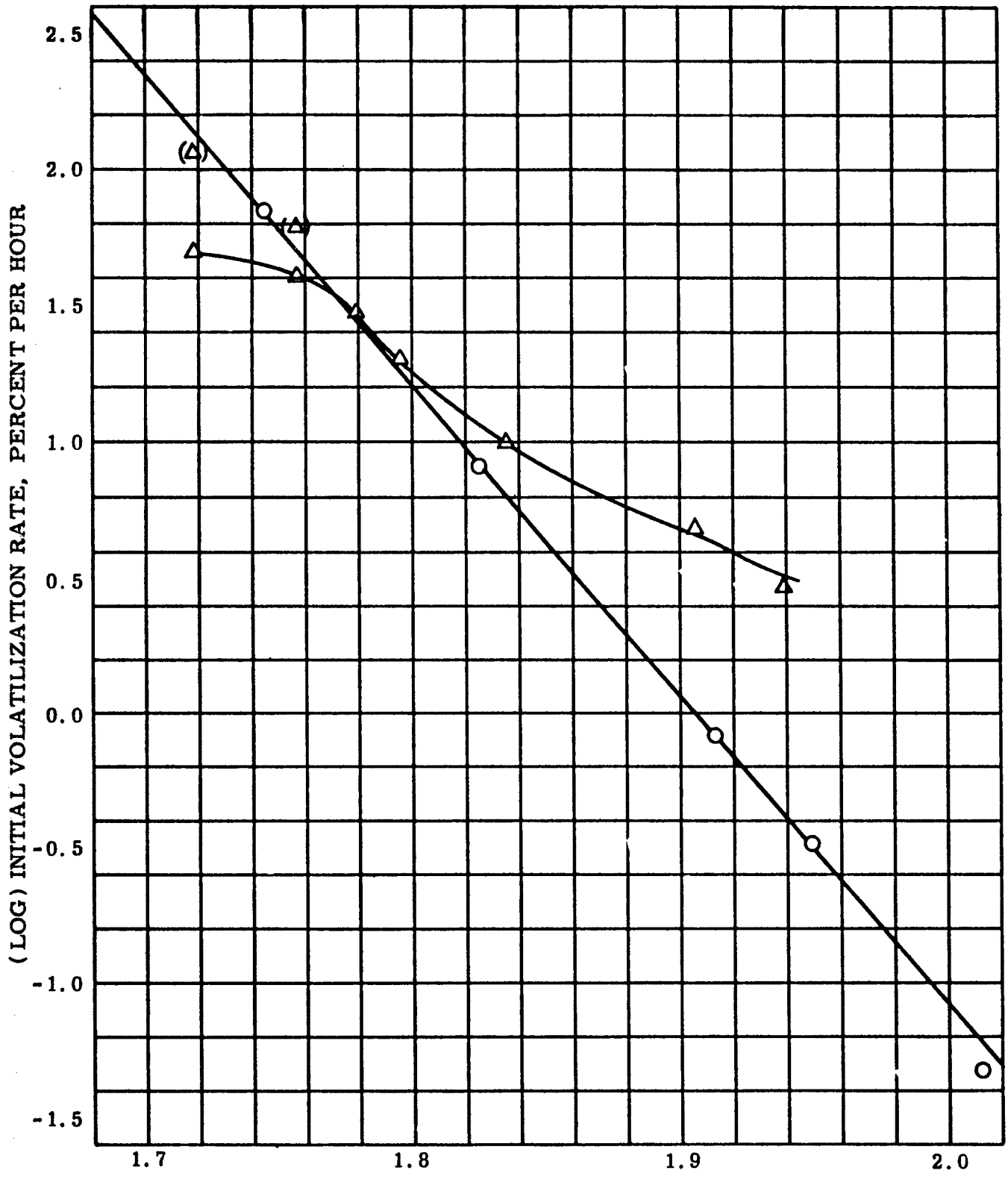

Figure 30 COMPARISON OF VOLATILIZATION RATES, "Δ" AND ESTIMATED APPARENT RATE CONSTANTS, "(Δ)" FROM THE MAGNIFIED THERMOGRAM WITH INITIAL VOLATILIZATION RATES, "O" FROM ISOTHERMAL AGING OF CHLORENDIC ANHYDRIDE-HARDENED EPOXY, CODE 22/10, IN DRY N_2

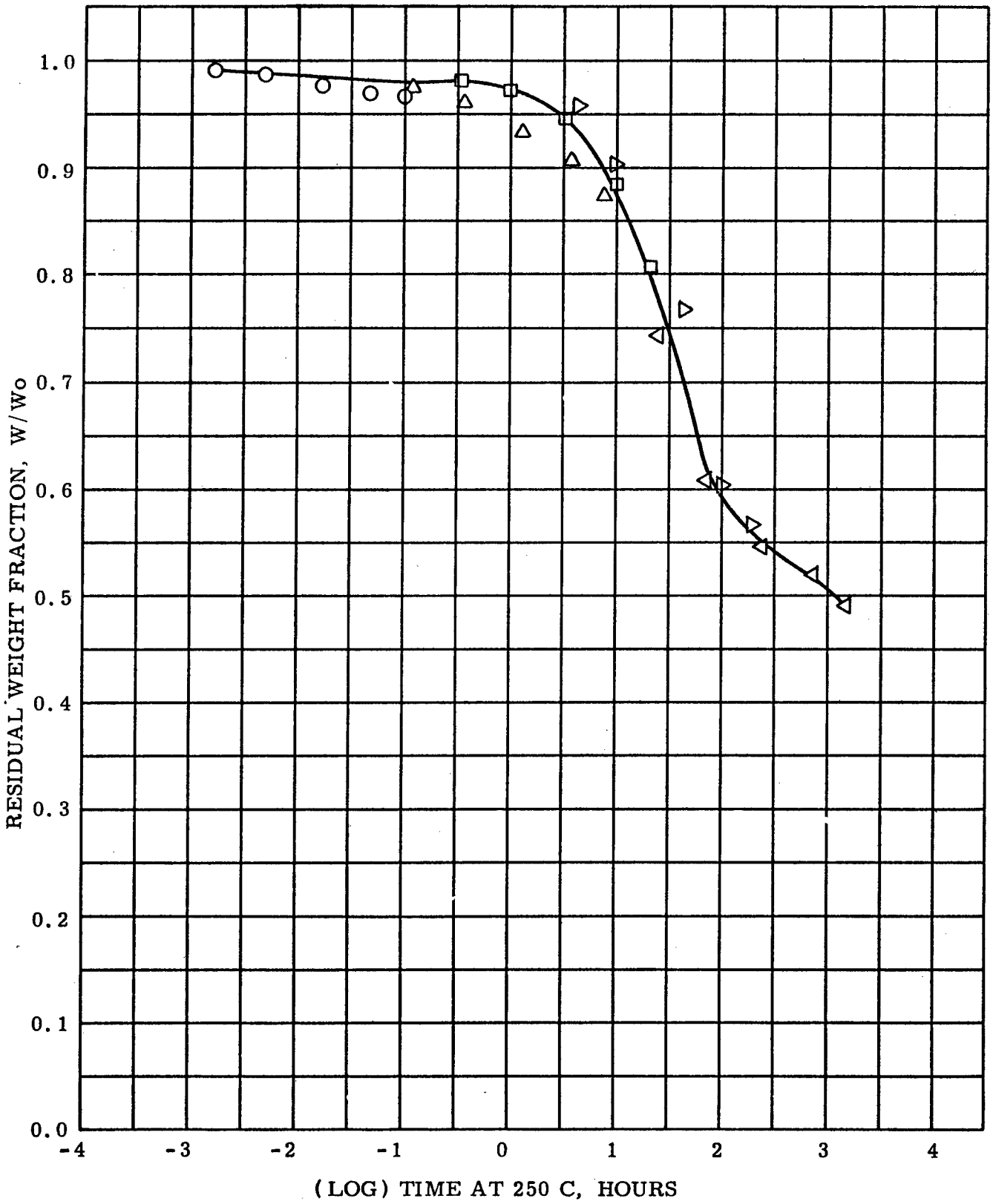

Figure 31 TIME-TEMPERATURE SUPERPOSITION OF AGING DATA FOR CHLORENDIC ANHYDRIDE-HARDENED EPOXY, CODE 22/10, IN DRY N_2 AT: ○ 200 C △ 240 C, □ 250 C, ▷ 275 C AND ◁ 300 C

validity. Eventually, however, cases are encountered which cannot be treated by the method of initial rates at all. The reaction product of aconitic acid and acetic anhydride, to be considered next, affords a case in point.

d. Reaction Product of Aconitic Acid with Acetic Anhydride.

The aging curves for this experimental polymer, hereinafter called "AcoAc," are wondrous to behold. As can be seen in Figure 32, the curve at each aging temperature peels away from the common heating curve, whereafter all of the aging histories assume virtually the same slope. Clearly, no initial volatilization rates are available from the data, but fortunately, the amount of trial and error involved in superposing these strange aging curves can be materially reduced by recognizing them as typical of volatilization via the logarithmic rate process (8).

In logarithmic volatilization, the true weight fraction volatilized (from Equation 4 in Subsection II A1 of this report) is related to aging time by (8):

$$\frac{v - L}{H} \cong \frac{\ln(\underline{k}k't + 1)}{k'} \qquad (31)$$

where k', unlike the empirical rate constant, $\underline{k}$, is independent of temperature. According to Equation 31, a plot of $\frac{v - L}{H}$ vs the log of time becomes linear for times which make $\underline{k}k't$ large compared with unity, and the slope, m', of the linear region yields the value of k':

$$k' = \frac{\ln 10}{m'} \qquad (32)$$

In quasi-kinetic analysis, however, the apparent, rather than the true residual weight fraction is used with the result that Equation 31 is arbitrarily changed to:

$$w \cong 1 - \frac{H}{k'}\ln\left(\frac{k_a k't}{H} + 1\right) \qquad (33)$$

Thus, the slope, $-m$, of a plot of w vs log t yields the value of k'/H, rather than k':

$$\frac{k'}{H} = -\frac{\ln 10}{m} \qquad (34)$$

The relationship between the apparent rate constant, k_a, and the empirical rate constant, $\underline{k}$, can be found with the help of the exponential forms of Equations 31 and 33:

$$e^{\frac{k'}{H}(v-L)} \cong \underline{k}k't + 1 \qquad (35)$$

and:

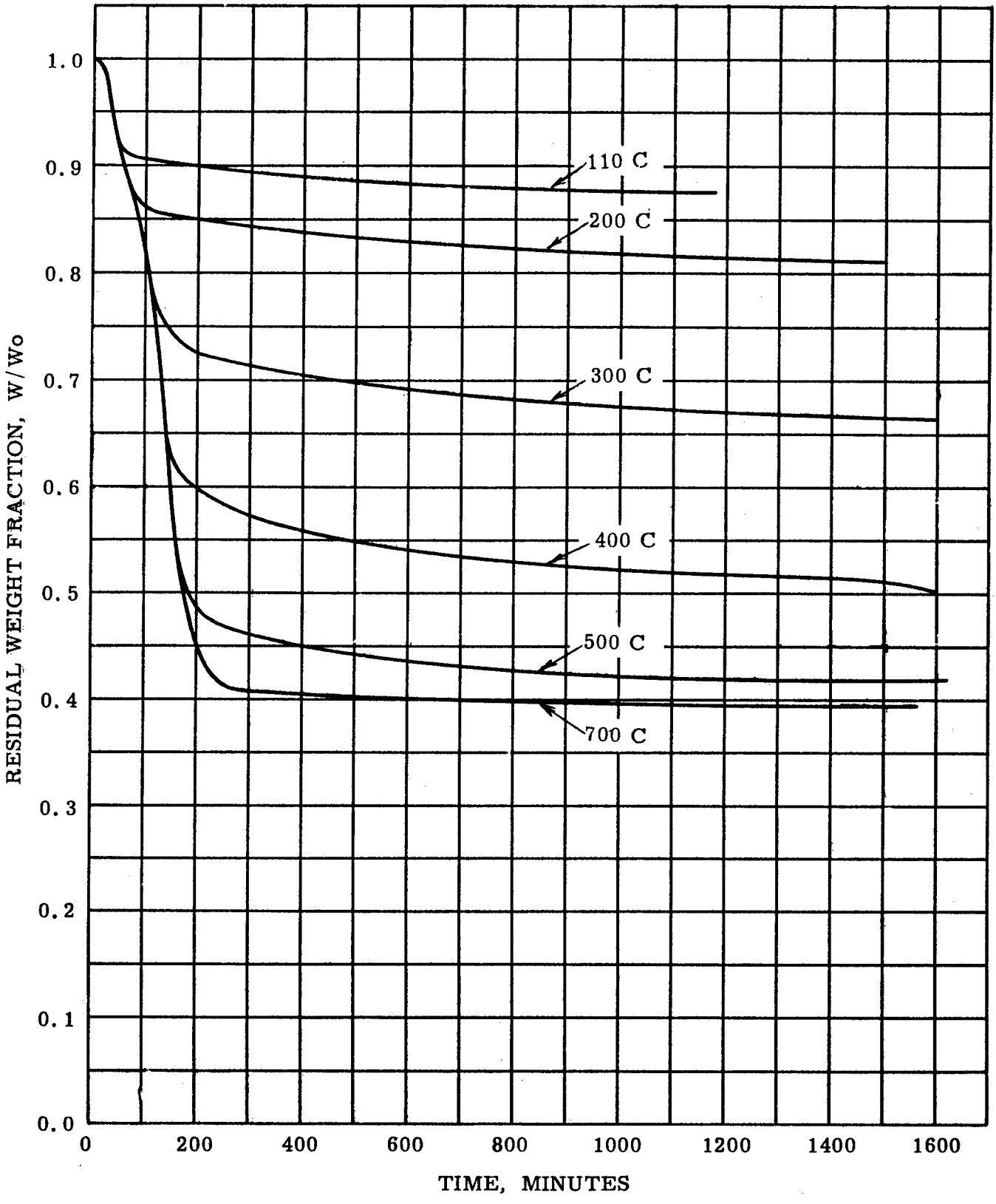

Figure 32 TGA IN DRY N_2 AT CONSTANT TEMPERATURE
REACTION PRODUCT OF ACONITIC ACID & ACETIC ANHYDRIDE, CODE 88, 8/58

$$e^{\frac{k'}{H}(1-w)} \cong \frac{k_a k' t}{H} + 1 \qquad (36)$$

The rate equations found by differentiating Equations 35 and 36 are:

$$\frac{dv}{dt} \cong \underline{k} H e^{-\frac{k'}{H}(v-L)} \qquad (37)$$

$$\frac{dv}{dt} \cong k_a e^{-\frac{k'}{H}(1-w)} \qquad (38)$$

From the ratio of Equation 37 to Equation 38:

$$\underline{k} \cong \frac{k_a e^{-\frac{k'L}{H}}}{H} \qquad (39)$$

Thus, $\underline{k}$ is a constant multiple of k_a, so that the use of w instead of $\frac{v - L}{H}$ does not affect the temperature-dependence of the resulting rate data; the same value of $\underline{E}$ is found in quasi-kinetic analysis as would be determined in more rigorous analysis of logarithmic volatilization data. Further, this is presumably true for all non-transcendental forms of g(h).

The plots of w vs log t for AcoAc are linear, as shown in Figure 33, but k'/H is not constant for all the curves or even within some of the curves. This is not an unusual finding from studies of solid polymers, since the value of k'/H, like that of $\underline{k}$, depends in as yet unspecified ways on the geometry and degree of subdivision of the sample. Inconstancy of k'/H is, however, a nuisance which bars the way to straightforward kinetic analysis.

To circumvent this difficulty, the data for AcoAc were superposed without the help of an Arrhenius plot by applying Equation 24 reversely. This could be done with unusual ease since aging data were available for most of the residual weight fraction range of interest, with only a few relatively short gaps unaccounted for. Thus, it was possible to extend the tail of each line in Figure 33 half-way down the range of unknown residual weight fractions to meet the back-extension of the beginning of the next lower curve. The resulting extrapolated matching points, shown as triangles in Figure 33, were then simply strung together head-to-tail on the logarithmic time-scale, as shown in Figure 34, using the data at 300 C to establish the location of part of the 300 C master curve. Also shown

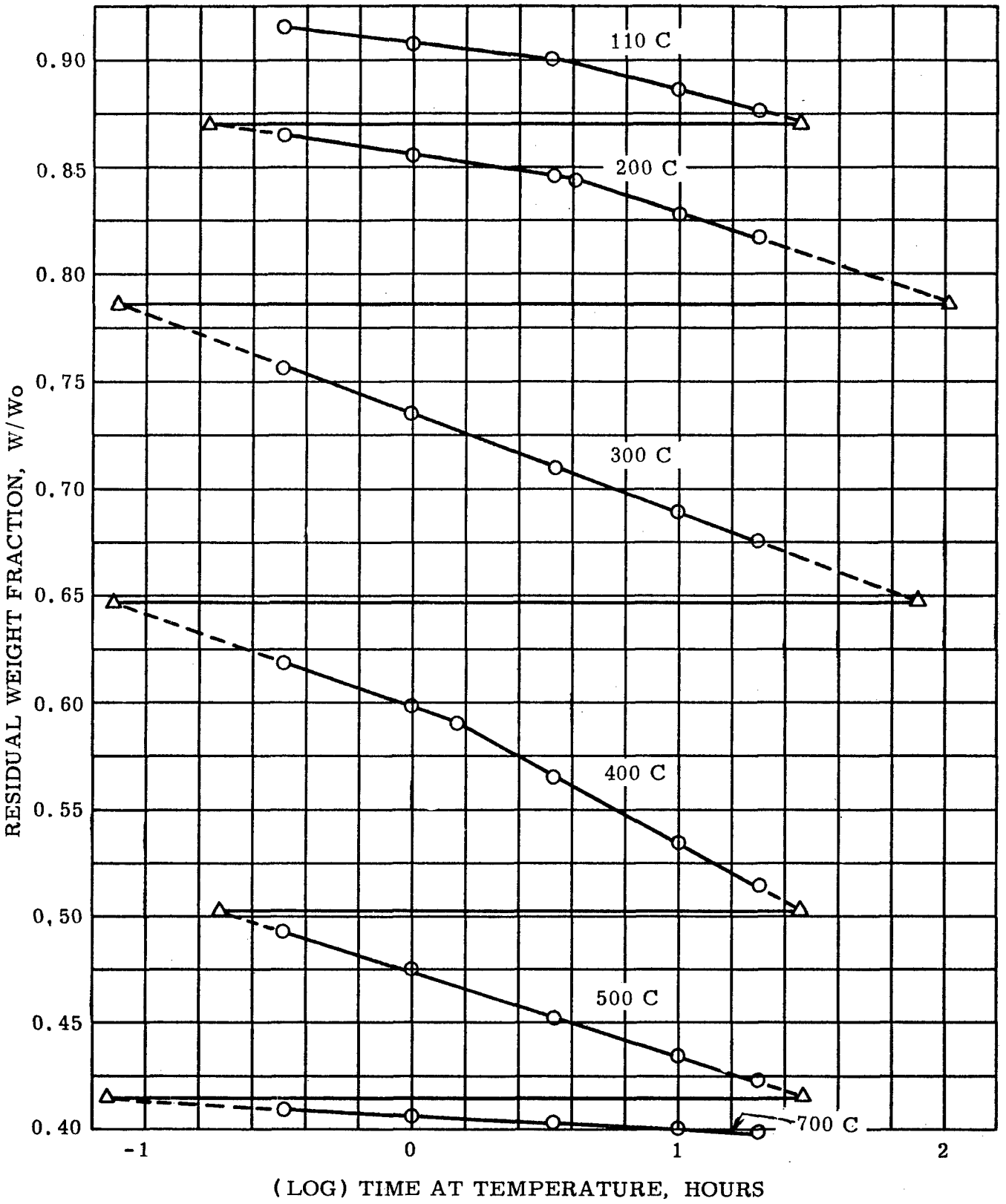

Figure 33 TGA IN DRY N_2 AT CONSTANT TEMPERATURE, REACTION PRODUCT OF ACONITIC ACID AND ACETIC ANHYDRIDE, CODE 88, 8/58
O DATA POINTS Δ EXTRAPOLATED MATCHING POINTS

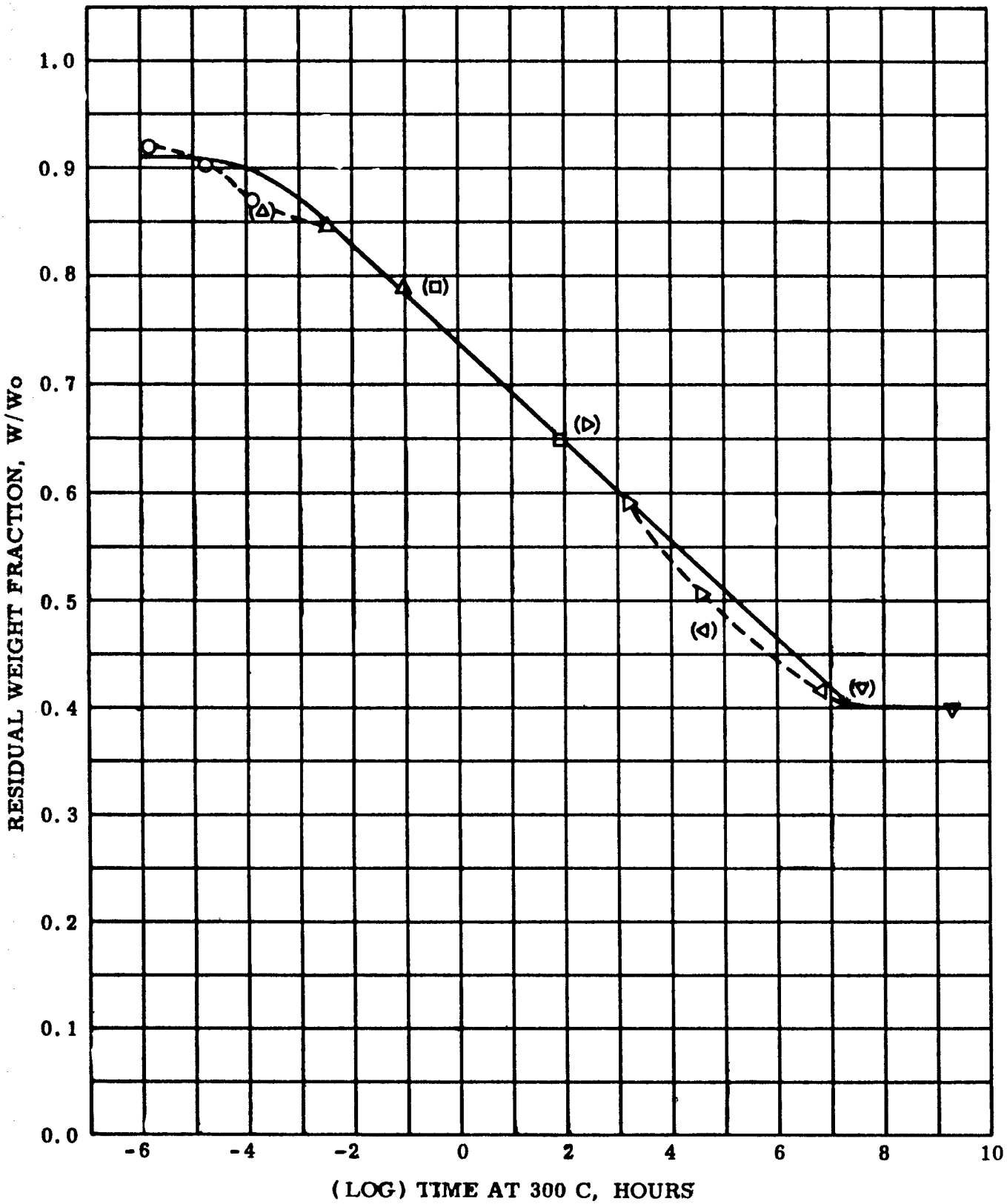

Figure 34 HEAD- TO- TAIL SUPERPOSITION OF AGING DATA FOR REACTION PRODUCT OF ACONITIC ACID AND ACETIC ANHYDRIDE, CODE 88, 8/58, IN DRY N_2 AT:

○ 110 C, △ 200 C, □ 300 C, ▷ 400 C, ◁ 500 C AND ▽ 700 C

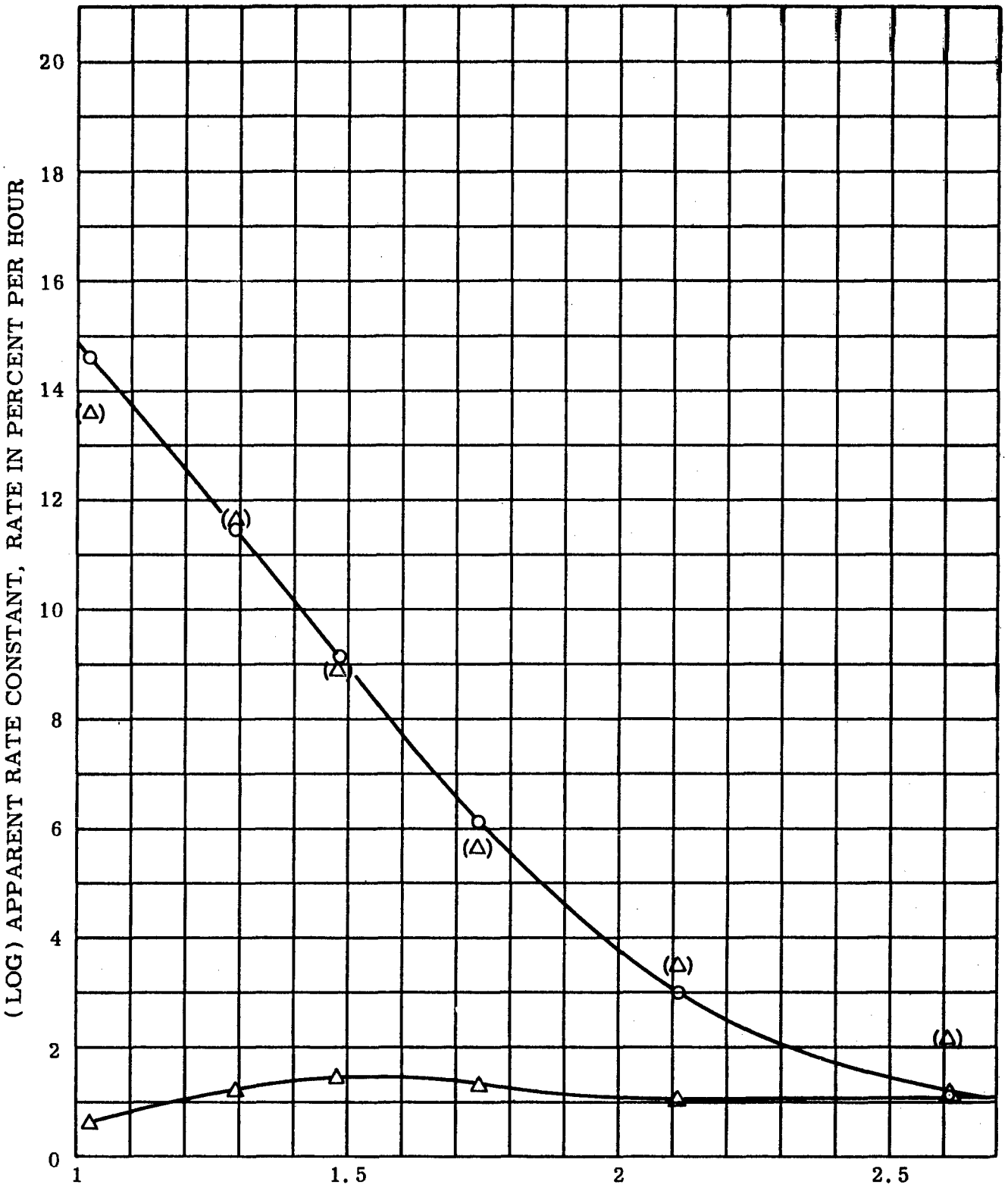

Figure 35 COMPARISON OF VOLATILIZATION RATES, " Δ " AND ESTIMATED APPARENT RATE CONSTANTS, "(Δ)" FROM THE MAGNIFIED THERMOGRAM WITH APPARENT RATE CONSTANTS, "O" FROM ISOTHERMAL AGING OF THE REACTION PRODUCT OF ACONITIC ACID AND ACETIC ANHYDRIDE, CODE 88, 8/58, IN DRY N_2

in Figure 34 are alternative matching points, given in parentheses near the corresponding plotted matching points. The remaining plotted points are those at which bends occurred in the individual curves.

From the dotted curve in Figure 34, appropriate values of α_T and then of b can be found readily for each volatilization step, using Equations 24 and 29, thus completing the quasi-kinetic analysis of the aging data for AcoAc. It is interesting, however, to go a little further with the help of Equations 34 and 36 in order to illustrate the effect of the logarithmic process on the shape of the TGA curve. For simplicity's sake, this can be done satisfactorily by regarding the curve in Figure 34 as representing a case of one-step volatilization from w = .91 to w = .40, as shown by the solid line. This simplification permits the derivation of values of k_a on the basis of a single value of k'/H.

From the slope of the solid curve in Figure 34, Equation 34 yielded a value of k'/H = 50.4 per unit apparent weight fraction. Next, k_a was found by substituting in Equation 36 a convenient value of t and the corresponding value of w read from the 300 C curve. The resulting value of k_a at 300 C, 12,910 per hour, was then taken as the master apparent rate constant, k_{am}, in finding values of k_a appropriate to the other aging temperatures using:

$$k_a \cong \frac{k_{am} t_{im}}{ti} \qquad (40)$$

as in Equation 26.

The resulting values of k_a for rates expressed in percent per hour, are given as logarithms in Table 17. Also given for reference in Table 17 are the values of log α_T found from k_a and k_{am} as in Equation 27, viz, by subtracting log k_{am} from each value of log k_a.

Table 17

Rate and Superposition Data for 200 mg Samples of "AcoAc" Powder Aged in Dry N_2

Aging Temperature, °C	log k_a, per hr	log α_T
110	1.173	- 4.94
200	3.021	- 3.09
300	6.111	0
400	9.141	3.03
500	11.491	5.38
700	14.651	8.54

The Arrhenius plot of the apparent rate constants in Table 17 is shown in Figure 35. The value of b found from the slope of the linear part of the curve was 11,800, corresponding to a value of E of 54 K cal. In the curved region of the Arrhenius plot, values of 36 and 26 K cal can be found at 200 and 110 C by the loose usage of Equation 28.

It is interesting to compare the apparent rate constants in Figure 35 with the corresponding apparent volatilization rates read from the TGA curve for AcoAc. Excepting those in the neighborhood of 10% per hour, the apparent volatilization rates bear little resemblance to the apparent rate constants, as might be expected from the form of f(w) in Equation 38. Because the exponential increase of the apparent rate constant with temperature is almost exactly compensated by the exponential decrease of f(w) with residual weight fraction, the apparent rate of volatilization remains almost constant over a long temperature range. Thus, the TGA curve for AcoAc is virtually linear over the same long temperature range.

In future, then, possible operation of the logarithmic rate process can be surmised from gently sloping TGA curves. Further, given a single logarithmic aging curve at a temperature in the gently sloped region of the TGA curve, the apparent rate constants at several temperatures can be found from the corresponding apparent volatilization rates read from the TGA curve, using Equation 38. The results of applying this procedure to the data for AcoAc are shown as triangles in parentheses in Figure 35.

Another way of applying a single aging curve as an aid to the quasi-kinetic analysis of a TGA curve is one suggested by the striking similarity of the shapes of the superposed curves in Figures 25, 28, 31, and 34 and the corresponding TGA curves. As will next be shown, rather extensively linear relationships are sometimes found between the log of aging time and the reciprocal absolute TGA temperature.

2. An Empirical Relationship between Aging Times and TGA Temperatures. The relationship between aging times and TGA temperatures to be given in this subsection cannot presently be regarded as anything but empirical. There does exist, however, some slight theoretical basis for it, as will next be shown.

Equation 25, the general equation of the isothermal aging curve, can be expressed in terms of the true residual weight fraction as:

$$g(h) \cong \underline{k}t \qquad (41)$$

From Equation 22 in Subsection IV B1 of this report, the analogous temperature relationship can be written:

$$g(h) \cong \frac{A}{B}\left(Te^{-x} - \frac{ES}{R}\right) \qquad (42)$$

provided terms with zero subscripts can be ignored.

If samples of the same geometry and degree of subdivision are used in both isothermal aging tests and TGA, then at identical values of w, the corresponding values of h and g(h) from aging and TGA are identical. Thus, at the time, t_i, and the absolute TGA temperature, T_i, at which the same value of w occurs:

$$kt_i \cong \frac{A}{B}\left(T_i e^{-x_i} - \frac{ES_i}{R}\right) \qquad (43)$$

At values of x greater than about 15, the value of S_i can be approximated roughly by:

$$S_i \cong e^{-x_i - e} \qquad (44)$$

then:

$$kt_i \cong \frac{Ae^{x_i}}{B}\left(T_i - \frac{E}{R}e^{-e}\right) \qquad (45)$$

The value of Re^e is about 30, so that the constant term in the parentheses in Equation 45 is usually a large negative number. Further, the logarithmic form of the Arrhenius rate equation suggests that when materials having similar $\underline{A}$ values (as do many carbonaceous polymers) are all compared on the same empirical rate constants, $\underline{k}_c$, the ratio of $\underline{E}$ to T is nearly constant:

$$(\log \underline{k}_c - \log \underline{A})R \cong C \cong -\frac{E}{T} \qquad (46)$$

where C is a constant.

From Equation 46, which suggests that the magnitude of T_i tends to be proportional to that of $\underline{E}$, the constant in the parentheses in Equation 45 will tend to be appreciably larger than all pertinent values of T_i likely to be encountered in a given TGA curve, making their difference nearly constant. With several grains of salt, then, Equation 45 is rewritten:

$$t_i \cong ae^{-\frac{b'\ln 10}{T_i}} \qquad (47)$$

or, more conveniently:

$$\log t_i \cong \log a - \frac{b'}{T_i} \qquad (48)$$

where t_i is time at some single aging temperature. As described earlier, however, data for other aging temperatures can be superposed on a common isothermal, and the usefulness of Equation 48 can thereby be extended:

$$\log t_i \cong \log a - \frac{b'}{T_i} - \log \alpha_T \qquad (49)$$

Plots of the logs of times at the superposition temperatures vs the corresponding reciprocal absolute TGA temperatures, drawn as suggested by the simplified approximate relationship in Equation 48, are shown in Figures 36, 37, 38, and 39 for 200 mg samples of pulverized "Teflon," polystyrene, chlorendic anhydride-hardened epoxy and AcoAc. Except in the inherently inaccurate TGA range, all four curves are remarkably linear. Further, the linear range encompasses the whole experimentally accessible range of residual weight fraction in every case except that of AcoAc. Even in this instance, however, the non-linearity which occurs at values of w greater than 0.872 arises only from the simplification arbitrarily used in deriving values of log α_T from Figure 34.

The constants of Equation 48 derived from the slopes and intercepts of Figures 36 through 39 are given for reference in Table 18.

Table 18

Constants of the Empirical Equation
Relating Isothermal Times to TGA Temperatures

Polymer	log a	b'
Polytetrafluoroethylene	22.1082	16,500
Polystyrene	18.8482	11,000
Epoxy	19.8182	10,000
AcoAc	22.2082	12,500

The life-times found from Equation 49, using the constants from Table 18 and the values of log α_T from Tables 14 through 17, are compared with observed life-times at five different levels of residual weight fraction in Table 19. In this case, the calculated life-times have been converted to minutes for convenient comparison with the raw aging data.

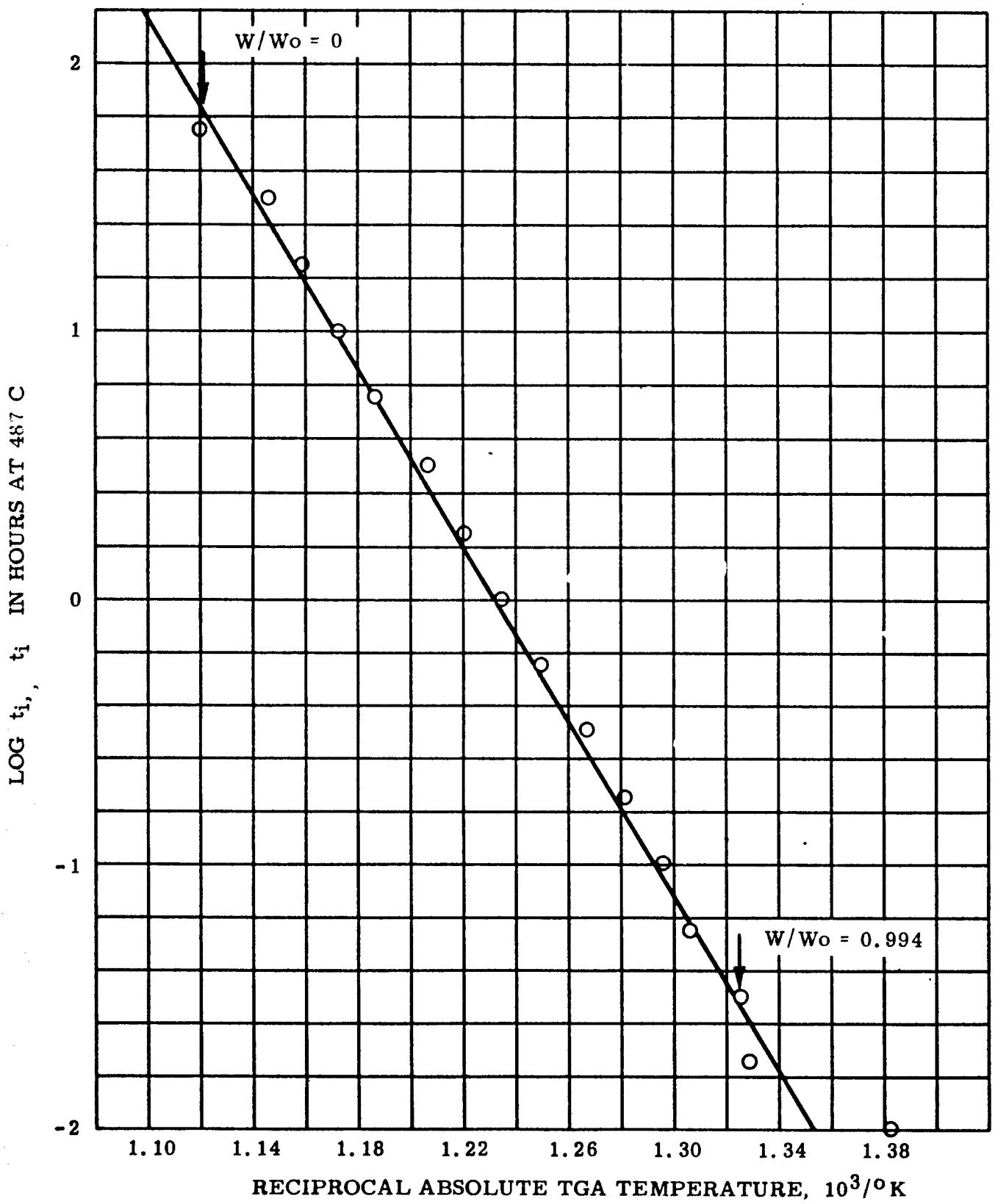

Figure 36. SIMPLIFIED APPROXIMATE RELATIONSHIP BETWEEN CORRESPONDING VALUES OF LIFE AT 487 C AND TEMPERATURE IN TGA, POLYTETRAFLUOROETHYLENE

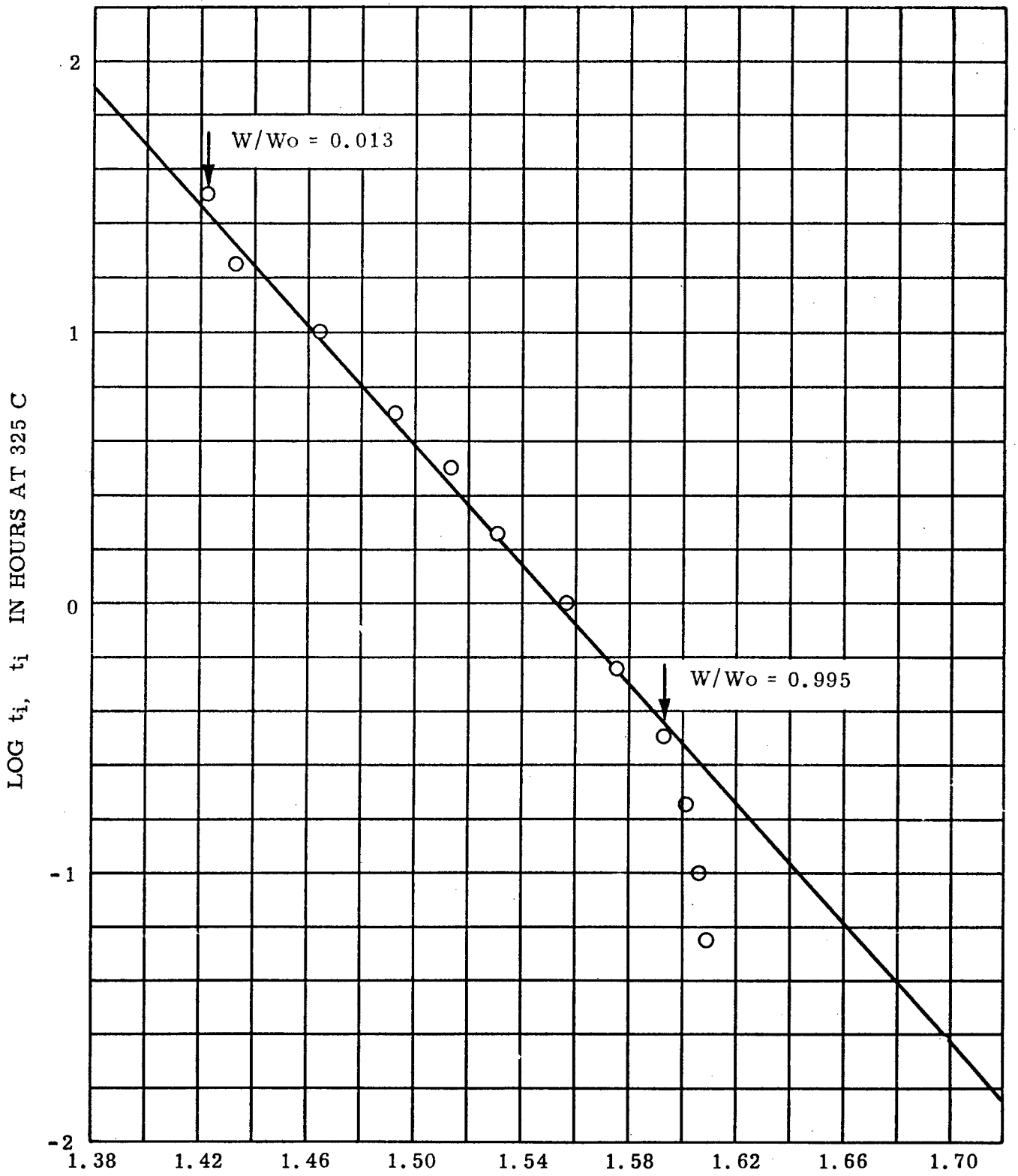

Figure 37 SIMPLIFIED APPROXIMATE RELATIONSHIP BETWEEN CORRESPONDING VALUES OF LIFE AT 325 C AND TEMPERATURE IN TGA, POLYSTYRENE

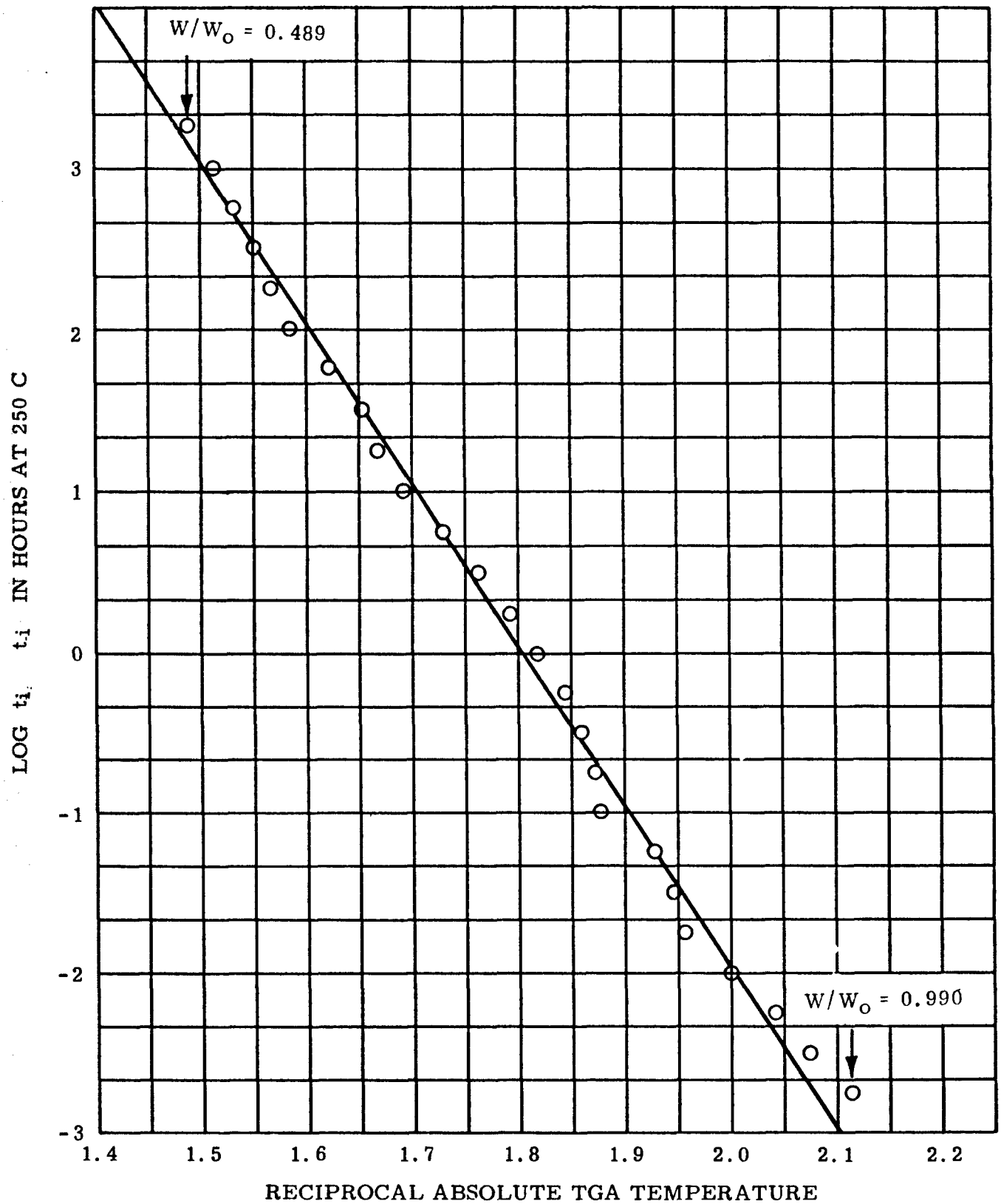

Figure 38 SIMPLIFIED APPROXIMATE RELATIONSHIP BETWEEN CORRESPONDING VALUES OF LIFE AT 250 C AND TEMPERATURE IN TGA, CHLORENDIC ANHYDRIDE - HARDENED EPOXY, CODE 22/10

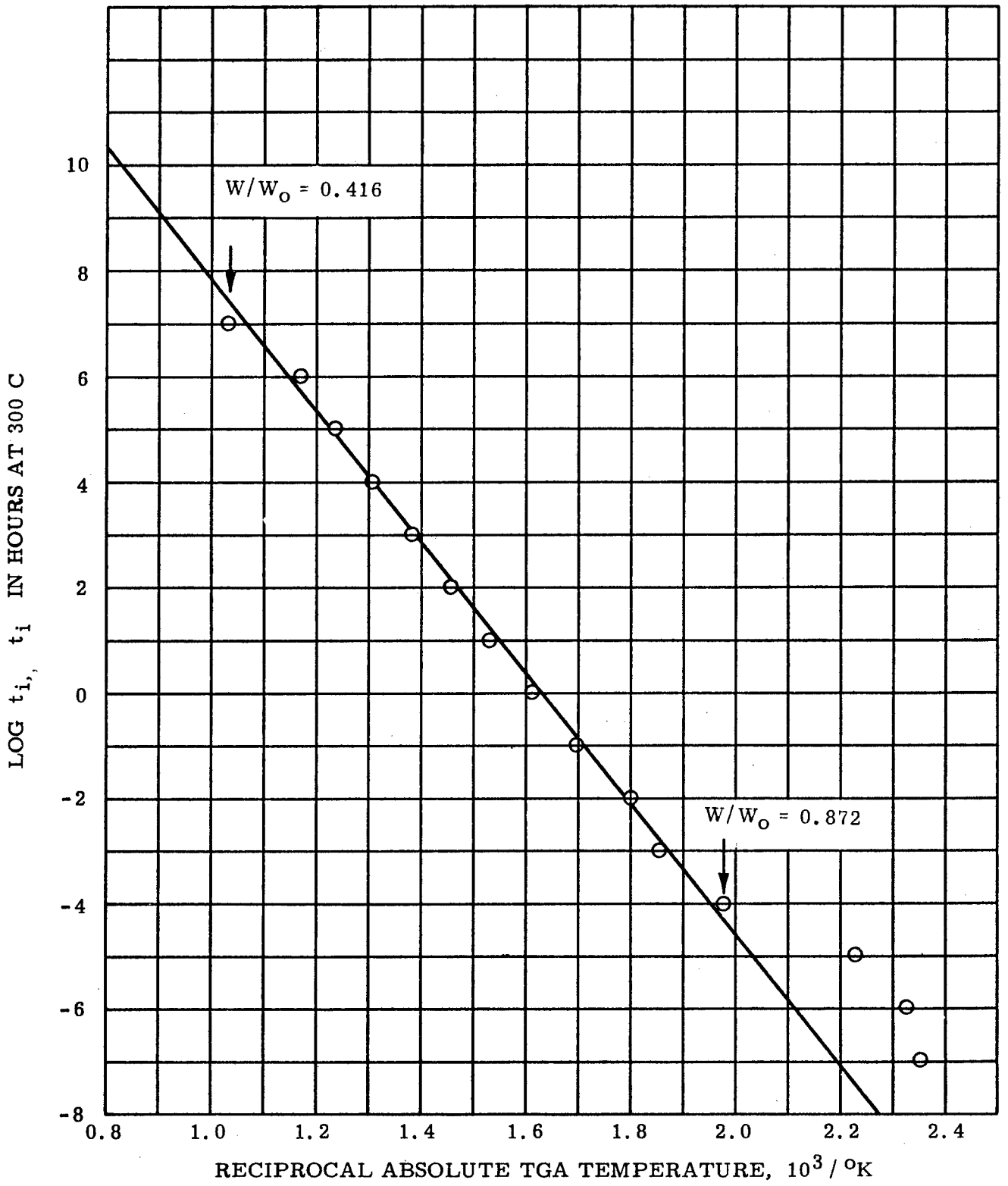

Figure 39 SIMPLIFIED APPROXIMATE RELATIONSHIP BETWEEN CORRESPONDING VALUES OF LIFE AT 300 C AND TEMPERATURE IN TGA, REACTION PRODUCT OF ACONITIC ACID AND ACETIC ANHYDRIDE, CODE 88, 8/58

Table 19

Calculated and Observed Lifetimes
of 200 mg Pulverized Polymer Samples, minutes in Dry N_2

Polytetrafluoroethylene

Aging Temp.°C	0.9 Obs.	0.9 Calc.	0.7 Obs.	0.7 Calc.	0.5 Obs.	0.5 Calc.	0.3 Obs.	0.3 Calc.	0.1 Obs.	0.1 Calc.	W/W_o
430	---	3380	---	1.22×10^4	---	2.67×10^4	---	5.01×10^4	---	9.24×10^4	
450	734	691	---	2490	---	5460	---	1.03×10^4	---	1.89×10^4	
480	87	75	304	270	580	593	1171	1110	---	2050	
490	44	39	170	141	320	309	642	581	---	1070	
500	29	23	91	84	187	184	422	345	927	636	
510	19	14	62	50	106	111	204	208	454	383	
520	6	9	31	31	58	68	114	127	250	234	

Polystyrene

Aging Temp.°C	0.9 Obs.	0.9 Calc.	0.7 Obs.	0.7 Calc.	0.5 Obs.	0.5 Calc.	0.3 Obs.	0.3 Calc.	0.1 Obs.	0.1 Calc.	W/W_o
300	255	344	1165	1020	---	1790	---	3450	---	5560	
320	104	93	424	277	696	487	1001	938	1504	1490	
325	79	68	257	203	---	356	---	687	---	1100	
337	35	33	124	98	201	172	393	331	454	533	
342	29	25	92	73	154	128	226	247	359	397	
350	13	16	49	46	79	81	110	155	171	250	

Chlorendic-Anhydride-Hardened Epoxy, Code 22/10

Aging Temp.°C	0.9 Obs.	0.9 Calc.	0.8 Obs.	0.8 Calc.	0.7 Obs.	0.7 Calc.	0.6 Obs.	0.6 Calc.	0.5 Obs.	0.5 Calc.	W/W_o
200	---	1.01×10^5	---	2.9×10^5	---	5.11×10^5	---	1.51×10^6	---	1.20×10^7	
240	711	1360	---	3880	---	6830	---	2.02×10^4	---	1.60×10^5	
250	523	512	1273	1460	---	2580	---	7620	---	6.03×10^4	
275	60	52	156	149	313	263	609	778	---	6150	
300	2	7	12	19	27	33	65	97	1004	766	

AcoAc

Aging Temp.°C	0.85 Obs.	0.85 Calc.	0.75 Obs.	0.75 Calc.	0.65 Obs.	0.65 Calc.	0.55 Obs.	0.55 Calc.	0.45 Obs.	0.45 Calc.	W/W_o
110	---	7390	---	7.14×10^6	---	5.45×10^8	---	3.89×10^{10}	---	4.25×10^{12}	
200	120	68	---	6.61×10^4	---	5.04×10^6	---	3.60×10^8	---	3.94×10^{10}	
300	---	8.53×10^{-2}	27	82	---	6280	---	4.49×10^5	---	4.90×10^7	
400	---	6.95×10^{-5}	---	6.72×10^{-2}	---	5	360	366	---	4.00×10^4	
500	---	3.57×10^{-7}	---	3.45×10^{-4}	---	2.63×10^{-2}	---	19	210	206	
700	---	2.43×10^{-10}	---	2.35×10^{-7}	---	1.79×10^{-5}	---	1.28×10^{-3}	---	1.40×10^{-1}	

Considering the tremendously broad ranges of time, temperature, and residual weight fraction encompassed by Table 19, the agreement between observed and calculated values is regarded as quite good. This is especially interesting in view of the widely different kinetic processes represented. Although it is unsafe to conclude that the empirical plot of log t_i vs $\frac{1}{T_i}$ will be extensively linear in all cases, further study of this interesting relationship is clearly warranted.

D. Summary of Observations Regarding Kinetic Analysis of TGA Curves

To sum up, kinetic analysis of inert atmosphere weight-loss data alone leads only to kinetic constants which are unauthentic until proven otherwise by corroborative studies. This is true because volatilization rates bear only an implied relationship to decomposition rates and because they depend on not only the temperature, but also the apparent kinetic process and the geometry and degree of subdivision of the sample, all of which may change with temperature. For the same reason, the kinetic constants found from weight-loss data alone are of limited practical value; they cannot be extrapolated to different experimental conditions on present knowledge, and in many cases, they are valid only for narrow temperature ranges even for the procedural conditions employed.

While the nature of the apparent kinetic process can sometimes be surmised from weight-loss data, especially when both TGA and isothermal aging test results are available, little is known about the accompanying effects of geometry and degree of subdivision, especially as these sample characteristics change with extent of volatilization. Thus, present-day studies of the volatilization of laboratory samples lead to little more than logical starting points for more significant investigations.

The value of TGA curves alone as sources of kinetic data is further limited by inherent inaccuracy of TGA at small volatilization rates. Moreover, no powerful quasi-kinetic analytical technique comparable to empirical time-temperature superposition of aging curves has yet been found for TGA. Since it encompasses the whole temperature range of interest, however, the TGA curve does have value as an adjunct of short-time aging curves which can be satisfactorily treated by simple quasi-kinetic methods.

As far as can presently be seen, TGA in inert atmosphere will probably remain more valuable as an empirical screening test for polymers than as a source of kinetic data. Even in this role, however, TGA is not a sufficient test of intrinsic thermal stability in view of the possibility of reaction without weight change and in view of the eventual need to examine

promising materials in reactive atmospheres. For these reasons, corroborative screening test methods have also been studied. Two of these will next be discussed briefly and compared with TGA in dry N_2.

V. TWO CORROBORATIVE EMPIRICAL TECHNIQUES FOR MEASURING THERMAL STABILITY

The need for corroborative methods has been discussed previously(1), as has the use of differential thermal analysis (DTA) in this role. Because the value of DTA was found to be severely limited by broad irreproducibility and frequent insensitivity, means were sought for improving the experimental technique. Concurrently, other corroborative methods were also considered. Progress along these lines will next be summarized briefly.

A. Improved Differential Thermal Analysis

In order to minimize base-line drift, it has long been the practice in DTA to dilute the sample with the inert reference material to the greatest possible extent commensurate with reasonable sensitivity (1). Since reasonable sensitivity has frequently been unattainable in tests on polymers, several schemes have been tried in past attempts to improve matters (1). In the most drastic of such schemes, DTA of polymers has recently been conducted in the total absence of diluent with rather startling results: sensitivity was increased so greatly that even such diffuse heat effects as those associated with second order transitions were detectable in some cases, and large variations in the particle size of the sample appeared to have little untoward effect (9).

So promising a technique was tried immediately, but its use necessitated extensive redesign of the sample holder to prevent leakage of the unrestrained sample in case of melting. A photograph of the improved sample holder, designed in stainless steel by Mr. J. A. Hill, of the General Engineering Laboratory, is shown inFigure 40. The new holder is shown schematically in Figure 41.

In Figure 41 some additional improvements can be seen. For the sake of improved thermal uniformity within the wells, their ends have been made spherical rather than flat. To minimize errors due to partial volatilization of the sample, the vented cover section has been designed to gravitate downward as the sample volatilizes, thus keeping the sample thermocouple in constant contact with the sample. To eliminate chemical attack of the sample thermocouple by the decomposing sample material, a Pt foil "boot" was fashioned in a home-made jig to fit tightly over the ceramic lead-in insulator. The need for such protection is illustrated in Figure 42.

Figure 40 Improved DTA Sample Holder

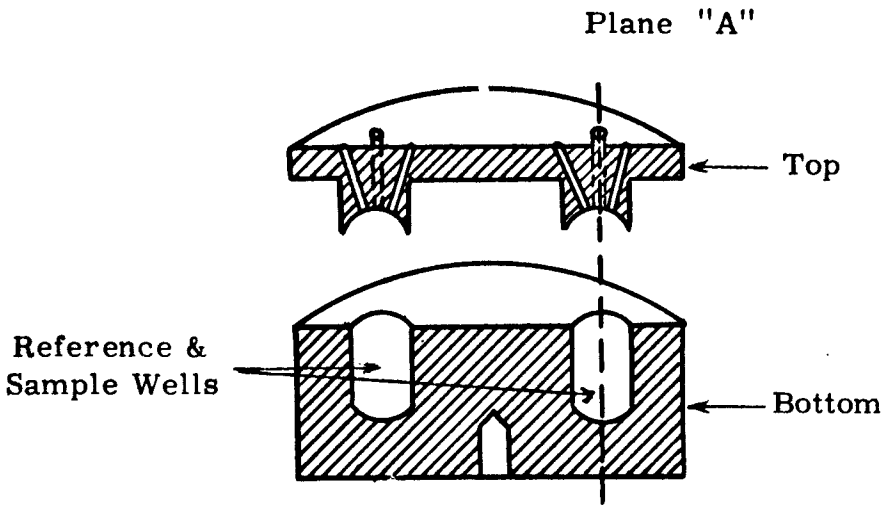

X - SECTION OF SAMPLE HOLDER

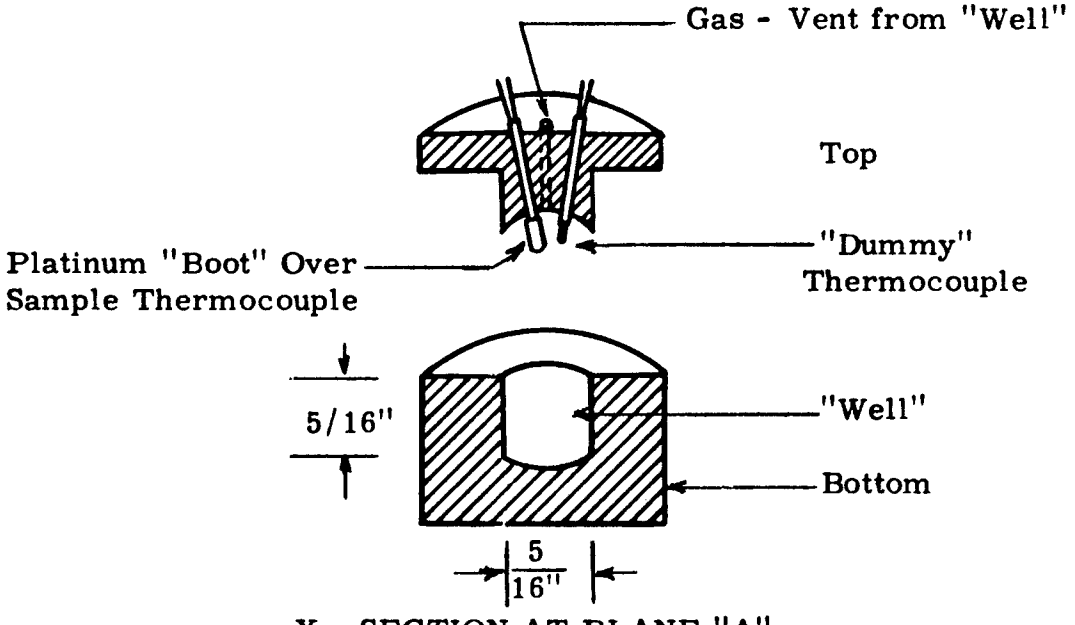

X - SECTION AT PLANE "A"

Figure 41
SAMPLE HOLDER FOR DIFFERENTIAL THERMAL ANALYSIS
OF UNDILUTED MATERIALS

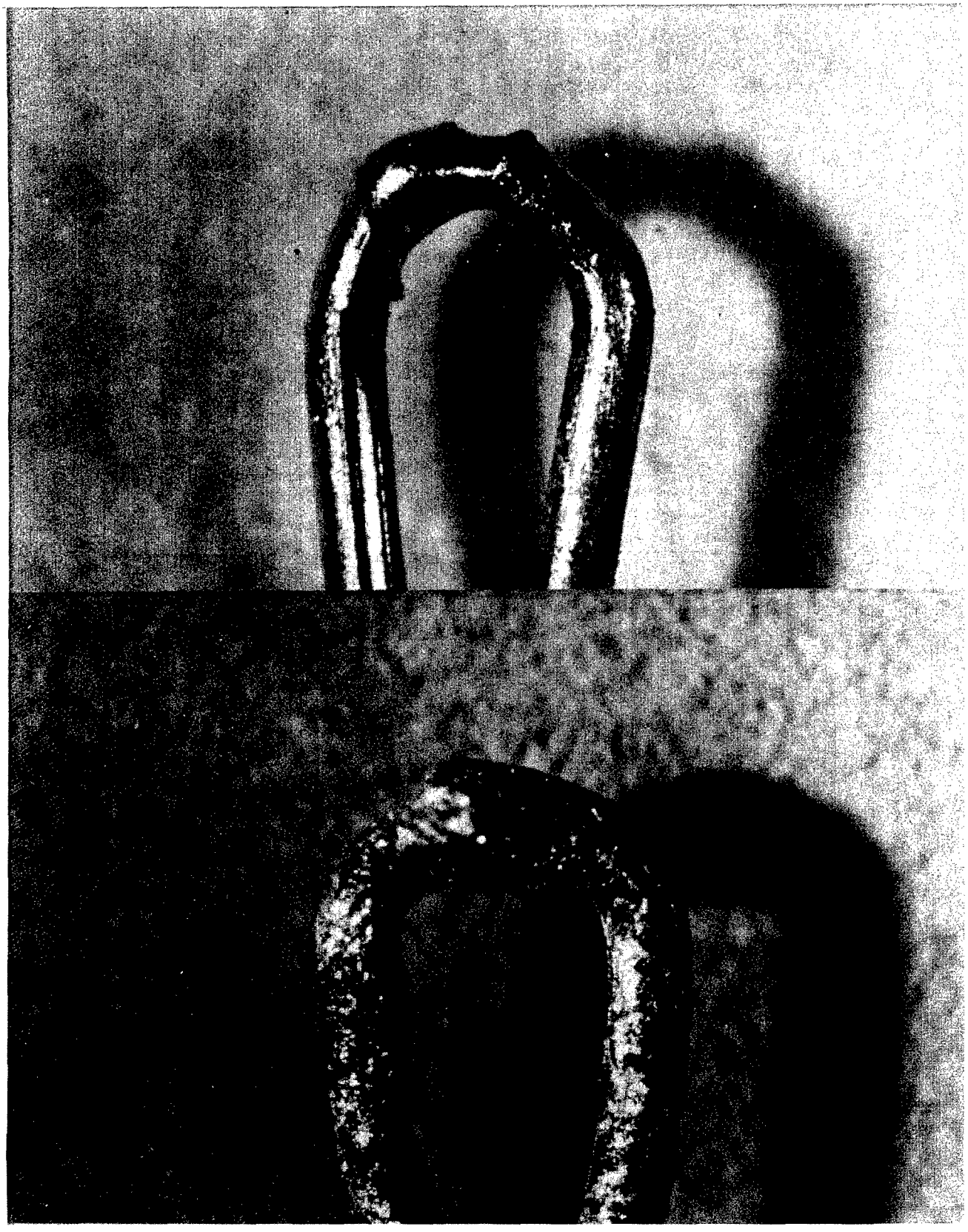

Figure 42 DTA Sample Thermocouple (13 mil dia. Pt-PtRh Wire)
Upper Photo: new
Lower Photo: after one run on resin of Me_2N + B + H (Burg)

DTA curves determined for 100 mg pulverized samples heated in the improved holder at 180 C degrees per hour in dry N_2 are compared with the corresponding TGA curves in Figures 43 through 50. In general, these show that irreproducibility of DTA still remains a problem. Further, while use of the new holder greatly increases the sensitivity of DTA, Figures 43, 45, 46, 48, 49, and 50 show that in many instances, the heat effects accompanying gradual volatilization still tend to be insensibly small.

On the other hand, however, Figures 47 through 50 illustrate the occasional value of DTA as a means of sensing appreciable reactions which occur in advance of catastrophic volatilization. Since such reactions are sometimes observed, the study of corroborative techniques has been continued and extended to include a method, here called "thermoparticulate analysis" (TPA), capable of detecting certain types of minute weight losses (10).

B. Thermoparticulate Analysis

TPA affords a means of sensing the escape of gas-borne particles from a polymer as it is heated. As such, it is insensitive to the volatilization of small molecules, but it is highly sensitive to the escape of colloidal fragments. Further, since such fragments are sensed in the gas phase, TPA, unlike TGA, is potentially applicable in reactive atmospheres, provided the escaping fragments are not burned to small molecules before they can be detected.

The apparatus employed is shown in block diagram form (10) in Figure 51, where it is seen that back-ground error is minimized by filtering the atmospheric gas to remove foreign particles ahead of the sample heating furnace. The exit gas, bearing volatilized fragments of the sample, is then cooled before being passed into the particle detectors.

Two detectors are used to provide sensitivity to a wide range of particle size. The condensation nuclei detector, essentially a form of Wilson cloud chamber, senses particles upon which water can condense. Particles which can be detected by this device range from 10^{-7} to $10^{-4.5}$ cm in diameter. The Sinclair-Phoenix Smoke Photometer, which has been employed widely in smoke pollution studies, senses particles in the range from 10^{-5} to $10^{-2.6}$ cm using the principle of light scattering.

Preliminary studies have indicated that TPA may indeed be applicable in reactive atmospheres, as shown in Figures 52 and 53, even at temperatures in the neighborhood of 400 C. Further, the comparable Figures 54 and 55 for the same materials in dry N_2 suggest that TPA may be dramatically sensitive to reactions unaccompanied by catastrophic volatilization. This is especially clear, and most encouragingly so, in Figure 56. Conversely, Figure 57 suggests that in cases of concurrent reaction and

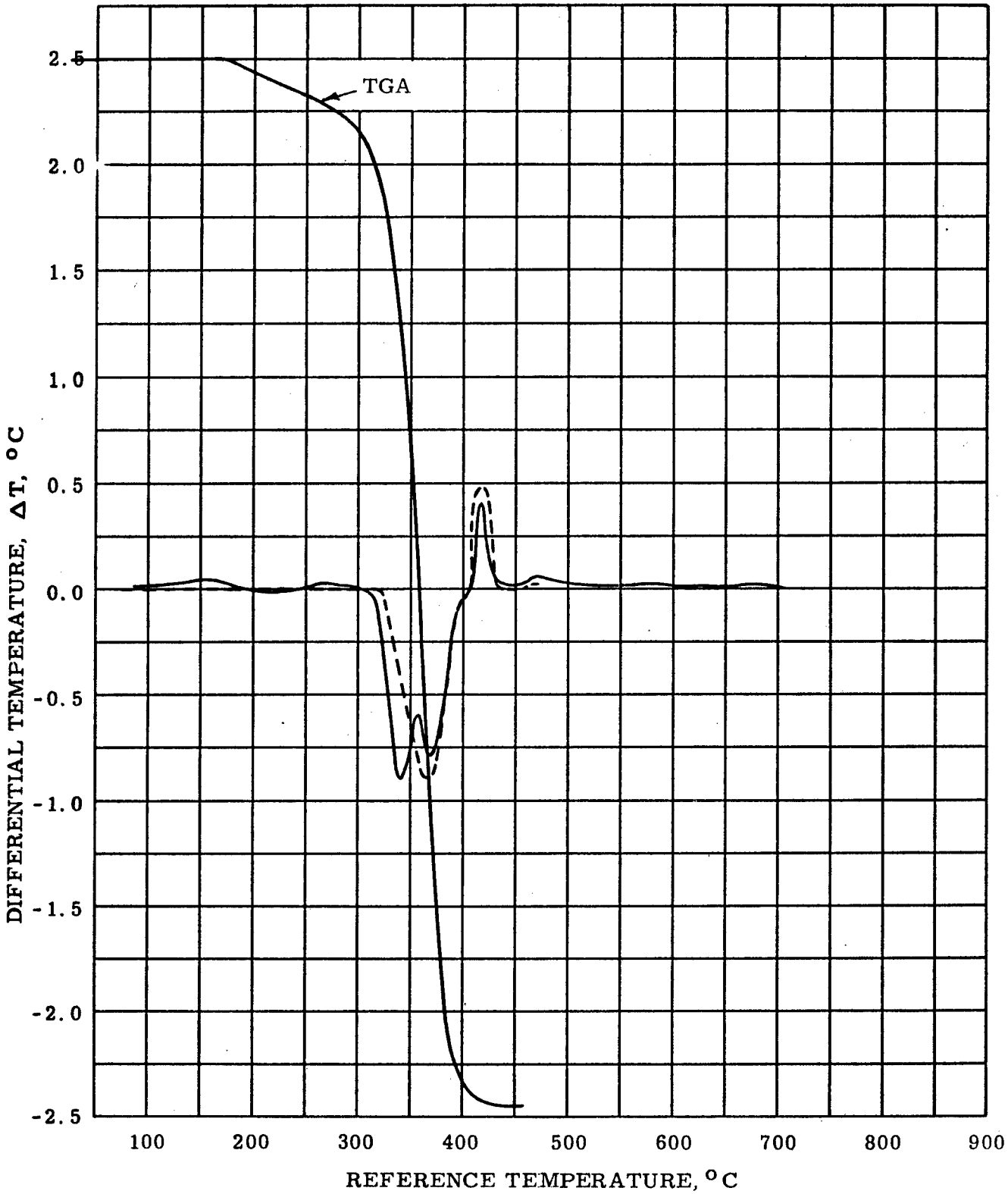

Figure 43 DTA IN DRY N_2 AT 180 C° PER HOUR, COMPARED WITH TGA AT THE SAME HEATING RATE, (POLY) METHYL METHACRYLATE ("PLEXIGLAS")

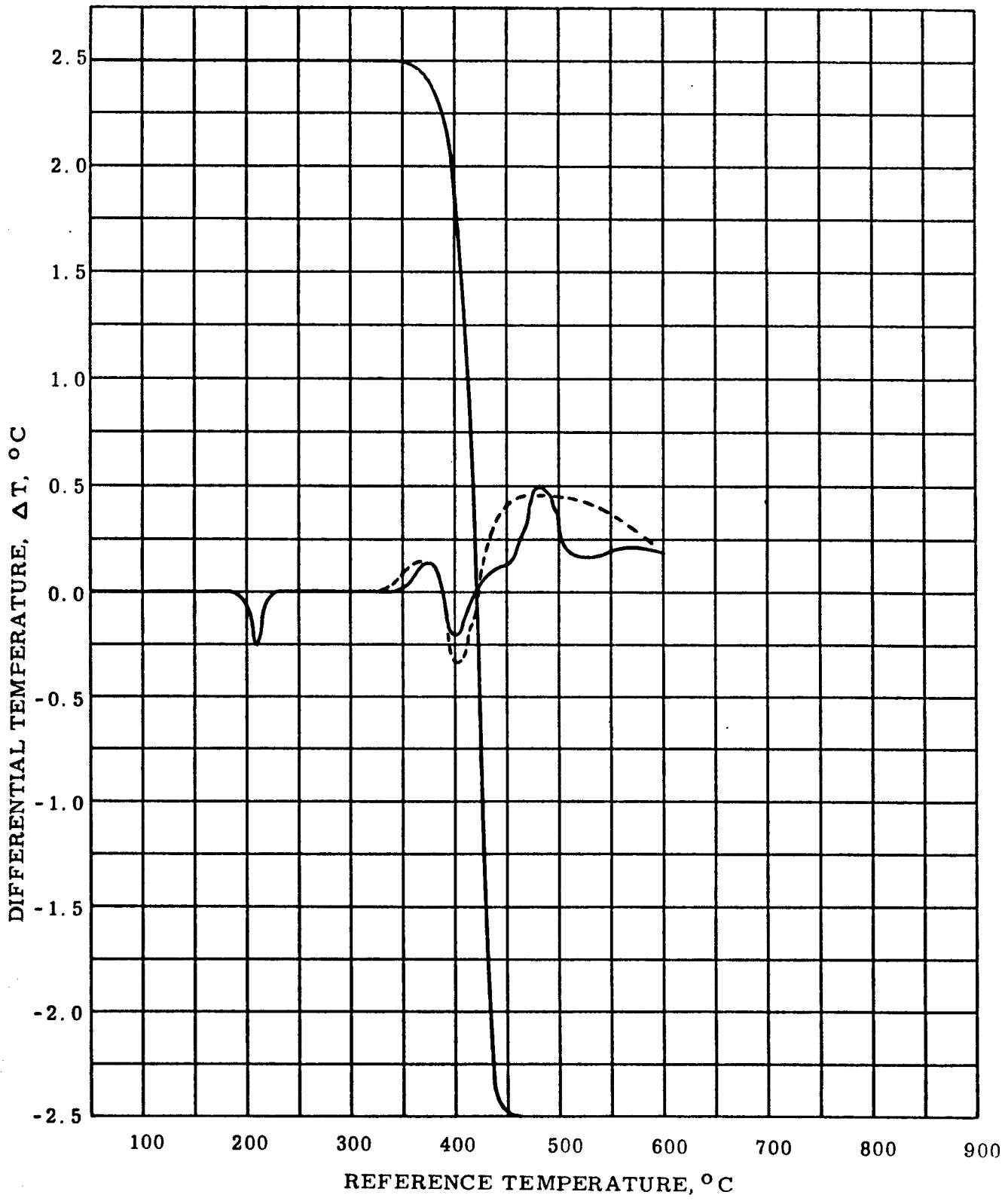

Figure 44 DTA IN DRY N_2 AT 180 C° PER HOUR, COMPARED WITH TGA AT THE SAME HEATING RATE, POLYCHLOROTRIFLUOROETHYLENE

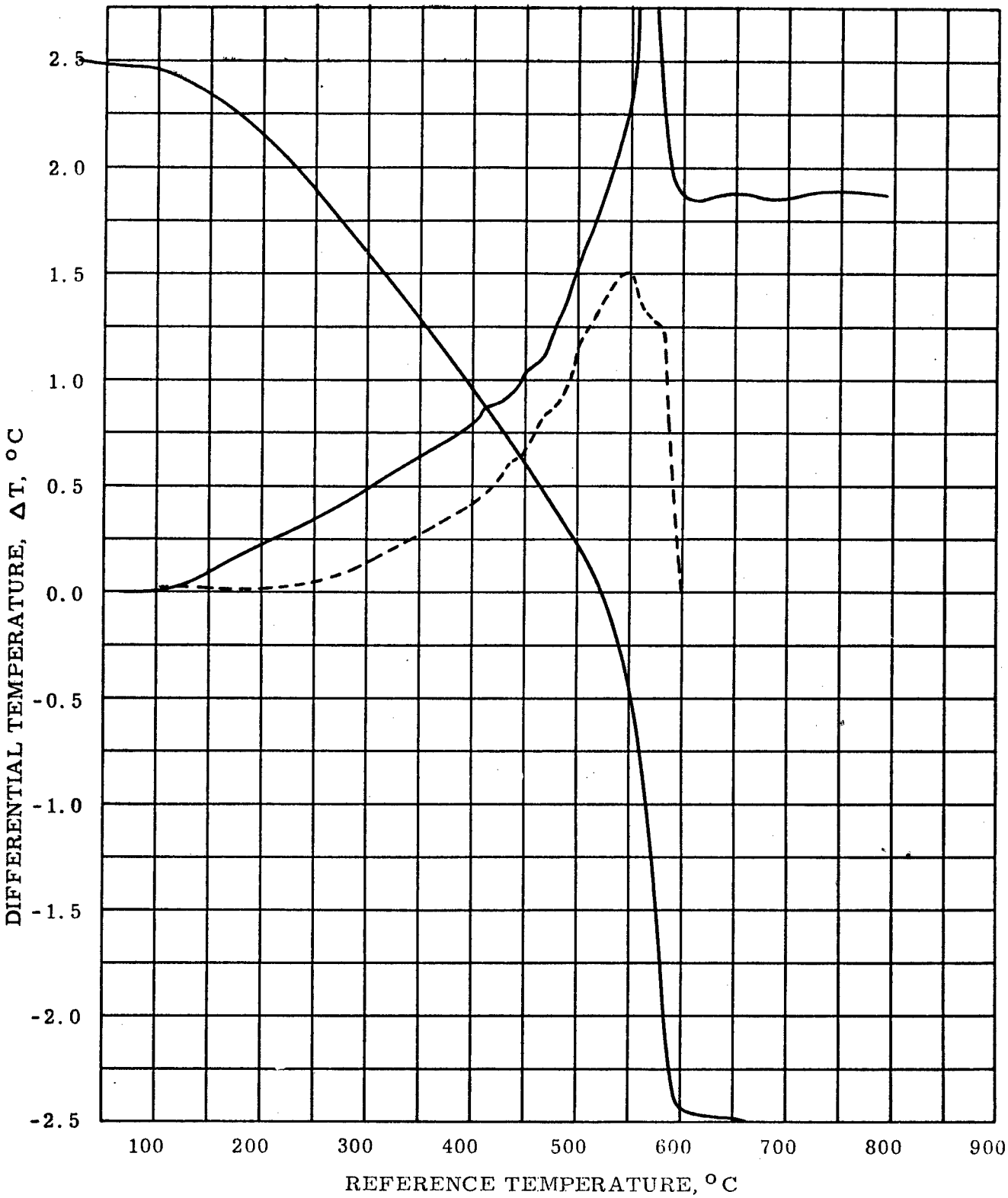

Figure 45 DTA IN DRY N_2 AT 180 C° PER HOUR, COMPARED WITH TGA AT THE SAME HEATING RATE, PERFLUOROGLUTARODIAMIDINE-PERFLUOROBUTYRAMIDINE COPOLYMER, CODE 282

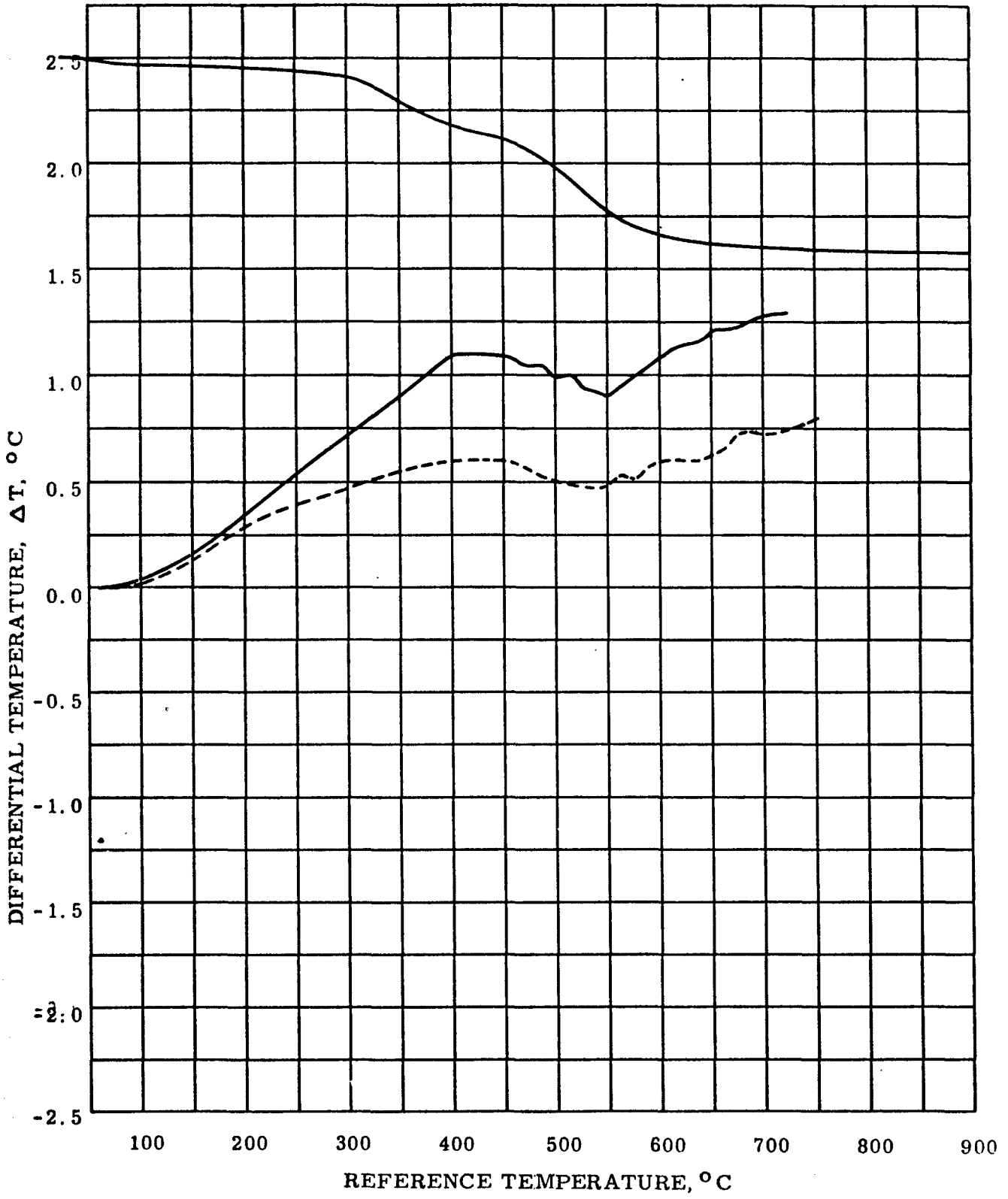

Figure 46 DTA IN DRY N_2 AT 180 C° PER HOUR, COMPARED WITH TGA AT THE SAME HEATING RATE, RESIN OF $Me_2N + Me_2P + B + H$ (BURG)

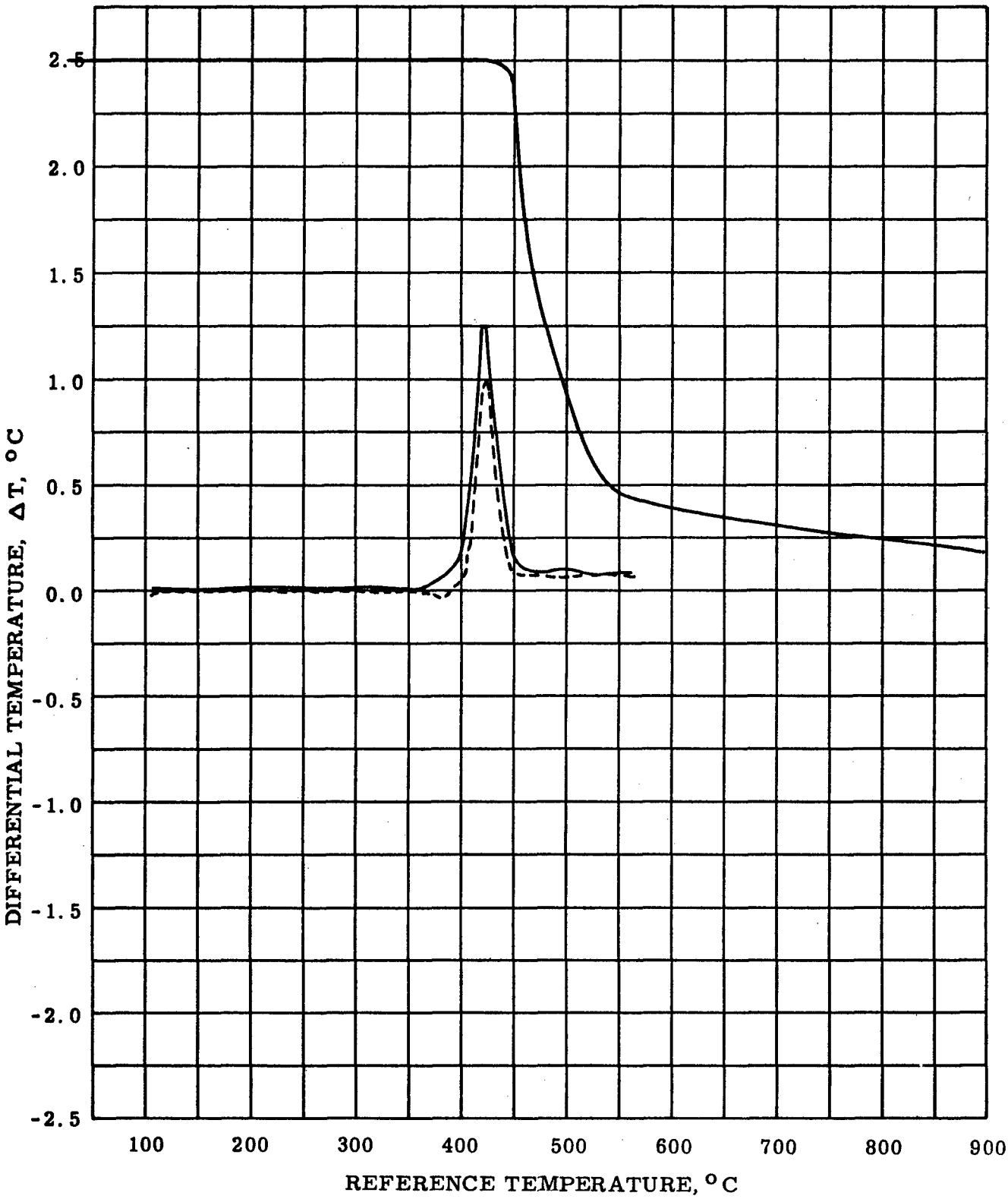

Figure 47 DTA IN DRY N_2 AT 180 C° PER HOUR, COMPARED WITH TGA AT THE SAME HEATING RATE, ZINC 4, 4' - BIS- THIOPICOLINAMIDODIPHENYL

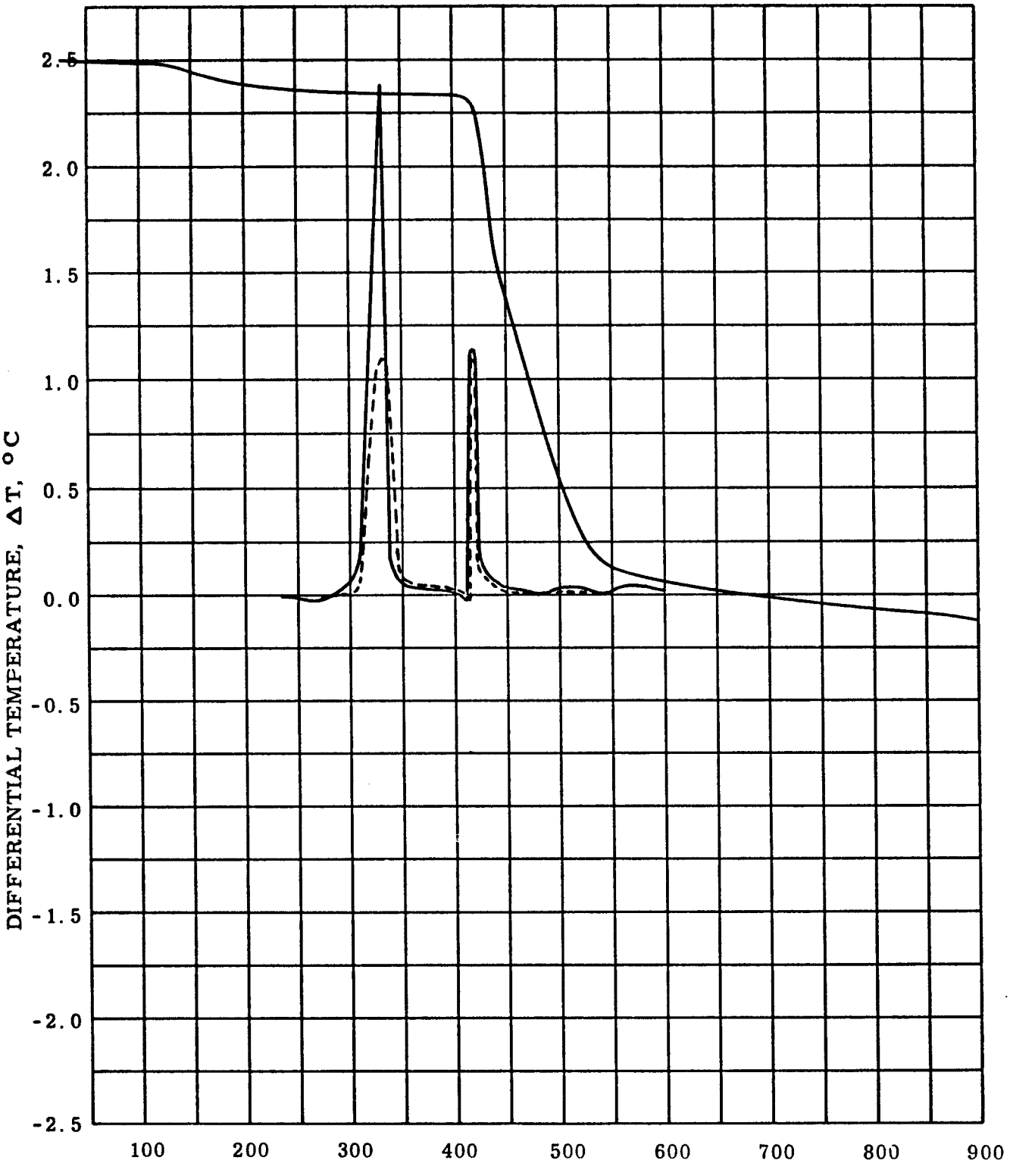

Figure 48 DTA IN DRY N_2 AT 180 C° PER HOUR, COMPARED WITH TGA AT THE SAME HEATING RATE, ZINC 4, 4 - BIS- THIOPICOLINAMIDODIPHENYL ETHER

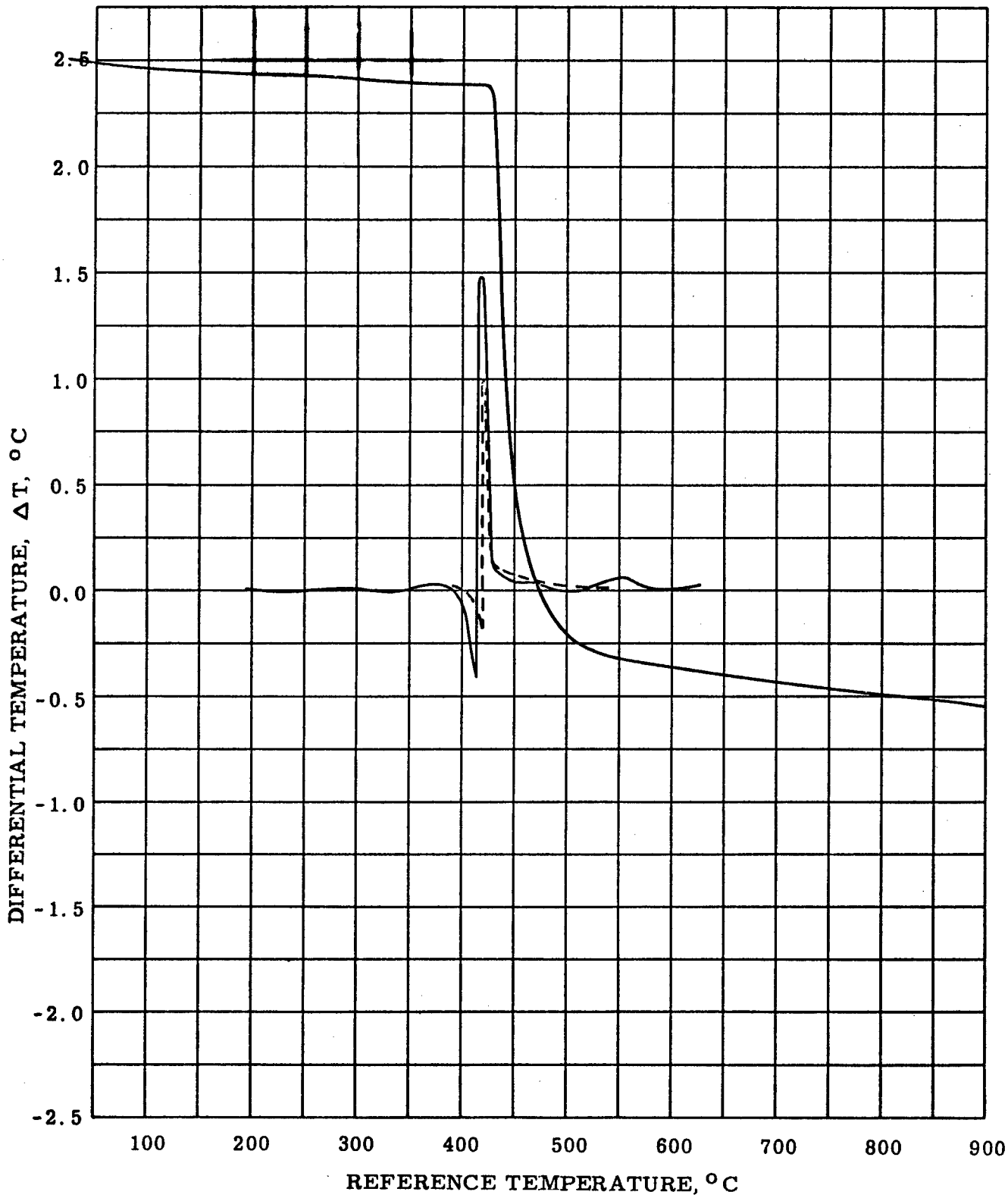

Figure 49 DTA IN DRY N_2 AT 180 C° PER HOUR, COMPARED WITH TGA AT THE SAME HEATING RATE, ZINC 4, 4' - BIS - THIOPICOLINAMIDODIPHENYL SULFONE

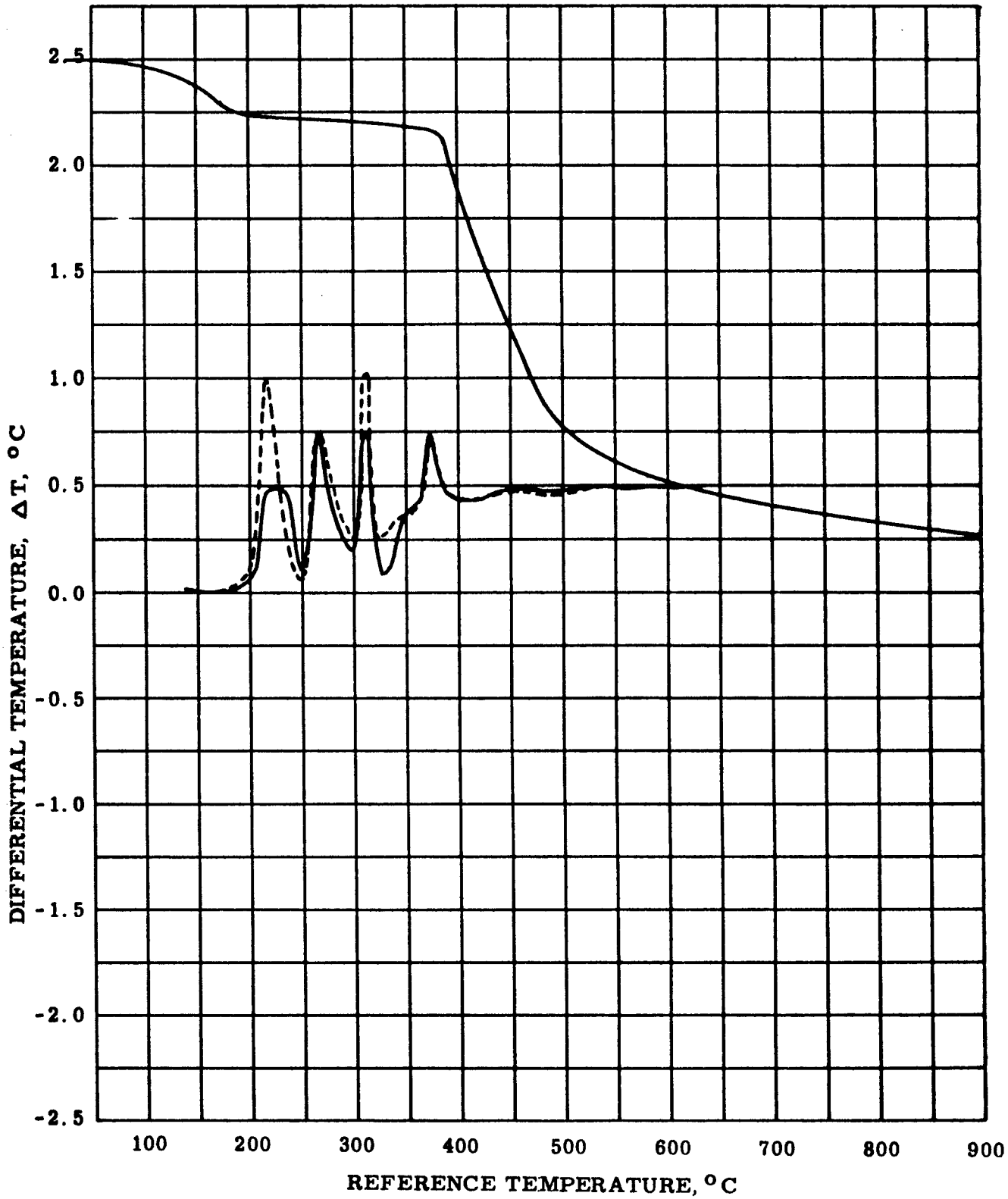

Figure 50 DTA IN DRY N_2 AT 180 C° PER HOUR, COMPARED WITH TGA AT THE SAME HEATING RATE, ZINC 4, 4' - BIS - THIOPICOLINAMIDODIBENZOPHENONE

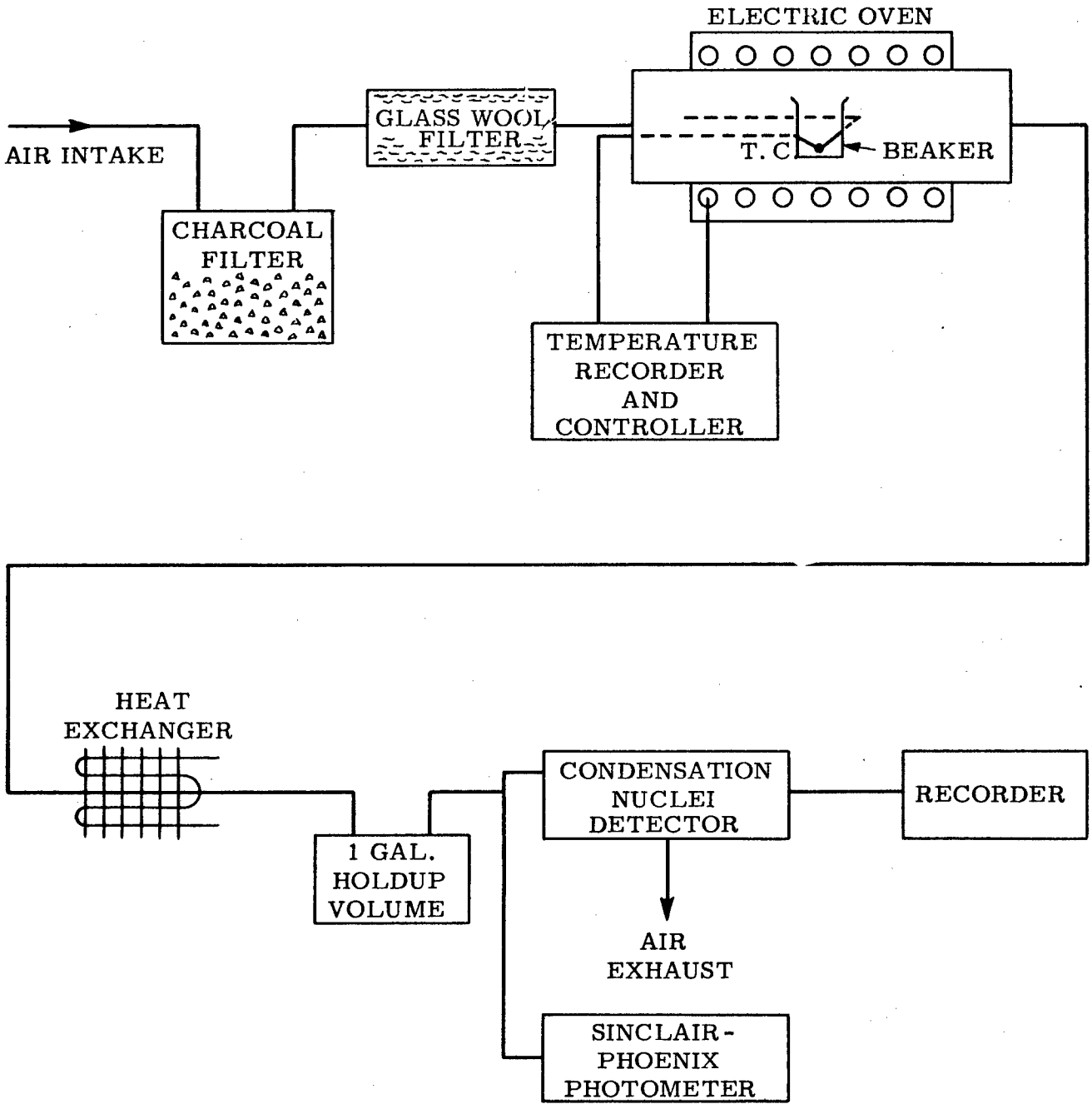

Figure 51 BLOCK DIAGRAM OF TPA TEST ASSEMBLY

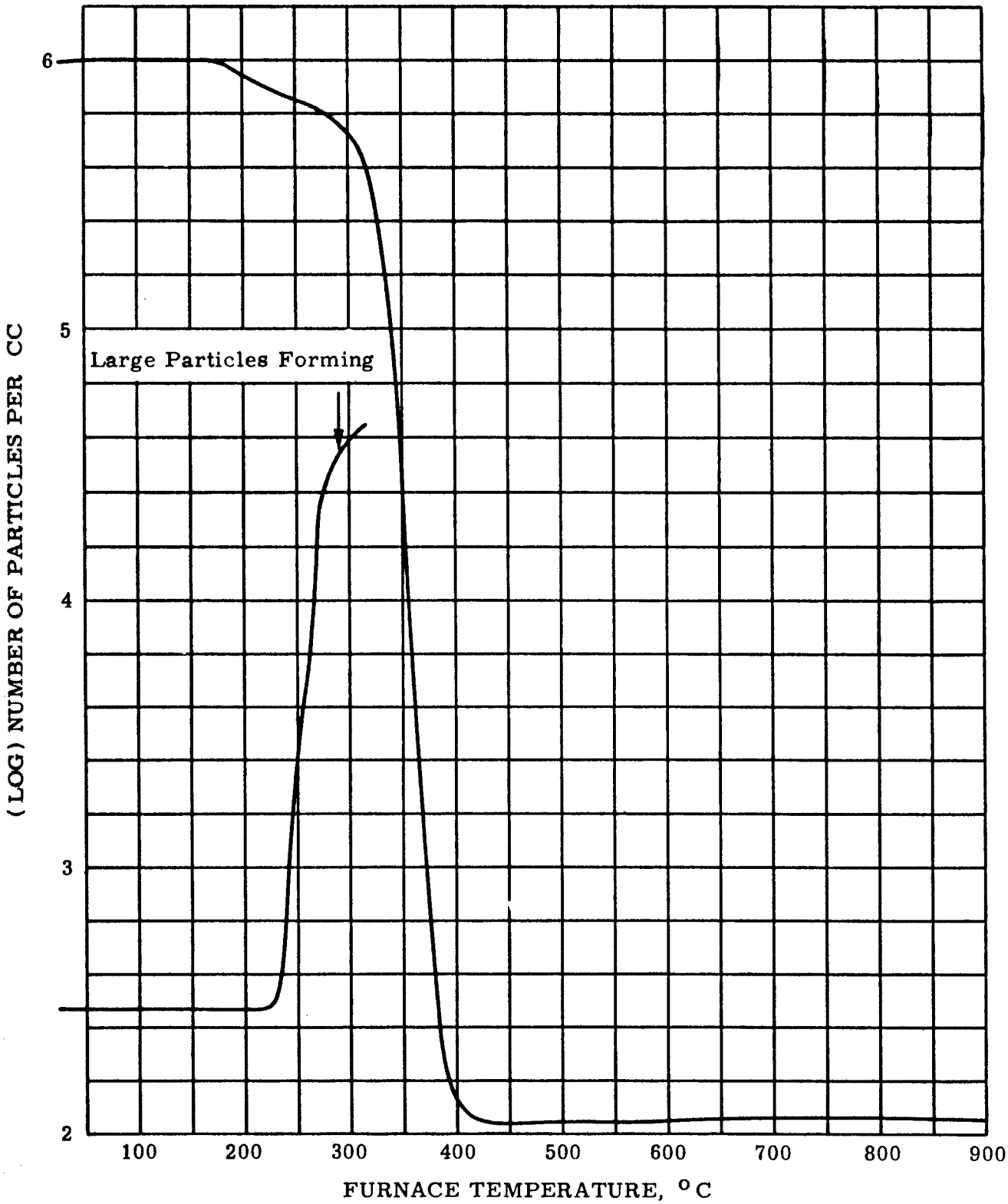

Figure 52 TPA IN AIR AT APPROXIMATELY 180 C° PER HOUR, COMPARED WITH TGA AT THE SAME HEATING RATE (IN N_2), (POLY) METHYL METHACRYLATE

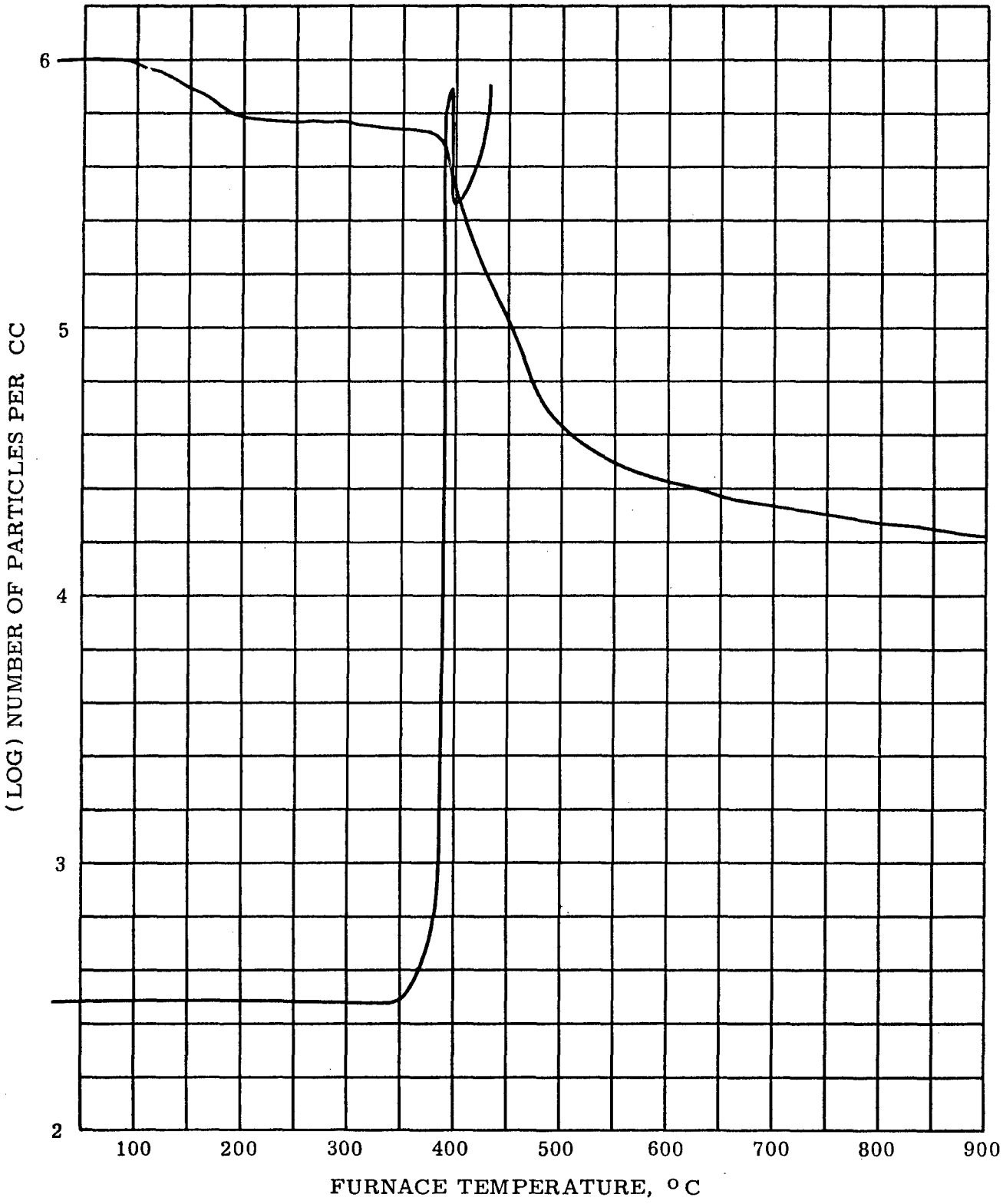

Figure 53 TPA IN AIR AT APPROXIMATELY 180 C° PER HOUR, COMPARED WITH TGA AT THE SAME HEATING RATE (IN N_2), ZINC 4, 4' - BIS - THIOPICOLINAMIDO - DIBENZOPHENONE

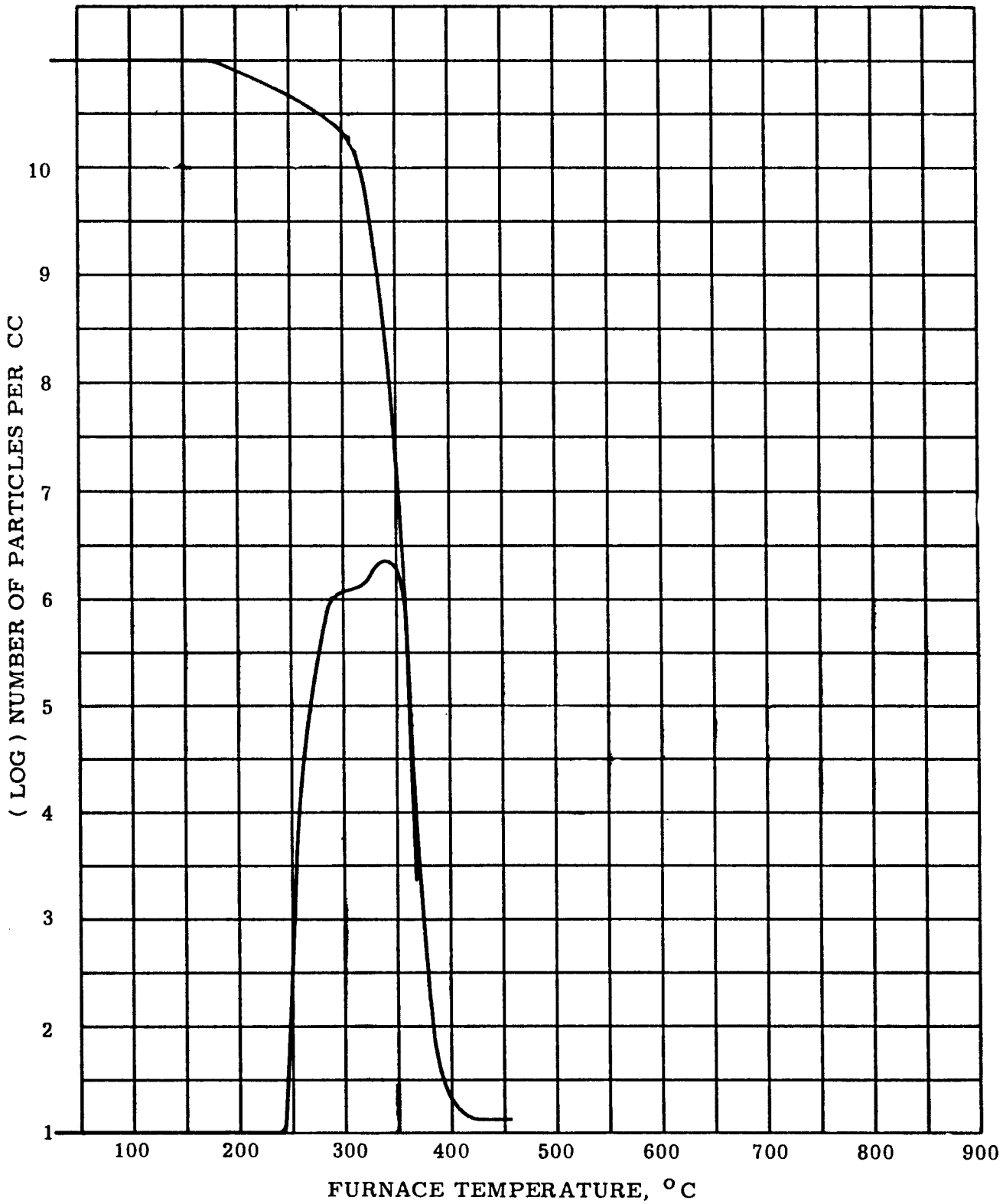

Figure 54 TPA IN DRY N_2 AT 180 C° PER HOUR, COMPARED WITH TGA AT THE SAME HEATING RATE, (POLY) METHYL METHACRYLATE

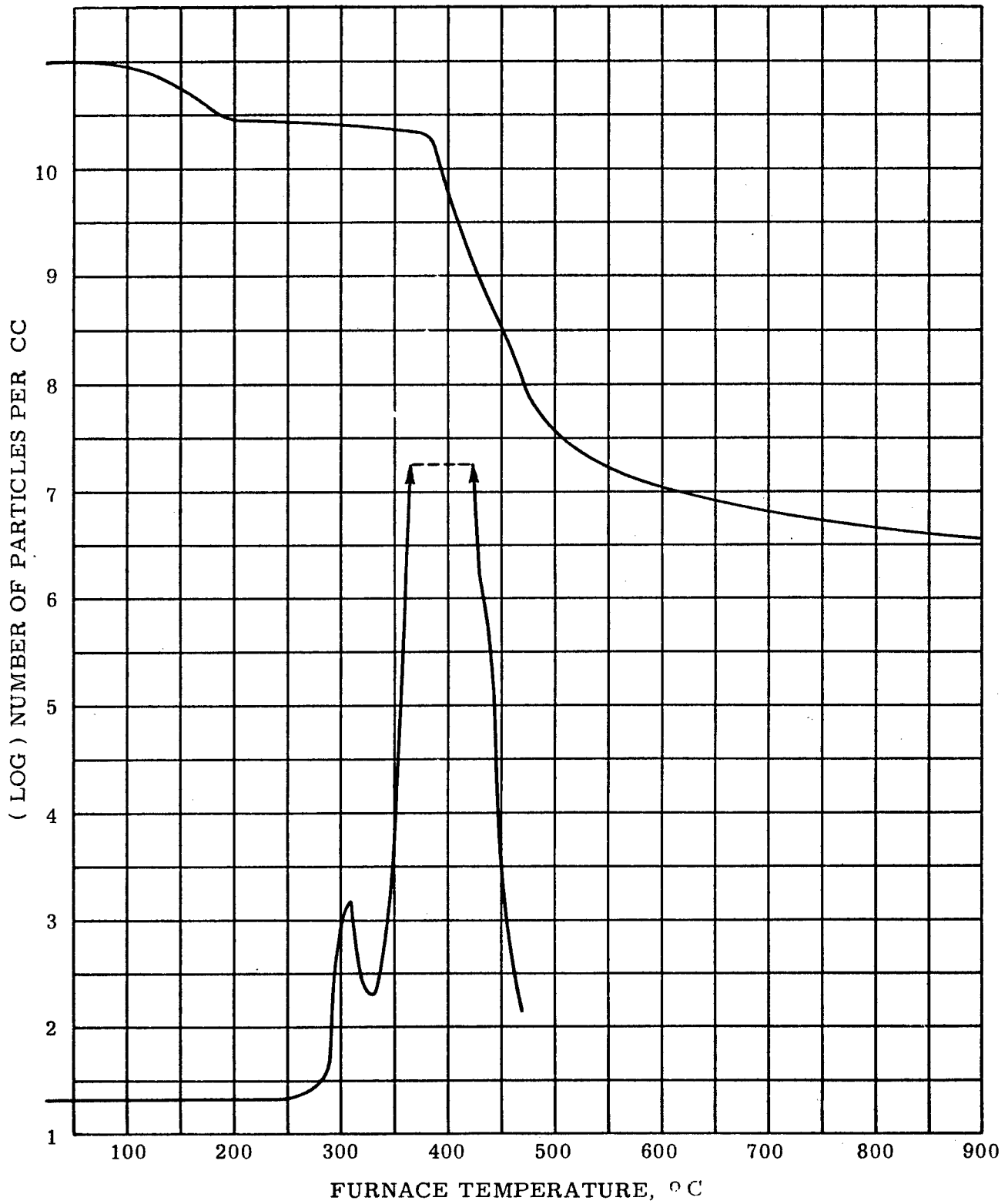

Figure 55 TPA IN DRY N_2 AT 180 C° PER HOUR, COMPARED WITH TGA AT THE SAME HEATING RATE, ZINC 4, 4' - BIS- THIOPICOLINAMIDODIBENZOPHENONE

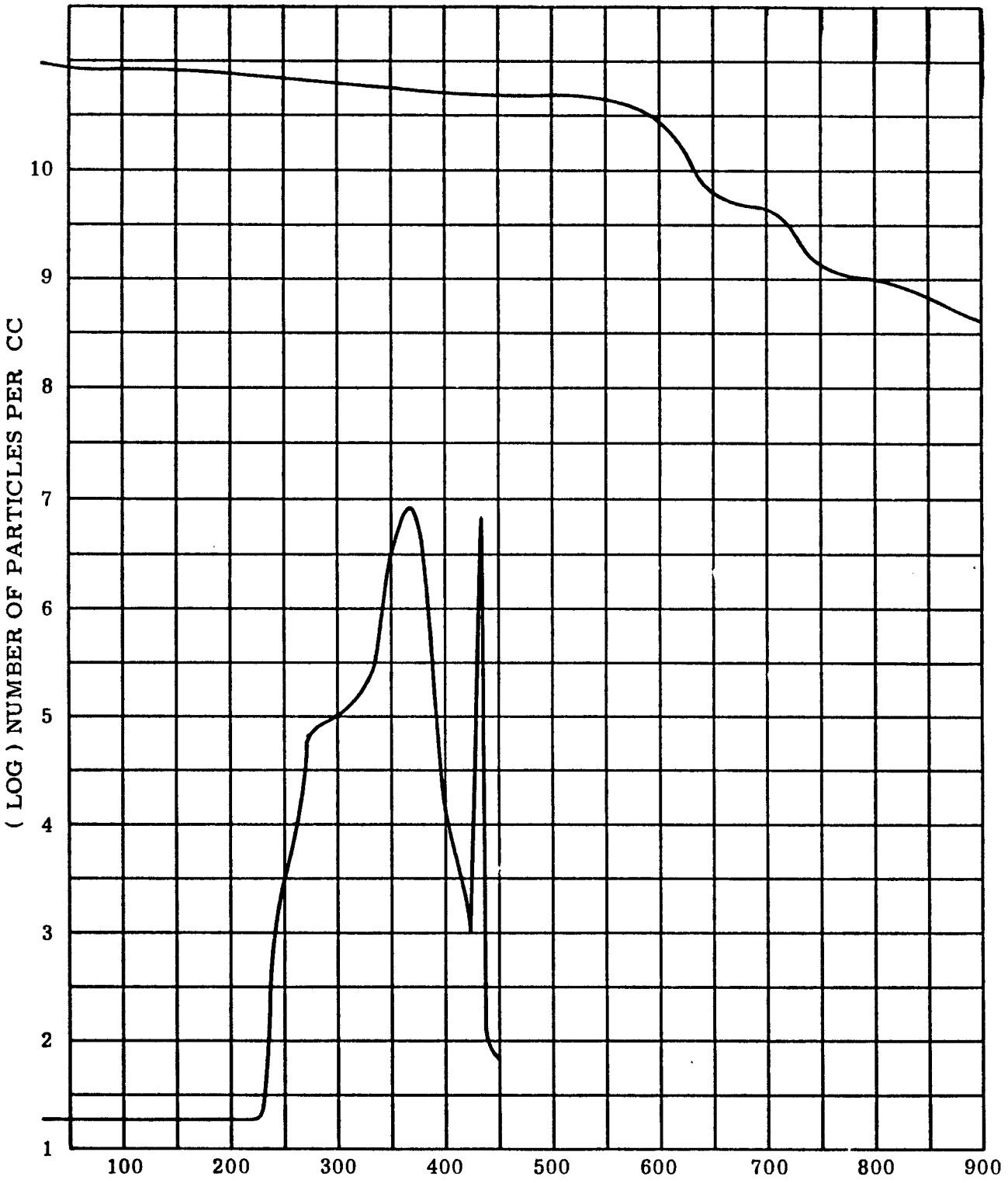

Figure 56 TPA IN DRY N_2 AT 180 C° PER HOUR, COMPARED WITH TGA AT THE SAME HEATING RATE, COPPER PHTHALOCYANINE (MATERIAL 22)

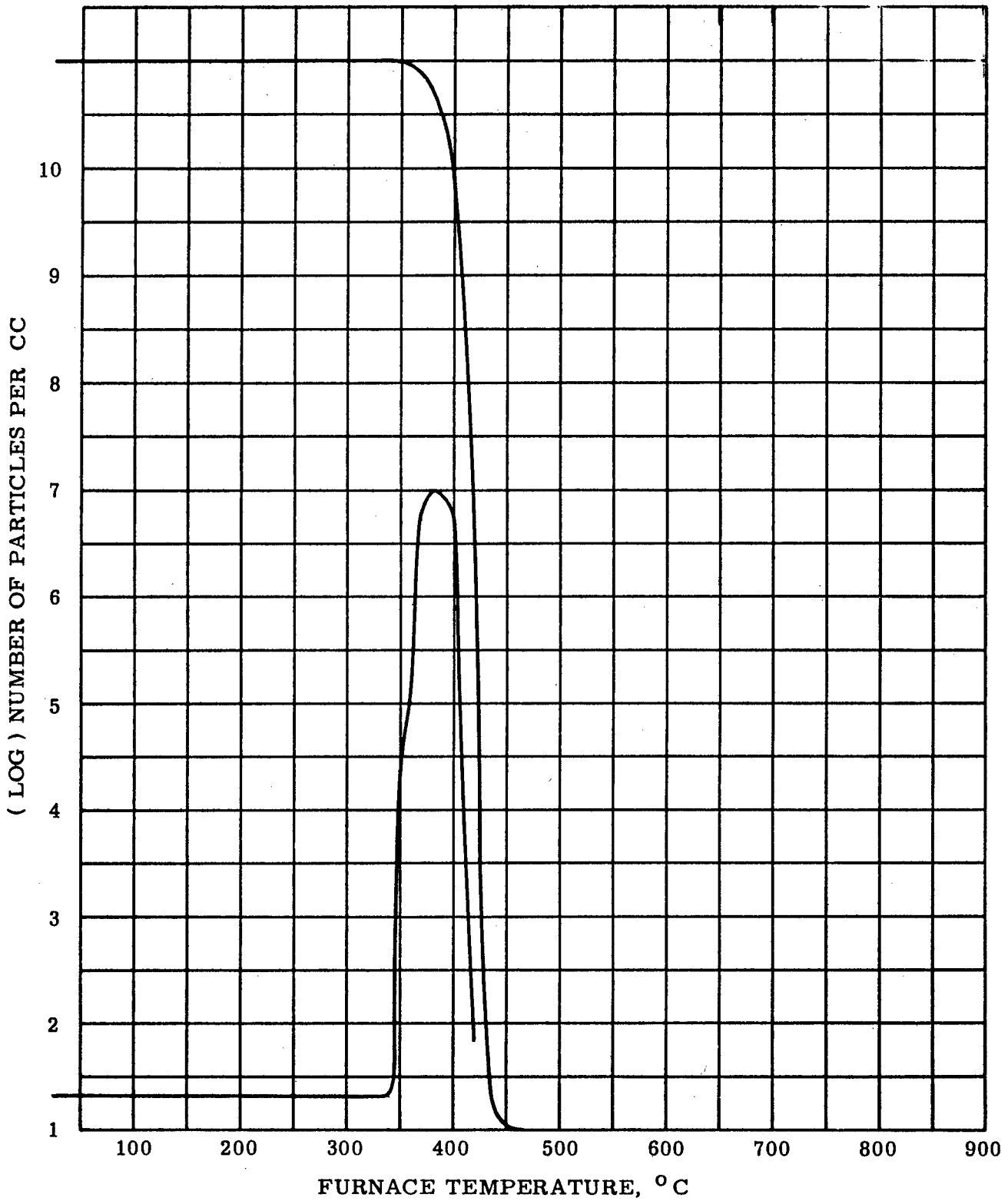

Figure 57 TPA IN DRY N_2 AT 180 C° PER HOUR, COMPARED WITH TGA AT THE SAME HEATING RATE, POLYCHLOROTRIFLUOROETHYLENE

volatilization, good agreement will be found between TGA and TPA.

Clearly, TPA is a corroborative technique which should be studied further. How materials should be compared on TPA data, however, is not yet quite so clear. As an empirical approach, the differences in the relative weights of polymer fragments might be ignored, in which case comparisons could be based on the number concentration of escaping particles under a given set of procedural conditions. From Figures 52 to 57, an end point concentration of 1000 particles per cc might prove broadly applicable. In any case, the location of recognizable curve features should be much easier in TPA than in TGA or DTA; unlike the TGA curve, the TPA curve is not confounded by gradual changes, and unlike the DTA curve, it is highly reproducible.

VI. CONCLUSIONS

1. Thermogravimetric analysis in inert atmosphere is a uniquely versatile method for empirically assessing intrinsic thermal stability because quantitative information is always available from the cumulative data record.

2. Of the two corroborative methods so far studied, namely, differential thermal analysis and thermoparticulate analysis, the latter is by far the more promising.

2a. Although it is sometimes capable of detecting reaction without catastrophic weight change, and although its sensitivity has been increased, the value of differential thermal analysis as a corroborative technique is still limited by irreproducibility and insensitivity to reactions which occur slowly over broad temperature ranges.

2b. Thermoparticulate analysis, a method of detecting escaping polymer fragments, can be applied in reactive atmospheres and gives dramatic and reproducible evidence of decomposition in cases of gradual volatilization.

3. Of the two procedural decomposition temperatures so far defined for thermogravimetric analysis in inert atmosphere, namely, the differential procedural decomposition temperature and the integral procedural decomposition temperature, only the latter is consistently applicable and equitable.

3a. The differential procedural decomposition temperature, defined as the procedural temperature at which the specific decomposition rate constant increases through a prescribed value, is generally inapplicable to the comparison of materials by means of thermogravimetric analysis because the specific decomposition rate constant cannot be found from volatilization data without corroborative knowledge of the relationship between the

apparent volatilization rate and:

i. The true volatilization rate for the volatilization step of interest.

ii. The nature of the apparent kinetic process and any changes in its nature in the temperature range of interest.

iii. The geometry and the degree of subdivision of the sample and any changes in these characteristics with extent of volatilization.

3b. The differential procedural decomposition temperature, determined empirically on a fixed apparent volatilization rate, is an inequitable basis for comparing materials, but serves as a basis for comparing recognizable features of thermogravimetric data records and those from corroborative techniques.

3c. In the practical sense, the fixed-rate differential procedural decomposition temperature is ambiguous or unacceptably imprecise or even unavailable from the data record in cases of gradual or step-wise volatilization.

3d. The integral procedural decomposition temperature, being based on areas under the data record in a fixed temperature range, is always available from the data record from thermogravimetric analysis in inert atmosphere, and it is an equitable basis for comparing materials because it can always be derived from the data record in a consistent manner.

3e. In the practical sense, the integral procedural decomposition temperature is a highly reproducible index of thermal stability and a comprehensive one which rewards refractoriness but which penalizes early volatilization in proportion to refractoriness. It is also a real temperature having the significance of an integrated-half-volatilization point.

4. As a means of determining kinetic constants, thermogravimetric analysis, like isothermal volatilization studies, is of limited value for the reasons given under Conclusion 3a; the constants found from volatilization studies alone are unauthentic until proven otherwise, and cannot be extrapolated to other experimental conditions. They are of value primarily as means of establishing logical starting points for more significant investigations.

4a. Thermogravimetric analysis is inherently inaccurate in the range of small volatilization rates. This limits its value as a kinetic method, especially with respect to the determination of long-time aging characteristics.

4b. Use of the Arrhenius integral as the equation of the data record for thermogravimetric analysis in inert atmosphere results in the determination of kinetic constants which satisfy each other ambiguously. Uniquely appropriate constants cannot be found without precise knowledge of the nature of the apparent kinetic process, as well as the effects of changing geometry and degree of subdivision of the sample on true volatilization rates.

4c. Empirically valid kinetic constants are readily found from isothermal aging data, but not from thermogravimetric data, by simple quasi-kinetic time-temperature superposition.

4d. For materials of widely different apparent kinetic process, isothermal aging times can be related to corresponding temperatures in thermogravimetric analysis by an empirical equation which is frequently linear over surprisingly long ranges of residual weight fraction.

VII. BIBLIOGRAPHY

1. Doyle, C. D., WADC TR 59-136 (1959).

2. Wall, L. A. and R. E. Florin, J. Res. NBS, 60, 451 (1958).

3. Tsonis, C. A., General Engineering Laboratory, General Electric Company, Private Communication.

4. Friedman, H. L., Missile and Space Vehicle Dept., General Electric Company, Private Communication.

5. Jahnke, E. and F. Emde, "Tables of Functions with Formulae and Curves," Dover (New York), 1945.

6. Coulson, C. A. and W. E. Duncanson, Phil. Mag., 33, 754 (1942).

7. Doyle, C. D., Modern Plastics, 34, No. 11, 141 (1957).

8. Doyle, C. D., J. Pol. Sci., 31, 95 (1958).

9. Keavney, J. J. and E. C. Eberlin, Abstr., 135th A.C.S. Mtg., 28S (1959).

10. Van Luik, F. G. and E. L. Johnson, General Engineering Laboratory, General Electric Company, Report 59GL65 (1959).

UNCLASSIFIED

GENERAL ELECTRIC COMPANY, Schnectady, New York, EVALUATION OF EXPERIMENTAL POLYMERS, by C. D. Doyle, May 1960. 106p. incl. illus. tables, 10 refs. (Project 7340; Task 73404) (WADD TR 60-283) (Contract AF 33(616)-5576) Unclassified report

Thermogravimetric analysis (TGA) in dry N_2 is considered in detail as a method for comparing the intrinsic thermal stabilities of experimental polymers on both empirical and fundamental grounds. Two procedural decomposition temperatures are defined and discussed. One, the "differential procedural decomposition temperature" (dpdt), is based on the locations of recognizable curve features, while the second, the "integral

(over)

UNCLASSIFIED

UNCLASSIFIED

GENERAL ELECTRIC COMPANY, Schnectady, New York, EVALUATION OF EXPERIMENTAL POLYMERS, by C. D. Doyle, May 1960. 106p. incl. illus. tables, 10 refs. (Project 7340; Task 73404) (WADD TR 60-283) (Contract AF 33(616)-5576) Unclassified report

Thermogravimetric analysis (TGA) in dry N_2 is considered in detail as a method for comparing the intrinsic thermal stabilities of experimental polymers on both empirical and fundamental grounds. Two procedural decomposition temperatures are defined and discussed. One, the "differential procedural decomposition temperature" (dpdt), is based on the locations of recognizable curve features, while the second, the "integral

(over)

UNCLASSIFIED

UNCLASSIFIED

procedural decomposition temperature" (ipdt), is based on areas under the curve. Kinetic analysis of volatilization data is discussed on the basis of both the Arrhenius rate equation and its integral. Two quasi-kinetic methods are discussed, one based on empirical time-temperature superposition; the other, on an empirical relationship between isothermal times and temperatures in TGA. Two corroborative test methods, differential thermal analysis and thermoparticulate analysis are discussed briefly.

UNCLASSIFIED

UNCLASSIFIED

procedural decomposition temperature" (ipdt), is based on areas under the curve. Kinetic analysis of volatilization data is discussed on the basis of both the Arrhenius rate equation and its integral. Two quasi-kinetic methods are discussed, one based on empirical time-temperature superposition; the other, on an empirical relationship between isothermal times and temperatures in TGA. Two corroborative test methods, differential thermal analysis and thermoparticulate analysis are discussed briefly.

UNCLASSIFIED

UNCLASSIFIED

GENERAL ELECTRIC COMPANY, Schnectady, New York, EVALUATION OF EXPERIMENTAL POLYMERS, by C. D. Doyle, May 1960. 106p. incl. illus. tables, 10 refs. (Project 7340; Task 73404) (WADD TR 60-283) (Contract AF 33(616)-5576)
Unclassified report

Thermogravimetric analysis (TGA) in dry N_2 is considered in detail as a method for comparing the intrinsic thermal stabilities of experimental polymers on both empirical and fundamental grounds. Two procedural decomposition temperatures are defined and discussed. One, the "differential procedural decomposition temperature" (dpdt), is based on the locations of recognizable curve features, while the second, the "integral

(over)

UNCLASSIFIED

UNCLASSIFIED

GENERAL ELECTRIC COMPANY, Schnectady, New York, EVALUATION OF EXPERIMENTAL POLYMERS, by C. D. Doyle, May 1960. 106p. incl. illus. tables, 10 refs. (Project 7340; Task 73404) (WADD TR 60-283) (Contract AF 33(616)-5576)
Unclassified report

Thermogravimetric analysis (TGA) in dry N_2 is considered in detail as a method for comparing the intrinsic thermal stabilities of experimental polymers on both empirical and fundamental grounds. Two procedural decomposition temperatures are defined and discussed. One, the "differential procedural decomposition temperature" (dpdt), is based on the locations of recognizable curve features, while the second, the "integral

(over)

UNCLASSIFIED

UNCLASSIFIED

procedural decomposition temperature" (ipdt), is based on areas under the curve. Kinetic analysis of volatilization data is discussed on the basis of both the Arrhenius rate equation and its integral. Two quasi-kinetic methods are discussed, one based on empirical time-temperature superposition; the other, on an empirical relationship between isothermal times and temperatures in TGA. Two corroborative test methods, differential thermal analysis and thermoparticulate analysis are discussed briefly.

UNCLASSIFIED

UNCLASSIFIED

procedural decomposition temperature" (ipdt), is based on areas under the curve. Kinetic analysis of volatilization data is discussed on the basis of both the Arrhenius rate equation and its integral. Two quasi-kinetic methods are discussed, one based on empirical time-temperature superposition; the other, on an empirical relationship between isothermal times and temperatures in TGA. Two corroborative test methods, differential thermal analysis and thermoparticulate analysis are discussed briefly.

UNCLASSIFIED

UNCLASSIFIED